Abstracts 6928-7225

SOLID STATE ABSTRACTS

an abstract journal devoted to the theory, production and use of solid state materials and devices

VOLUME 1 NUMBER 4

PHYSICS

METALLURGY

ELECTRONICS

METALS

SEMICONDUCTORS

SUPERCONDUCTORS

PHOSPHORS

MAGNETICS

DIELECTRICS

SOLID STATE ABSTRACTS

VOLUME 1, NUMBER 4

January, 1961

Abstracts 6928–7225

TABLE OF CONTENTS

Abstracts of the Solid State Literature

Metallurgy and Chemistry of Solids

General . . . 161
Chemical Reactions . . . 161
Alloys . . . 161
Crystal Structure . . . 161
Crystal Growth . . . 164
Crystal Surfaces and Crystal Processing . . . 168
Effects of Radiation . . . 170

Solid State Physics

General . . . 170
Crystal Physics . . . 171
Dielectric Properties . . . 172
Carrier Properties . . . 172
Conductivity . . . 173
Galvanomagnetic Properties . . . 174
Other Electrical Properties . . . 174
Electrical Properties of Specific Materials . . . 175
Magnetic Properties . . . 176
Optical Properties . . . 181
Thermal Properties . . . 183
Mechanical Properties . . . 184

Solid State Devices

Point Contact Diodes . . . 184
Junction Diodes . . . 185
Junction Transistors . . . 187
Field Effect Transistors . . . 188
Functional Units . . . 188
Galvanomagnetic Devices . . . 189
Other Conductive Devices . . . 189
Photodevices . . . 190
Thermal Devices . . . 190
Magnetic Devices . . . 190
Other Solid State Devices . . . 191

Solid State Device Measurements . . . 191

Basic Solid State Device Circuits

General . . . 191
Amplifiers . . . 193
Oscillators . . . 196
Switching Circuits . . . 196
Signal Converters . . . 197
Waveform Generators . . . 197

Applications of Solid State Devices

Medical . . . 198
Military . . . 198
Television . . . 198
Telephony . . . 199
Radar . . . 199
Microwaves . . . 199
Recording and Reproduction . . . 199
Computers . . . 200
Power . . . 203
Control . . . 204
Instrumentation . . . 204

New Products . . . 205

Subject Index . . . 207

Author Index . . . 214

List of Journals Abstracted . . . 215

Conference Programs Abstracted in Solid State Abstracts, Vol. 1, No. 3 and No. 4; see page 213

Editor: GEOFFREY KNIGHT, JR.

Assistant Editor: MYRON A. COHEN

PUBLISHED MONTHLY BY

Cambridge Communications Corporation, 238 Main Street, Cambridge 42, Massachusetts, Tel. Klrkland 7-1997

Subscription Rate: $25.00 per year. Single Copies and Back Issues: $2.50. Advertising Rates on Request.

Cambridge Communications Corp. is not prepared to furnish copies of the articles abstracted. However, there are many libraries throughout the country which maintain photocopying services.

SYMBOLS USED IN THE ABSTRACTS

L: Letter to the Editor. A: Only an abstract is given in the reference. R: Only a review is given in the reference. E: Erratum.

The reference numbers in the indices are the abstract numbers, not the page numbers.

Copyright 1961 by Cambridge Communications Corp. Printed in the U.S.A. by the University Press, Inc.

Second-class mail privileges applied for at Boston, Massachusetts

ABSTRACTS OF THE SOLID STATE LITERATURE

METALLURGY AND CHEMISTRY OF SOLIDS

GENERAL

Commercial Availability of Yttrium-Gadolinium Garnets - See 7216

CHEMICAL REACTIONS

6928 REACTIONS BETWEEN GALLIUM AND QUARTZ by L. M. Foster and R. A. Kramer (Alcoa Res. Labs.); 1960 Fall Mtg. Electrochem. Soc.

It can be shown from simple thermodynamic considerations that gallium metal cannot react with silica. For the reaction $SiO_2 + Ga \rightarrow Si + Ga_2O_3$ the free energy change at 1273°K is +138 kcal. Because of the considerable solubility of silicon in gallium at high temperatures, however, this reaction can proceed until the silicon content reaches 1×10^{-7} atom % in the gallium. Vacuum heating experiments in all quartz environments have shown that attack on the quartz is much greater than this. The findings can be explained by the reaction $SiO_2 + Ga \rightarrow Si + Ga_2O$ and the volatilization of the gallium sub-oxide.

ALLOYS

6929 THERMODYNAMIC STUDY OF THE BINARY SYSTEM CARBON-SILICON USING A MASS SPECTROMETER by J. Drowart and G. De Maria (U. Chicago); Proc. Conf. Silicon Carbide, Pergamon Press, 1960, pp. 16-23

Mass spectrometric analysis of the molecules in a molecular beam issuing from a graphite Knudsen cell containing hexagonal SiC to determine the nature and pressure of the gaseous species in thermodynamic equilibrium with SiC is reported. The predominant species are Si, SiC_2, and Si_2C, less important molecules being C, C_2, and C_3, Si_2, Si_3, SiC, Si_2C_2, Si_2C_3, and Si_3C. Partial pressures have been measured for each of these molecules by comparing their intensity with that of silver and of C, C_2 and C_3 used as pressure standards, with corrections for the relative ionization cross-sections. These pressures, together with estimated free-energy functions, are used to calculate heats of sublimation and dissociation energies. The Si decomposition pressure determined, combined with the heat of formation of SiC, gives a heat of sublimation of Si, $\Delta H^\circ_{298} = 113 \pm 3$ kcal/g atom, in agreement with directly measured values.

6930 TRANSFORMATION STUDIES OF GRAY TIN SINGLE CRYSTALS by R. G. Wolfson, M. E. Fine and A. W. Ewald (Northwestern U.); J. Appl. Phys., Vol. 31, pp. 1973-1977, Nov. 1960

Measurements of the linear growth rate of white tin into thin single crystal wafers of gray tin, over the temperature range from 24.2° to 46.5°C, are presented. The rate is not a single-valued function of the temperature. Imposed upon the strong temperature dependence of the average rate is a variation which is well defined at a given temperature; the spread in the observed values decreases sharply with increasing temperature. The variation is attributed to two observed stress-relaxation processes: cleavage in the gray tin and plastic deformation, accompanied by recrystallization, in the white tin.

6931 PROPERTIES OF HgSe-HgTe ALLOYS by T. C. Harman, A. J. Strauss and L. B. Farrell (Lincoln Lab.); 1960 Fall Mtg. Electrochem. Soc.

Determination of the phase diagram for the pseudo-binary system HgSe-HgTe by differential thermal analysis and x-ray diffraction techniques was reported. Melting points measured for HgSe and HgTe are 799° and 670°C, respectively. Continuous solid solution occurs over the whole range of composition. Large single crystals of the alloys have been prepared by the Bridgman method. Data on the electrical properties of the alloys as a function of composition, impurity concentration, and temperature were presented.

Incongruent Melting of the Ternary Compound $AgSeTe_2$ - See 6954

Solid Solutions of Metals and Tungsten Trioxide - See 6998

Solubility of Si in Ga - See 6928

CRYSTAL STRUCTURE (including Imperfections and Impurities)

Polytypism in SiC Crystals - See 6937 and 6952

6932 DISLOCATIONS, STACKING FAULTS AND TWINS IN THE SPINEL STRUCTURE by J. Hornstra (N. V. Philips); J. Phys. Chem. Solids, Vol. 15, pp. 311-323, Oct. 1960

The slip plane in crystals of the spinel type is assumed to be the (111) plane in analogy with the basal slip of corundum. This is also in agreement with experimentally observed deformation twinning, which may be explained as a mechanism involving partial dislocations with a (111) slip plane. Dislocations with a (111) slip plane may consist of four partial dislocations separated by three stacking faults. The detailed structure of these stacking faults is compared with the perfect

spinel lattice. During slip the cations move in a direction different from that of the oxygen ions. This process, the synchro-shear process, is discussed for the case that cations with four-fold coordination take part in it. Another type of stacking fault shows relationship to the olivine lattice. Two possible configurations of the (111) twin boundary are discussed.

6933 MECHANISM FOR COLORATION OF ALKALI HALIDES AT LOW TEMPERATURES by C. C. Klick (U.S. Naval Res. Labs.); Phys. Rev., Vol. 120, pp. 760-762, Nov. 1, 1960

A mechanism for low-temperature coloration of alkali halides is proposed in which double ionization of a halide ion or single ionization of two adjacent halide ions leads to the formation of an uncharged halogen molecule which occupies two adjacent halide ion sites. If the molecule is localized at one of these sites by the jump of a nearby halide ion into the other site, a vacancy and interstitial are formed. Capture of an electron by each of these imperfections leads to the production of the F center and H center.

6934 DIFFUSION OF F CENTERS INTO POTASSIUM CHLORIDE SINGLE CRYSTALS by H. Mizuno and M. Inoue (Matsushita Electronics); Phys. Rev., Vol. 120, pp. 1226-1229, Nov. 15, 1960

Measurements at various temperatures of the diffusion of F centers into potassium chloride crystals during an additive coloring process are reported. A diffusion process which can be explained by a simple theory of volume diffusion seems to be predominant at higher temperatures. At lower temperatures, however, the occurrence of a disordered interfacial diffusion with an F-center concentration decreasing exponentially with the first power of penetration depth is confirmed.

Color Centers in Alkaline Earth Fluorides - See 7059 and 7060

6935 GERMANIUM STRUCTURAL DEFECTS — THEIR CAUSE AND EFFECT by D. H. Lyon (GE); 1960 Fall Mtg. Electrochem. Soc.

Line defects and point defects found in germanium single crystals were discussed. The line defects are dislocations, and the point defects are believed to be a precipitated phase. Etching methods have been used to detect each type of defect by the production of characteristic etch pits, called dislocation pits and saucers. Several observations were made regarding the origin and control of the defect during crystal growth as well as possible effects on device performance.

Implications of the Dangling Bond Model for Dislocation Theory - See 7000

6936 SOME EFFECTS OCCURRING IN DISLOCATED TELLURIUM by J. S. Blakemore, J. W. Schultz and K. C. Nomura (Honeywell Res. Ctr.); J. Appl. Phys., Vol. 31, pp. 2226-2231, Dec. 1960

Dislocation densities as small as $1000\,cm^{-2}$ are sometimes found in carefully produced single crystals of tellurium, but since the material is very soft a quite mild stress can introduce 10^6 dislocations/cm^2 or more. Dislocation etch pits of sharply geometric shape can be developed on the cleavage $(10\bar{1}0)$ planes by the slow attack of sulphuric acid; their planar surfaces correspond to $(1\bar{1}00)$, $(10\bar{1}3)$, $(01\bar{1}1)$, and $(0\bar{1}1\bar{1})$ faces. Effects are noted on faces exposed by cleavage at 77°K which suggest that even at this temperature the material can suffer localized plastic damage, for brief etching of such faces produces small flat-bottomed pits; these may be interpreted by supposing that the mild stress of cleavage at 77°K generates shallow dislocation loops. The flat-bottomed pits disappear when a surface layer $\geq 25\mu$ is etched away. A marked increase in electron-hole recombination rate is noted in plastically deformed crystals. If the additional recombination occurs through the dislocations themselves, then each has a capture radius of some 4×10^{-8} cm at 300°K. Dislocated crystals also show more prominent trapping effects at low temperatures than structurally pure samples, and contain additional readily ionizable acceptor sites; these may be derived from the dislocations themselves or from other defects created or activated by plastic flow.

6937 SURFACE FEATURES ON SILICON CARBIDE CRYSTAL FACES by S. Amelinckx and G. Strumane (Lab. Kristalkunde, Ghent); Proc. Conf. Silicon Carbide, Pergamon Press, 1960, pp. 162-201

Observations of industrial silicon carbide crystals to demonstrate the role played by dislocations in crystal growth are presented. The remarkable polytypism of SiC is at least partially explained by the spiral growth mechanism. Interesting relations exist between the geometry of the growth features and the polytypic structure of the crystals. SiC is also the first substance for which the relation dislocation-etchpit has been demonstrated without ambiguity. Some more recent work on etching of SiC is discussed in relation to dislocations in this substance.

6938 ELECTRON OPTICAL STUDY OF BASAL DISLOCATIONS IN GRAPHITE by S. Amelinckx and P. Delavignette (Centre d'Etude de l'Energie Nucléaire, MOL Belgium); J. Appl. Phys., Vol. 31, pp. 2126-2135, Dec. 1960

A study of dislocations in graphite which have a Burgers vector in the basal plane and which lie in this plane by the use of thin foil transmission electron microscopy is reported. The dislocations are dissociated into ribbons consisting of two partials separated by a stacking fault. Specific models for these dislocations are presented. Hexagonal networks contain extended and contracted nodes. The presence of two types of stacking faults gives rise to singularities which are analyzed in terms of experimentally determined Burgers vectors. The dislocations and even the networks are very mobile along the basal plane. The stacking fault energy is determined as 3 to 5×10^{-2}ergs/cm^2.

6939 FRICTIONAL STRESS ACTING ON A MOVING DISLOCATION IN AN OTHERWISE PERFECT CRYSTAL by D. Kuhlmann-Wilsdorf (U. Penn.); Phys. Rev., Vol. 120, pp. 773-781, Nov. 1, 1960

The problem of the frictional stress suffered by moving dislocations in otherwise perfect crystals is investigated. This is done without calculating the core energies of dislocations, but by considering stresses and strains on the slip plane. The level of frictional stresses obtained is much higher than reported previously. Since common glide dislocations in metals with close packed structures apparently do not suffer significant frictional stresses, mechanisms which tend to reduce their effect are discussed. A new such mechanism which is based on the idea that the positions of dislocation axes are not defined with precision, but only within one to a few times the average displacement of the oscillating atoms is considered. The expected result of this is a depression of the frictional stress for close packed

metals even at very low temperatures, almost no effect on dislocations in crystals with diamond structures, and a temperature dependence proportional to $e^{-\text{const } T/T_M}$ for NaCl type salts, and, probably, for bcc metals.

6940 ANALYSIS OF IMPURITIES IN SILICON CARBIDE by G. H. Morrison and R. L. Rupp (Sylvania); Proc. Conf. Silicon Carbide, Pergamon Press, 1960, pp. 227-234

A review of the various techniques of analysis for trace impurities in SiC and other semiconductors is presented and their advantages and limitations are discussed. Results to date on an emission spectrographic method of enhanced sensitivity are given. The method is based on the selective volatilization of impurities from the silicon carbide matrix. Preparation of spectrographic standards is described and the present limits of sensitivity are presented.

6941 DETERMINATION AND IDENTIFICATION OF IMPURITIES IN SILICON FROM LOW-TEMPERATURE HALL DATA by R. T. Bate (Battelle Mem. Inst.), L. R. Weingarten and D. J. Shombert (Merck, Sharp, Dohme); J. Electrochem. Soc., Vol. 107, pp. 908-911, Oct. 1960

The use of low-temperature measurements of the Hall effect to determine donor and acceptor concentrations and in some cases to identify the major impurity in silicon is discussed and a simple apparatus for making these measurements with liquid helium is described. Typical results are presented and correlated with lifetime data at room temperature. Interpretation of the Hall coefficient measurements is discussed, and a simplified analysis of the case of the two types of donor impurity is suggested.

6942 PRACTICAL NEUTRON ACTIVATION ANALYSIS FOR THE ELECTRONIC SCIENTIST by J. P. Cali and J. R. Weiner (Air Force Camb. Res. Ctr.); J. Electrochem. Soc., Vol. 107, pp. 1015-1019, Dec. 1960

Neutron activation analysis is an extremely sensitive analytical method for determining trace impurities in semiconductor materials. Theoretical aspects are discussed, and procedures are outlined. Parameters which determine sensitivity are considered, as well as the techniques whereby they may be varied to increase sensitivity. Tables which list elements that can be determined by neutron activation analysis, their half-lives, and minimum detectable amounts are included. Elemental matrix materials of electronic interest are also tabulated together with naturally occurring associated impurities which can be determined by neutron activation analysis and other methods. These matrices are also ranked according to extent of flux perturbations, degree of self-activation, and ease of chemical separation.

6943 NEUTRON ACTIVATION ANALYSIS OF SILICON CARBIDE by L. F. Lowe, H. D. Thompson and J. P. Cali (Air Force Camb. Res. Ctr.); Proc. Conf. Silicon Carbide, Pergamon Press, 1960, pp. 221-226

Neutron activation analysis of silicon carbide for seven elements (Ni, Mn, Cu, Zn, Sb, Mo, and Fe) is discussed. After irradiation with thermal neutrons, the SiC sample was decomposed at 1250°C with chlorine and oxygen. The induced impurity activities were separated from one another and counted by means of a Geiger counter to determine their impurity levels. The results are in agreement with available spectrographic data. It is suggested that this method, which is several orders of magnitude more sensitive than the spectrographic method for many elements, could be extended well beyond the seven elements checked.

6944 ANALYSIS OF IMPURITIES IN COMPOUND SEMICONDUCTORS by G. D. Perkins, C. F. Robinson, and R. K. Willardson (Con. Electrodynamics); 1960 Fall Mtg. Electrochem. Soc.

Problems involved in the application of mass spectrometry to the detection and identification of impurities in compound semiconductors were discussed. A typical problem is the detection of silicon in InSb, AlSb, or GaAs. At mass 28 ± 0.03 a quadruplet consisting of Si, Co, N_2, and C_2H_2 is usually found, and a resolution of at least 1:1600 is required. Mass spectrographic analyses were compared with impurity concentrations expected from controlled impurity additions and electrical analysis.

6945 INVESTIGATIONS OF CRYSTAL PERFECTION OF SEMICONDUCTOR CRYSTALS BY X-RAY DIFFRACTION MICROSCOPY by G. H. Schwuttke (Gen. Tel. and Electronics Labs.); 1960 Fall Mtg. Electrochem. Soc.

The application of x-ray diffraction microscopy to the detection of impurities in semiconductor crystal lattices was described. Segregation, cluster formation, and precipitated second phases can be revealed in the diffraction image. The sensitivity of this method makes possible, for instance, the detection of oxygen concentrations in silicon as small as $10^{17}/cm^3$.

6946 SEPARATION OF SULFUR, SELENIUM, AND TELLURIUM FROM ARSENIC by J. M. Whelan, J. D. Struthers, and J. A. Ditzenberger (Bell Labs.); J. Electrochem. Soc., Vol. 107, pp. 982-985, Dec. 1960

Three methods for separating trace amounts of sulfur present in high-purity arsenic are discussed. These are: (a) vacuum sublimation, (b) sublimation in a hydrogen stream, and (c) distillation of arsenic from an arsenic-lead solution. The last method is somewhat more effective than the second. The first was unsatisfactory. The lead process yielded arsenic containing the following atom fractions of sulfur, selenium, and tellurium; 1×10^{-9}, $\leq 2.7 \times 10^{-8}$, and $\leq 2 \times 10^{-8}$, respectively. Concentrations of these impurities were measured with the aid of radiotracer techniques.

6947 SOME STATISTICS OF DOPING SILICON CRYSTALS by J. W. Brownson and R. Saphir (Raytheon); 1960 Fall Mtg. Electrochem. Soc.

The application of statistical techniques to crystal doping problems, which has yielded several valuable process techniques as well as improved understanding of impurity variations in silicon material, was discussed. These techniques include evaluation of raw silicon, optimization of doping, doping process control, analysis of scrap and its recovery, and the detection of unsuspected contaminants in the material. One result has been the analytical quantification of the variations of impurity levels within and among samples of the various forms of silicon. The causes of these variations have been partially analyzed.

6948 RESISTIVITY OF GRANULAR SILICON CARBIDE — IMPURITY AND CRYSTAL STRUCTURE DEPENDENCE by P. Carroll (Carborundum); Proc. Conf. Silicon Carbide, Pergamon Press, 1960, pp. 341-346

The use of granular resistivity and color observations as a

qualitative means to demonstrate diffusion of nitrogen into α-silicon carbide grain is discussed. The range of resistivity obtained covers seven orders of magnitude. Observed color changes are related to the resistivity changes. Darker green coloration indicates lower resistivity. The conductivity of β-silicon carbide grain has been found to be higher than that of α-silicon carbide.

6949 A MODIFIED CLOSED BOX SYSTEM FOR THE DIFFUSION OF BORON IN SILICON by R. S. Yatsko and J. S. Kesperis (USASRDL); J. Electrochem. Soc., Vol. 107, pp. 911-915, Oct. 1960

An investigation of a modified closed box diffusion system over a wide range of conditions is reported. Boron layers have been diffused in silicon from B_2O_3-SiO_2 sources ranging from concentrations of 0.2 %B by weight to pure B_2O_3. Non-melting source conditions have been varied to melting source conditions, yielding surface concentrations ranging from 10^{18} to 10^{21} carriers/cc. Some effects of environmental atmospheres and materials are discussed. Applications to photo-voltaic devices and double diffused transistors are described.

6950 DIFFUSION OF Ag^+, Cl^-, AND Cd^{++} IN SILVER CHLORIDE SINGLE CRYSTALS by R. F. Reade and D. C. Martin, Jr. (Iowa State U.); J. Appl. Phys., Vol. 31, pp. 1965-1968, Nov. 1960

The results of an investigation of the diffusion rates of silver, chlorine, and cadmium ions in single crystals of silver chloride by means of a modification of the surface counting method are reported. The diffusion coefficient of the silver ion from 200° to 400°C can be represented by the equation $D = 9.36 \exp(-1.01\ ev/kT)\ cm^2/sec$. Estimates of chloride ion activation energies give a value of 1.57 ev between 350° and 400°C, and a value of 0.37 ev below 280°C. The silver and chloride ion diffusion data are compared with results of workers who used sectioning methods. The diffusion coefficient of the cadmium ion may be expressed by the equation $D = 32.8 \exp(-1.36\ ev/kT) cm^2/sec + 2.35 \times 10^{-5} \exp(-0.56/kT)\ cm^2 sec$.

6951 DIFFUSION OF SILVER INTO CUPROUS OXIDE by A. I. Andrievskii, A. V. Sandulova and M. I. Yurkevich (L'vov Polytechnical Inst.); Soviet Phys.-Solid State, Vol. 2, pp. 581-584, Oct. 1960

The results of an experimental investigation of the diffusion of silver in cuprous oxide (Cu_2O) mono- and polycrystals are reported. Diffusion was investigated using the Ag^{110} isotope as a tracer. The diffusion coefficient was found to vary exponentially with temperature. The numerical values of the diffusion coefficients of silver in cuprous oxide crystals of various structure are given, the preexponential multiplier and the activation energy are calculated, and the mechanism of diffusion is discussed as a function of the structure of cuprous oxide and of temperature.

Electron Microscope Studies of Cleaved KCl Surfaces - See 6981

6952 POLYTYPISM AND SURFACE STRUCTURE OF SILICON CARBIDE CRYSTALS-INTERFEROMETRIC AND X-RAY STUDIES by A. R. Verma (U. Delhi); Proc. Conf. Silicon Carbide, Pergamon Press, 1960, pp. 202-216

Studies of the surface structure of a number of SiC crystals of different polytypes by a combination of phase-contrast microscopy and multiple-beam interferometry are reported. The structure of different polytypes has been determined by x-ray diffraction methods. A correlation between the spiral step-heights and x-ray unit cells has helped to explain the origin of polytypism in SiC crystals in terms of the dislocation theory. A mixture of polytypes and their variation on a microscopic scale is reported, and a variety of observations on SiC surfaces, some of which are still to be explained, is noted.

6953 CRYSTAL ORIENTATION EFFECTS OBSERVED IN TIN-TELLURIDE THIN FILMS by S. H. Shortes and D. P. Miller (Texas Instr.); 1960 Fall Mtg. Electrochem. Soc.

Tin-telluride thin films may be oriented crystallographically to certain preferred directions either during evaporation or during subsequent annealment. An investigation of the degree of orientation for different evaporation pressures and for effects of annealment ambient was reported. X-ray diffraction measurements reveal that either 111 or 110 crystal planes may be preferentially aligned parallel to the evaporation substrate. The results indicate that variations from stoichiometry of the film is sufficient for orientation. A tin-rich film orients to the 111 direction while a tellurium-rich film orients to the 110 direction.

Structure of Single Crystal Gold Films Grown by Vacuum Deposition - See 7079

Effect of Plating Parameters on the Structure of Co and Co-Ni Alloys - See 6994

Spiral Walls in Thin Magnetic Films - See 7038

Structure of Thin Ferrite Films - See 6974 and 6976

6954 A STRUCTURAL STUDY OF THE COMPOUND $AgSbTe_2$ by R. W. Armstrong, J. W. Faust, Jr. and W. A. Tiller (Westinghouse Res. Lab.); J. Appl. Phys., Vol. 31, pp. 1954-1959, Nov. 1960

The use of x-ray, optical and electron microscope, and chemical etching techniques to investigate a striated microstructure, observed in zone refined single crystals of the $AgSbTe_2$ structure is reported. This microstructure, originally thought to be fine twin lamellas, has been identified as a Widmanstatten precipitate of Sb_2Te_3 upon the {111} planes of the matrix face-centered cubic material. In addition, the evidence obtained from all the measurements made on this material indicates that the ternary compound of the $AgSbTe_2$ type does not melt congruently.

Crystal Structure of Ag_2Se - See 7077

Crystal Structure of Tri-Clinic Copper Tungstate - See 6998

CRYSTAL GROWTH

Role Played by Dislocation in the Growth of SiC Crystals - See 6937

6955 HORIZONTAL GROWTH OF GERMANIUM SINGLE CRYSTALS USING A SILICON NITRIDE RECEPTACLE by J. L. Porter (Sylvania); 1960 Fall Mtg. Electrochem. Soc.

The use of silicon nitride as a replacement for quartz in the horizontal formation of germanium single crystals was described. The complete nonwettability of the silicon nitride offers a distinct advantage and thus facilitates the formation of large cross-sectional ingots of high crystallographic perfection.

6956 SYNTHESIS AND CRYSTAL PULLING OF GALLIUM ARSENIDE IN A MAGNETIC CRYSTAL PULLER by K. Weiser and S. Blum (IBM); 1960 Fall Mtg. Electrochem. Soc.

An all-quartz magnetic crystal puller in which GaAs is synthesized in situ and then pulled from the melt was described. Details of the puller were given, and the preparation of both doped and undoped material was described. Some electrical properties in the temperature range from 4° to 750°K of n- and p-type single crystals prepared in this manner were reported.

6957 GROWTH FROM THE MELT. Part II. CELLULAR INTERFACE MORPHOLOGY by G. F. Bolling and W. A. Tiller (Westinghouse Res. Labs.); J. Appl. Phys., Vol. 31, pp. 2040-2045, Nov. 1960

A theoretical examination of the microscopic shape of a solid-liquid interface for those growth conditions which give rise to a cellular morphology is presented. The method of obtaining a general solution is set forth, and approximate treatments are used to compare the theoretical approach with experimental data. The variation of cell size with temperature gradients, growth velocity, stirring in the liquid, interfacial free energy, and solute content is examined, and the conditions governing the stability of a cellular interface compared to that of a smooth interface are predicted.

6958 THE SHAPE OF MELT-CRYSTAL INTERFACES DURING FLOAT ZONING OF SILICON by J. H. Braun and R. A. Pellin (du Pont); J. Electrochem. Soc., Vol. 107, p. 268C (A), Dec. 1960

The thermal environment of the interface of growth of a silicon crystal during float zoning was described. Depending on operating conditions, the interface between the melt and the growing crystal can be convex, near flat, or concave. The shape of the interface has been made visible by slot doping of n-type silicon with an excess of boron dope to give a p-n junction between n-type crystal and p-type melt. This junction, delineating an interface, can be decorated with a staining etchant.

6959 PROPERTIES OF PbSe PREPARED BY POWDER-METALLURGY TECHNIQUES by J. F. Miller and R. C. Himes (Battelle Mem. Inst.); J. Electrochem. Soc., Vol. 107, pp. 915-919, Nov. 1960

The application of powder-metallurgy techniques to the preparation of bulk specimens of lead selenide is discussed; both the hot-press and the press-and-sinter methods have been employed. Compacting pressure, sintering temperature, sintering time, and the particle size of the powder were treated as variables. Electrical and thermoelectric properties, densities, and microstructures of the specimens were studied. Sound specimens of near-theoretical density and with electrical and thermoelectric properties similar to those of the best of cast lead selenide were prepared successfully by the hot-press method. Densities of hot-pressed specimens, which were highest for those prepared at 750°C, 8100 psi, were observed to decrease with sintering temperature in the range 750°-450°C, and with compacting pressure in the range 8100-2000 psi. The pressed-specimen density was not affected appreciably by variations of sintering time (in the range 5 min-5 hr at 750°C) or variations of the particle size of the powder (in the range -60 to -200 mesh). Electrical properties of specimens with densities in the range 90-98% of theoretical, which were prepared by both the hot-press and the press-and-sinter methods, did not change significantly as density varied in this range.

6960 EPITAXIAL AND SINGLE CRYSTAL GROWTH ON TO SILICON CARBIDE SEEDS by K. M. Hergenrother, S. E. Mayer and A. I. Mlavsky (Transitron); Proc. Conf. Silicon Carbide, Pergamon Press, 1960, pp. 60-66

Studies of the theoretical aspects of crystal growth from the vapor phase, particularly with respect to factors which prevent secondary nucleation during growth onto a seed, are reported. The theory is applied to the problem of growing single-crystal SiC from the vapor phase epitaxially onto seeds. A furnace, designed to meet the limiting parameters, has been used to grow layers of high-purity SiC onto seeds. The electrical and physical properties of films prepared in this manner, which are dependent on various growing parameters as well as the purity of the starting materials, are discussed. Single crystals of the cubic modification several cubic millimeters in volume have been grown in the furnace by random nucleation, and means of growing larger cubic crystals onto cubic as well as onto hexagonal seeds are described. The properties of junctions made by epitaxial deposition films are also presented.

Thermocouple Furnace for SiC Device Fabrication - See 7093

6961 AN IMPROVED METHOD OF GROWING CdS CRYSTALS FROM THE VAPOR PHASE by P. D. Fochs (Assoc. Elec. Ind.); J. Appl. Phys., Vol. 31, pp. 1733-1734, Oct. 1960

A technique which utilizes the gradual increase in the difference in temperatures of two Kanthal heating elements to permit CdS crystals to be grown directly on the inside of a silica tube, remote from one another, instead of on a continuous polycrystalline CdS substrate as in most existing methods is described.

6962 GROWTH OF LARGE CRYSTALS BY GRAIN GROWTH by L. R. Shiozawa and A. Carlson (Clevite); J. Electrochem. Soc., Vol. 107, p. 268C, Dec. 1960

The growth of monocrystals of CdS-type compounds weighing up to a half pound by "grain-growth" recrystallization is described. As in growth and destruction of froth bubbles, molecules diffuse across cell walls in response to curvature-induced differences in vapor pressure, resulting in reduction of interfacial boundary area ultimately to zero. A temperature gradient is used to form and maintain maximum density. The method appears useful for any solid having a reasonable sublimation pressure.

Crystallographic Orientation of Evaporated SnTe Films - See 6953

6963 GROWTH STEPS ON THE SURFACES OF GERMANIUM, SILICON, AND III-V COMPOUND DENDRITES by G. R. Booker (Westinghouse); 1960 Fall Mtg. Electrochem Soc.

Use of optical, interference, and electron microscopy to study the growth steps occurring on the "flat" surfaces of germanium, silicon, and III-V compound dendrites was described. Variations in height, slope, form, and distribution of the steps have been observed. The role of the steps in increasing the thickness of the dendrites was discussed.

6964 SILICON DENDRITE STUDIES by S. N. Dermatis and J. W. Faust, Jr. (Westinghouse); 1960 Fall Mtg. Electrochem Soc.

The growth and evaluation of dendrites of silicon was discussed. Pertinent information on growth processes, segregation, and crystal perfection was given.

Preparation of a Graded Energy Gap Alloy - $GaAs_xP_{1-x}$ - See 7076

6965 PREPARATION OF GALLIUM PHOSPHIDE UNDER MODERATE PRESSURES OF PHOSPHORUS VAPOR by J. F. Miller, R. C. Himes and H. L. Goering (Battelle Mem. Inst.); 1960 Fall Mtg. Electrochem. Soc.

Results of experiments on the crystallization of GaP under moderate pressures of phosphorus vapor (1 - 5 atm) were presented. Sound transparent ingots of the compound have been prepared by the Bridgman method (2 - 5 atm) and by the Czochralski technique (1 - 3 atm). Apparatus and procedures used were described in some detail. Exploratory work on other "low-pressure" preparation methods and results of recent experiments were also discussed briefly.

6966 GROWTH OF CESIUM CHLORIDE CRYSTALS FROM SOLUTION AND MELT by P. Avakian and A. Smakula (MIT); J. Appl. Phys., Vol. 31, pp. 1720-1722, Oct. 1960

Large cesium chloride crystals obtained from solution upon addition of urea are described. These crystals show NH_4^+ impurity. Since CsCl undergoes a phase transition between its melting point and room temperature, normal growing methods from the melt could not be used, but a modified ("double-run") Bridgman method yielded good results.

6967 THE STUDY OF PROPERTIES OF SINGLE CdS AND ZnS CRYSTALS FOR USE AS DETECTORS IN CRYSTAL COUNTERS by S. J. Czyzak and H. Payne (Detroit U.); U. S. Gov. Res. Rep., Vol. 34, p. 640 (A), Nov. 18, 1960 PB 149 503

Progress on the growing of single CdS and ZnS crystals is reported. A new technique in powder preparation has produced single crystals of greater purity. By heat treating the grown crystals hexagonal ZnS crystals are produced more easily than the cubic ZnS crystals, the reaction in the latter being sluggish. More accurate data has been obtained by employing new techniques and more sensitive apparatus in the measurement of the electrical properties of CdS and ZnS. Rechecking of data shows the results to be consistent. Electron polarizabilities of free positive ions has been calculated. The work on dislocation studies of ZnS single crystals is being continued.

Preparation of HgSe-HgTe Single Crystals by the Bridgman Method - See 6931

Preparation of Ag_2Se by Fusion Techniques - See 7077

6968 FORMATION OF PHOSPHOR FILMS BY EVAPORATION by L. R. Koller and H. D. Coghill (GE); J. Electrochem. Soc., Vol. 107, pp. 973-976, Dec. 1960

Three processes for making ZnS phosphor films are described. One process for ZnS activated with Cu, Ag, or Mn involves evaporation of powder phosphor onto a room-temperature substrate followed by heat treatment of the film in an H_2S + HCl atmosphere. A process for ZnS:Mn alone involves the single step of evaporating the phosphor onto a substrate held between 250° and 400°C. The third process involves evaporating the phosphor in a single step onto a heated substrate in a uniformly heated enclosure such as the "Hot Wall Bell Jar." A fourth process used for silicate, phosphate, and borate phosphors involves a reaction during the course of evaporation between ZnF_2 and a heated substrate.

6969 PARTICLE GROWTH DURING ZINC SULFIDE PHOSPHOR PREPARATION by A. Kremheller and S. Faria (Gen. Tel. Electronics Labs.); J. Electrochem. Soc., Vol. 107, pp. 891-895, Nov. 1960

The influence of processing conditions, such as time and temperature, and the effect of fluxing agents on the particle size and concomitant properties observed during zinc sulfide phosphor preparation are discussed. The particle size increases exponentially with the reciprocal firing temperature and as the square root of the firing time when phosphors are prepared in open boats; the activation energy and frequency constant depend on the flux employed. A particle size anomaly is observed when zinc sulfide powder containing zinc chloride is processed near 1000°C in sealed quartz vials. This anomaly, which can be ascribed to the Hedvall effect, is accompanied by anomalies in chloride retention and crystal structure.

Growth of Single Crystal Gold Films by Vacuum Deposition - See 7079

6970 MECHANISM OF HYDROGEN REDUCTION OF CUPROUS IODIDE VAPOR by C. R. Morelock and G. W. Sears (GE Res. Lab.); 1960 Fall Mtg. Electrochem. Soc.

A study of the growth of copper whiskers by the hydrogen reduction of cuprous iodide vapor was reported. Alternative mechanisms have been proposed involving a homogeneous vapor phase reduction and a surface catalyzed reduction at the whisker tip. A necessary consequence of the homogeneous vapor phase reaction is the existence of a highly supersaturated copper vapor. It was shown that the vapor was not appreciably supersaturated in copper vapor and that the catalytic site is probably the step associated with an axial screw dislocation in the growing whisker.

6971 THE GROWTH OF SINGLE CRYSTAL IRON FERRITES BY THE CZOCHRALSKI METHOD by F. H. Horn (GE); 1960 Fall Mtg. Electrochem. Soc.

A procedure for growing iron ferrites into single crystals by pulling from the melt was described. An iridium crucible is used which, unlike platinum or platinum-rhodium alloys, does not react with ferrites. The melting and growing is performed in a carbon dioxide atmosphere. Problems attending this method of growth, such as the maintaining of stoichiometry and purity, were discussed.

6972 PREPARATION, GROWTH AND STUDY OF ULTRA FINE FERRITE PARTICLES by W. J. Schuele and V. D. Deetscreek

(Franklin Inst. Labs.); Sixth Conf. Magnetism and Magnetic Materials, Nov. 14-17, 1960, New York, N.Y.

The preparation of ultra fine ferrite particles by a chemical precipitation process below 100°C in an aqueous medium was described. Variations in the initial preparation resulted in materials with different magnetic and physical properties. The resulting materials were grown hydrothermally at moderate temperatures for extended periods of time. Samples were removed at various times during the growing process and their magnetic and physical properties were determined. Coercive forces varied from zero for some truly superparamagnetic samples to ca. 800 oersteds at room temperature for some hydrothermally grown cobalt ferrites. At liquid nitrogen temperature coercive forces to 10,000 oersteds were measured. Crystallite size measurements were made by x-ray line broadening and the particle size was determined by electron microscopy. An apparatus to measure hysteresis loops in pulsed fields was constructed and used for measuring magnetic properties of samples difficult to saturate, i.e., cobalt ferrite samples at -196°C. Good agreement was obtained between pulsed fields and d-c measurements where samples could be measured by both systems.

6973 PERMALLOY FILMS EVAPORATED AT GRAZING INCIDENCE by M. S. Cohen (Lincoln Lab.); Sixth Conf. Magnetism and Magnetic Materials, Nov. 14-17, 1960, New York, N. Y.

The results of an investigation of oblique-incidence evaporated Permalloy films have been reported previously. This investigation showed that "chains" of crystallites form in the film perpendicular to the direction of the vapor beam because of a "self-shadowing" effect. The geometric anisotropy of these chains causes the films to be dichroic with the axis of greatest optical absorption parallel to the chains; the magnetic easy axis is also parallel to the chains because of the geometric anisotropy. Most of these films were made at incidence angles which were less than about 60°. The present study showed new effects for angles greater than 65°. Electron micrographs demonstrate that the crystallites become elongated in the direction of the vapor-beam for such high angles, although the chains are still present. The cause of this elongation is simply a geometric phenomenon. At very high incidence angles the vapor deposits more rapidly on the front face of a crystallite than on its top; the effect becomes more pronounced as the incidence angle increases. For angles greater than about 75° the axis of greatest optical absorption is parallel to the vapor beam, i.e. the crystallite shape anisotropy outweighs the anisotropy due to chains. Anomalous magnetic characteristics are also observed for such films.

6974 PREPARATION AND PROPERTIES OF THIN FERRITE FILMS by E. Banks, N. H. Riederman, H. W. Schleuning and L. M. Silber, (Polytech. Inst. Brooklyn); Sixth Conf. Magnetism and Magnetic Materials, Nov. 14-17, 1960, New York, N.Y.

The preparation of thin films of ferrites, of the order of 1000 Angstroms thick, by vacuum evaporation of the metals and subsequent high temperature oxidation, was described. Films of iron, nickel, cobalt, magnesium, and copper ferrites, mixed ferrites and mixed ferrite-aluminates, as well as yttrium iron garnet, have been prepared. X-ray powder diffractometry indicates that the ferrite films are single phase spinels, while the garnet shows the garnet structure. In many respects, the properties of the films are the same as those of bulk ferrites of similar composition. The resistivity of the films can be controlled by proper oxidizing procedures. X-band magnetic resonance measurements indicate that the saturation magnetizations of the films are comparable to those of the corresponding bulk ferrites, though the films show larger resonance linewidths. It has been possible to prepare magnesium ferrite films with magnetizations from 2200 gauss to less than 500 gauss by proper annealing and quenching. The possible advantages of thin films are that they allow optical studies of the material by transmission, and should permit determination of magnetic exchange constants through observation of spin wave resonance.

6975 MAGNETIC THIN FILMS BY IMPACT EVAPORATION by E. Kay (IBM); Sixth Conf. Magnetism and Magnetic Materials, Nov. 14-17, 1960, New York, N.Y.

The use of impact evaporation for the preparation of magnetic thin films was discussed. Data which indicates that a controlled glow discharge system can be compatible with contemporary demands in thin film technology was presented. Reproducible thin films of iron whose structural and magnetic properties depend on the location of the substrate within the discharge have been prepared. Very uniform iron films 1000 A thick having coercivities up to 250 oersted and Br/Bs ratio very nearly equal to unity have been prepared with unusually high remanence values. These results differ considerably from iron films of equal thickness prepared by thermal evaporation under high vacuum conditions at similar substrate temperatures. Films prepared by impact evaporation showed no evidence of either preferred crystallographic orientation or preferred direction of magnetization. In sharp contrast to findings by several authors, ferromagnetic nickel films can be deposited by impact evaporation. Results to date indicate that transport of alloys by impact evaporation holds considerable promise.

6976 FERRITE THIN FILMS by H. P. Lemaire and W. J. Croft (RCA); Sixth Conf. Magnetism and Magnetic Materials, Nov. 14-17, 1960, New York, N.Y.

The preparation of thin films of ferrites of various compositions was described. Two methods, both involving a spray technique using hot suspensions of hydroxides directed onto a heated substrate, have been used. The ferrite films are formed essentially through a co-precipitation mechanism. The films have been identified by x-ray diffraction as having a cubic spinel structure. Various compositions have been attained — magnetite, nickel ferrite, a magnetite-zinc ferrite series, and other mixed ferrites. Hysteresis loops for the films were obtained on a 1000 cycle loop tracer and indicate a high squareness ratio. The films as prepared are magnetically isotropic. Film thicknesses can be varied from a few hundred angstroms to about 1 micron. Thicknesses of some films were measured by interferometry and were compared to relative thicknesses estimated using a spectrophotometric technique. Coercive force measurements were related to thickness in a set of nickel ferrite films and to composition variations in a series of films of differing composition in magnetite-zinc ferrite series.

Electrodeposition of Thin Magnetic Films in a Magnetic Field - See 7039

6977 ON THE INCORPORATION OF NEODYMIUM IN MIXED YTTRIUM-NEODYMIUM-IRON GARNETS by G. Goldring, M. Schieber and Z. Vager (Weizmann Inst. Sci.); J. Appl. Phys. Vol. 31, pp. 2057-2059, Nov. 1960

The preparation and saturation magnetization of yttrium-iron

garnets containing various amounts of neodymium is described. The amount of Nd which can be incorporated in the garnet structure has been determined crystallographically and magnetically. The chemical analysis of the Nd/Y ratio was carried out by counting the characteristic x-rays of Nd produced by proton bombardment in a Van de Graaff accelerator. A compound with a formula of $YNd_2Fe_5O_{12}$ was found to be the richest iron garnet containing Nd; it has a saturation magnetization, at room temperature, of 4.25 ± 0.13 Bohr magnetons per formula weight compared to that of 3.55 ± 0.13 of $Y_3Fe_5O_{12}$ or $Sm_3Fe_5O_{12}$.

6978 FERROELECTRIC FILMS by R. A. Fotland (Horizons); U.S. Gov. Res. Rep., Vol. 34, p. 640 (A), Nov. 18, 1960 PB 148 817

A procedure which has been evolved for preparing uniform 20 micron thick films of ferroelectric sodium niobate and barium-lead titanate ceramic materials is described. The procedure involves first grinding the materials to colloid size. The fine particles are then dispersed in water using a colloid mill and a deflocculent. Films are then formed on a glass plate, using an organic film as an interlayer, by pouring the suspension on the plate and allowing the water to evaporate. Separation of the film from the glass plate is accomplished by rapidly volatilizing the interlayer at a high temperature. Strict attention to details of cleanliness must be observed in order to prevent the formation of pinholes in the film. Vitrification of the films is performed with the films resting on a fine particle size, partially sintered zirconia layer.

CRYSTAL SURFACES AND CRYSTAL PROCESSING

6979 SEPARATION OF THE DEFECT CONCENTRATION AND DIFFUSION COEFFICIENT IN DIFFUSION-LIMITED SCALING REACTIONS by A. J. Rosenberg (Lincoln Lab.); J. Electrochem. Soc., Vol. 107, pp. 795-799, Oct. 1960

In diffusion-limited scaling reactions the rate constant is proportional to the quantity DC_0, where D and C_0 are the diffusion coefficient and the solubility of the defect whose motion through the growing scale is essential to continued reaction. In order to separate D and C_0, recourse is usually made to an independent measurement of one or the other, which is a difficult and frequently unreliable procedure. A new technique which permits the accurate and simultaneous determination of D and C_0 from reaction rates alone is proposed. The method is based on the controlled interruption of a scaling reaction and possesses a rigorous internal check. It is applicable in principle to any such reaction, and the necessary mathematical formulation is presented in a convenient analytical form. Conventional experimental techniques can be used when $C_0 \gg 10^{17} cm^{-3}$. The treatment is illustrated for the oxidation of InSb.

6980 QUANTITATIVE CONSIDERATIONS CONCERNING CATALYSIS AT A SEMICONDUCTOR SURFACE by C. G. B. Garrett (Bell Labs.); J. Chem. Phys., Vol. 33, pp. 966-979, Oct. 1960

The theory of charge-transfer catalysis, originally proposed by Wagner and Hauffe, is set up in quantitative form. The objects of the treatment are to write down quantitative expressions for the absolute reaction rate, to show the consequences of the Wagner-Hauffe mechanism insofar as they concern the adsorption properties of the individual reacting materials, and to outline an experimental program for determining, by means of experiments on the semiconductor, alone and in association with each of the reacting substances in turn, the values prevailing in a practical case for the various parameters occurring in the theory.

6981 ELECTRON MICROSCOPE STUDIES OF COLLOIDS IN KCl by R. E. Simon and R. L. Sproull (Cornell U.); J. Appl. Phys., Vol. 31, pp. 2224-2225, Dec. 1960

Electron microscope studies of surfaces of potassium chloride crystals containing excess potassium are reported. The crystals were cleaved in a vacuum and the surfaces were replicated in the same vacuum. Large potassium colloids were observed with distinctive shapes and orientations determined by the host lattice.

Semiconductor Slicer - See 7217

Dissolution of Quartz by Ga - See 6928

6982 A SIMPLE METHOD FOR MONITORING THE CHEMICAL ETCHING RATE OF GERMANIUM AND SILICON by D. R. Turner (Bell Labs.); 1960 Fall Mtg. Electrochem. Soc.

Use of the excess holes and electrons produced at the surface of germanium or silicon during chemical etching to monitor the dissolution rate was discussed. When an n-type semiconductor electrode is made the cathode of an electrolytic cell in the etching solution, the saturation current density is proportional to the rate of etching the semiconductor. The technique also provides a convenient means of determining the fluoride ion concentration in HNO_3-HF mixtures.

6983 CHARACTERISTICS OF THE {111} SURFACES OF THE III-V INTERMETALLIC COMPOUNDS, III. EFFECT OF COLD WORK ON DISSOLUTION by H. C. Gatos and M. C. Lavine, (Lincoln Lab.); 1960 Fall Mtg. Electrochem. Soc.

The dissolution rate of the {111} surfaces of the III-V intermetallic compounds increases sharply as a result of surface damage introduced by abrasion. This increase in rate can be employed for determining the depth of surface damage. In the present case the observed increase in rate is not due to the higher reactivity of the cold worked surface since the dissolution processes studied are under diffusion control. The experimental results are interpreted on the basis of the surface roughness as affected by the presence of cold work.

6984 ORIENTATION-DEPENDENT DISSOLUTION OF GERMANIUM by F. C. Frank (U. Bristol); J. Appl. Phys., Vol. 31, pp. 1996-1999, Nov. 1960

The dissolution of single crystals of undoped germanium in Superoxol etchant is shown to be very closely completely orientation-dependent by the applicability of recent theorems on crystal dissolution shapes. The results of the theory are outlined and the method of application is described in detail.

6985 CHEMICAL ETCHING OF GERMANIUM, I. COMPARISON OF THE ETCHING OF GERMANIUM AND SILICON IN SOLUTIONS OF HF-HNO_3 by B. Schwartz and H. Robbins

(Hughes Aircraft); 1960 Fall Mtg. Electrochem. Soc.

The kinetics of the dissolution of germanium and silicon in solutions of nitric acid and hydrofluoric acid was discussed. The etching of germanium is in general more difficult than that of silicon. The etch rates of the latter are reproducible and constant in time, whereas the etch rates of germanium are extremely erratic. In addition, the etch rates of silicon are independent of crystallographic orientation, whereas those of germanium are strongly affected by the crystal orientation over large ranges of composition of etchant. There are also significant differences between the two elements in the temperature dependence of the etch rates.

6986 CHEMICAL ETCHING OF GERMANIUM, II. THE SYSTEM HF, H_2O_2, H_2O by H. Robbins and B. Schwartz (Hughes Aircraft); 1960 Fall Mtg. Electrochem. Soc.

The kinetics of the reaction of germanium with solutions of HF and H_2O_2 as a function of the composition and temperature of the etchant was discussed. The effect of conductivity type and surface orientation on the kinetics has been studied. At low weight ratios of HF to H_2O_2 the etch rates are linearly dependent on the HF concentration, and at high ratios the rates are linearly dependent on the H_2O_2 concentration. The activation energy goes through a maximum at a composition of about 1 H_2O_2 to 1 HF.

6987 ON THE MECHANISM OF CHEMICALLY ETCHING GERMANIUM AND SILICON by D. R. Turner (Bell Labs.); J. Electrochem. Soc., Vol. 107, pp. 810-816, Oct. 1960

The electrode potential of germanium or silicon in a chemical etching solution is a function of solution pH, rate of etching, physical condition of the surface, conductivity type, and resistivity. The results suggest that excess holes and electrons are produced at the surface of the semiconductor during chemical etching. Holes are injected at cathode sites, but only a portion of these holes are consumed at anode sites since the anode reaction involves current multiplication.

6988 STEADY-STATE LIQUID-SOLID INTERFACE REACTIONS AS APPLIED TO SILICON ETCHING BY HNO_3-HF-H_2O by J. J. Grossman (Hughes Aircraft); 1960 Fall Mtg. Electrochem. Soc.

Phenomenological equations for steady-state etching of silicon surfaces by diffusion across a bounding liquid film were written using the known homogeneous phase reaction mechanism of HNO_3 with HNO_2, NO_2, and NO. Minimal sets of measurements required to define, unambiguously, the solid-liquid interface reaction were discussed including contributions from semiconductor properties and oxide films. Finally it was shown that activation energies measured in terms of bulk solution concentrations can be misleading.

6989 THE ETCHING OF SILICON CARBIDE by J. W. Faust, Jr. (Westinghouse); Proc. Conf. Silicon Carbide, Pergamon Press, 1960, pp. 403-419

Various reasons for etching are reviewed and a brief discussion of the various physical and chemical processes used for etching SiC are presented. Experimental evidence showing that the action of boiling phosphoric acid on SiC produces a layer of silicon oxide on the surface is given. The action of various molten-salt etches on SiC is described. Sodium peroxide causes etching at 350°C. Dislocations are revealed by these etchants for both hexagonal and cubic SiC, and the shapes of the pits are related to edge and screw dislocations. Dislocation densities along intersecting lineage lines indicate a one-to-one correspondence between untruncated pits and dislocations.

6990 PHOSPHORIC ACID AND FUSED SALT ETCHING OF SILICON CARBIDE by R. C. Ellis, Jr. (Raytheon); Proc. Conf. Silicon Carbide, Pergamon Press, 1960, pp. 420-422

Aqueous phosphoric acid solutions of a density of 1.75 slowly decompose silicon carbide at 215°C to form SiO_2, CO_2, H_2, and CH_4. The results of etching SiC, Si, C, B, and Ge in a variety of fused salts are discussed.

Characteristic Etch Pits of Line and Point Defects — Dislocation Pits and Saucers - See 6935

Dislocation Etch Pits in Te - See 6936

Dislocation-Etch Pit Relation in SiC - See 6937

6991 MECHANISMS OF ELECTROLESS DEPOSITION OF METALS ON SILICON by S. L. Matlow (Hoffman Electronics); 1960 Fall Mtg. Electrochem. Soc.

Studies on the electroless deposition of metals onto silicon which indicate that there are at least four independent mechanisms by which the deposition can occur were discussed. These are (a) displacement plating, (b) displacement-replacement plating, (c) autocatalytic, homogeneous, and (d) autocatalytic-heterogeneous. These mechanisms can be distinguished by the apparent rate laws which are obeyed and by the nature of the metallic deposit. Examples of each case were given. Except for case (c) details of the mechanisms and the experimental data on which they are based were presented.

6992 'ELECTROLESS' DEPOSITION OF GOLD FROM AQUEOUS SOLUTION ON BASE METALS OF NICKEL, IRON-NICKEL-COBALT ALLOYS, AND GOLD by R. F. Walton (Texas Instr.); 1960 Fall Mtg. Electrochem. Soc.

A new solution formulation for the chemical (electroless) deposition of gold was proposed. The main constituents of this solution are potassium gold cynanide, citric acid or tartaric acid, tungstic acid, and N, N-diethylglycine sodium salt. Optimum concentrations of these constituents were determined by a statistical evaluation of the solution at four concentration levels. Investigation of such variables as immersion time, solution temperature, and pH, which affect the chemical deposition of gold from solution, enabled determination of the optimum operating conditions.

Study of the Initial Growth of Plating in Thin Electrodeposited Films of Fe-Ni Alloys - See 7078

6993 INFLUENCE OF THIOUREA ON THE DEPOSITION OF IRON-NICKEL FILMS by R. D. DeMars (IBM); 1960 Fall Mtg. Electrochem. Soc.

A polarographic investigation of the deposition reactions of iron and nickel in solutions containing the metal ion and potassium chloride and the metal ion, potassium chloride and thiourea was reported. Analysis of the polarographic waves using Koutecky's method yielded values for the kinetic param-

eters, an_a and $k^o_{f,h}$, for the reduction reactions. The effect of temperature and thiourea concentration on these parameters was studied. These results can lead to predictions about the composition of films plated from similar solutions. The predictions have been substantiated by a series of plated iron-nickel films.

6994 EFFECT OF PLATING PARAMETERS ON THE STRUCTURE AND MAGNETIC PROPERTIES OF Co AND Co-Ni ALLOYS by I. M. Croll and H. F. Quinn (IBM); 1960 Fall Mtg. Electrochem. Soc.

The preparation of electrodeposited Co and Co-Ni alloys under a wide range of plating conditions in an attempt to correlate specific bath conditions with grain orientation, grain size, and microstrain in the deposits was described. Striking changes in the texture of deposits prepared from simple baths have been found to occur in a critical pH region (3.5 - 4.0). Extreme preferred orientation has been obtained in deposits plated under combination a-c and d-c conditions. Specific ferromagnetic properties of the deposits have been correlated with their structure.

6995 ELECTRODEPOSITION OF NICKEL-COBALT ALLOYS FROM THE PYROPHOSPHATE BATH by V. Sree and T. L. Rama Char (Indian Inst. Sci.); 1960 Fall Mtg. Electrochem. Soc.

The codeposition of nickel with cobalt from a pyrophosphate bath was described. Detailed studies on alloy composition, cathode efficiency, and potential have led to the optimum conditions for obtaining satisfactory alloy plates with 10 - 91% nickel. The efficiency of cast alloy anodes is quite high. X-ray patterns of the deposits show the existence of fcc and hexagonal structures. The deposit composition can be altered appreciably only by varying the metal content of the bath.

6996 ELECTRODEPOSITION OF COBALT-MOLYBDENUM ALLOYS by A. Krohn and T. M. Brown (U. of Toledo); 1960 Fall Mtg. Electrochem. Soc.

An investigation which shows that cobalt-molybdenum alloys can be deposited from pyrophosphate solutions was reported. The addition of hydrazine sulfate to the plating bath prevents anodic oxidation of Co (II) to Co (III). It also causes an increase in the cathode current efficiency and an increase in the molybdenum content of the deposits. Efficiency is further increased by wiping the cathode during plating.

Fused Contacts to SiC - See 7026

EFFECTS OF RADIATION

6997 DYNAMICS OF RADIATION DAMAGE by J. B. Gibson, A. N. Goland, M. Milgram and G. H. Vineyard (Brookhaven Natl. Lab.); Phys. Rev., Vol. 120, pp. 1229-1253, Nov. 15, 1960

Radiation damage events at low and moderate energies (up to 400 ev) are studied by machine calculations in a model representing copper. Orbits of knock-on atoms are found and the resulting damaged configurations are observed to consist of interstitials and vacancies. Thresholds for producing permanently displaced atoms (i.e., interstitials) are about 25 ev in the <100> direction, 25 to 30 ev in the <110> direction, and around 85 ev in the <111> direction. Collision chains in the <100> and <110> directions are prominent; at low energies the chains focus; at higher energies they defocus. Above threshold, the chains transport matter, as well as energy, and produce an interstitial at a distance. The range of <110> chains has been studied in detail. Localized vibrational modes associated with interstitials agitations qualitatively like thermal spikes, ring annealing processes, and a higher energy process somewhat like a displacement spike have been observed. Replacements have been found to be very numerous. The configurations of various static defect have also been studied in this mode. The interstitial is found to reside in a "split" configuration, sharing a lattice site with another atom. The crowdion is found not to be stable, and Frenkel pairs are stable only beyond minimum separations, which are found to be very much dependent on orientation.

Production of Color Centers in Alkaline Earth Fluorides by X-Rays and Electron Bombardment - See 7059 and 7060

SOLID STATE PHYSICS

GENERAL

6998 INVESTIGATION OF PHYSICAL PROPERTIES OF SEMICONDUCTORS by M. E. Caspari (Pennsylvania U.); U.S. Gov. Res. Rep., Vol. 34, p. 642 (A), Nov. 18, 1960 PB 161 903

An investigation of materials which may have interesting semiconducting properties at high temperatures is reported. In particular solid solutions and compounds of metals and tungsten trioxide have been investigated. It was found that lead forms solid solutions with tungsten trioxide over a wide composition range but has metallic electrical properties. Copper tungstate and a compound containing a small amount of silver in tungsten trioxide were found to have interesting semiconducting properties. Aluminum boride was found to be a semiconductor with a large activation energy. Coupled with the preparation, chemical analysis and determination of electrical properties of these compounds, a crystal structure determination of tri-clinic copper tungstate was initiated. A study of the Faraday effect at microwave frequencies on n- and p-type germanium and silicon was carried out over a wide temperature range as a function of the static magnetic field, leading to information regarding the effective masses, life-times and mobilities of the charge carriers. Optical investigations of iodine single crystals showed the latter to be a semiconductor with a large activation energy. A large electrostrictive effect was measured in rutile single crystals and surface rather than volume imperfections were shown to have an effect on the breakdown strength in Harshaw KCl crystals.

6999 DIRECT MEASUREMENTS OF THE SURFACE ENERGIES OF CRYSTALS by J. J. Gilman (GE); J. Appl. Phys., Vol. 31, pp. 2208-2218, Dec. 1960

Measurements of the surface energies of several simple crystals at $-196^{\circ}C$ obtained by means of quantitative cleavage experiments are presented. The crystals and their cleavage planes are: LiF (100), MgO (100), CaF_2 (111), BaF_2 (111), $CaCO_3(10\bar{1}0)$, Si (111), and Zn (0001). Measured values of their respective surface energies (ergs/cm^2) are: 340, 1200, 450, 280, 230, 1240, and 105. The measured values for LiF and MgO are in good agreement with simple ionic lattice theory. Values for the other crystals seem consistent with their binding energies. Under irreversible conditions an effective surface energy is measured. This quantity increases rapidly with increasing temperature for the metallic crystals, Zn and Fe (3% Si). The increase correlates with increasing plastic flow in these crystals. In contrast, the effective surface energy of LiF and MgO is only moderately dependent on temperature. A small amount of cadmium (0.1 at. %) markedly increases the cleavage surface energy of zinc.

7000 FILLED AND EMPTY DANGLING BONDS IN III-V COMPOUNDS by D. B. Holt (U. Witwatersrand, So. Africa); J. Appl. Phys., Vol. 31, pp. 2231-2232, Dec. 1960

It is pointed out that the model of dangling bonds from the {111} and $\{\bar{1}11\}$ surfaces of III-V compounds proposed by Gatos, Moody, and Lavine is open to serious objection. The idea of resonance is introduced in order to develop a model which is not subject to the same difficulties. Certain implications of this model for dislocation theory are discussed.

7001 D BANDS IN CUBIC LATTICES. II by J. Callaway (U. Calif.); Phys. Rev., Vol. 120, pp. 731-740, Nov. 1, 1960

The results of a previous, perturbation theoretic treatment of d bands in the body-centered cubic lattice are extended in several respects: The methods of the previous calculation are applied to determine energy levels at the points Γ and X in the Brillouin zone of the face-centered cubic lattice. As before, the crystal potential is that of a lattice of point charges, screened by a uniform distribution of electrons. The perturbation expansion of the wave function of a d electron is developed for the body-centered cubic lattice. Calculations are reported for two states near the top and bottom of the d band, including terms of first order in the potential. These functions have the characteristic property that the wave function of a state near the top of the d band is more compact than that belonging to a state near the bottom. The energies of four states for the body-centered lattice are computed as a function of the binding parameter Za by a more accurate method than that employed in the previous work, making possible an estimation of the accuracy of perturbation theory and the dependence of bandwidth on binding parameter. The role of crystal field effects in the tight-binding limit is discussed, and the circumstances under which the d band may split into sub-bands based on functions of different cubic symmetries are determined. Estimation of the value of the binding parameter for which such separation occurs strongly suggests that this split does not occur for the actual transition metals. Finally, the effects of spin-orbit coupling on the band structure are studied in the tight-binding approximation. A formulation of $\vec{k} \cdot \vec{p}$ perturbation theory for d bands is given.

7002 SOME COMMENTS ON THE ELECTRONIC STRUCTURE OF GROUP IV AND III-V SEMICONDUCTORS by S. L. Mattlow (Hoffman Electronics); 1960 Fall Mtg. Electrochem. Soc.

The evidence for the structure of the valence band of the elements and intermetallics which crystallize in the diamond-cubic, zinc blende, or wurtzite structures being the $\sigma(sp^3)$ band is so extensive that the model is almost universally accepted. However, except for the C and BN systems it is not clear whether the conduction band is the $\sigma^*(sp^3)$ band or the π (d) band. Chemical crystallographic, spectroscopic, and electrical data which indicate that π (d) model is the more accurate are presented.

Variation of Energy Gap with Size of the Conjugated System in Organic Molecular Solids - See 7029

Energy Band Gap of Zn_3As_2 and Cd_3As_2 - See 7027

Energy Gap Width of AIB and I - See 6998

7003 VALLEY-ORBIT SPLITTING OF ANTIMONY IN GERMANIUM by H. Fritzsche (U. of Chicago); Phys. Rev., Vol. 120, pp. 1120-1124, Nov. 15, 1960

Measurements of the change of electrical conductivity under uniaxial tension and compression over the range $4^{\circ}K$ to $7^{\circ}K$ for single-crystal specimens of germanium doped with antimony are reported. The stress was varied from 1×10^7 to 5×10^8 dynes/cm^2. On the basis of Price's calculation of the effect of shear on the Kohn-Luttinger donor level structure, an expression for the piezoresistance which includes terms of high order in the strain has been derived. It is shown that for a finite valley-orbit splitting, i.e., a finite energy separation between the onefold and the threefold 1s-like donor states, shear increases the total electron concentration in the conduction band. For uniaxial stresses along the [110] direction this increase in electron concentration is an even function of stress and can, therefore, be determined from a linear combination of the piezoresistance measured under tension and compression. A comparison of the theoretical expression with the experimentally obtained change in electron concentration yields for antimony in germanium, a valley-orbit splitting of 0.57 ± 0.03 milli-electron volt.

7004 STUDY OF THE SURFACE STATES OF DIAMOND AND GRAPHITE BY A SIMPLE MO-LCAO METHOD by J. Koutecky and M. Tomasek (Czech. Acad. of Sci.); Phys. Rev., Vol. 120, pp. 1212-1218, Nov. 15, 1960

The surface states of diamond and two-dimensional graphite are investigated on the assumption that the delimitation of the crystal causes no perturbation within the elementary cells of the finite crystal. In both cases a plane perpendicular to the bond between a selected pair of carbon atoms is taken as the delimiting plane. The molecular orbitals are assumed in the form of a linear combination of sp^3 or sp^2 hybrids. In the case of graphite, molecular orbitals that are linear combinations of $2p_z$ orbitals, whose interaction with sp^2 hybrids is neglected, are further considered. It appears that in the case of diamond there exists a band of energies pertaining to Shockley surface states in the gap between the valence and conductivity bands. The number of atoms in this band equals the number of atoms

in the surface. From a discussion of the pertinent wave functions, it follows that these states are an expression of unsaturated bonds of the surface carbon atoms. The electron density on the hybrids projecting from the surface is essentially greater than the density on the other hybrids of the surface atoms. Further bands of surface states exist in the region of energies allowed for the volume valence and the conductivity states. In graphite, a quite analogous behavior is shown by those surface states whose wave functions are linear combinations of sp^2 orbitals. Surface states whose wave functions are linear combinations of p_z orbitals are a manifestation of unsaturated double bonds of surface atoms having only two neighbors. The analogy between these Shockley states and the nonbonding states of odd alternant aromatic hydrocarbons is pointed out.

7005 DISTRIBUTION OF ELECTRONS IN CADMIUM SULFIDE CRYSTALS by G. P. Mohanty and L. V. Azároff (Illinois Inst. Tech.); Phys. Rev., Vol. 120, pp. 1224-1225, Nov. 15, 1960

Very accurate x-ray diffraction intensities from a "pure" CdS crystal and one doped with chlorine are used to calculate electron density maps of their crystal structures projected along the c axis. To eliminate series termination errors, a difference map obtained by subtracting the electron density of the "pure" crystal from that of the doped crystal has also been prepared. According to this map, the electron distribution in the doped crystal is smeared out in the vicinity of the atom centers and an excess of electrons occurs in interstitial sites. This is contrary to the recently reported findings of Shuvalov who observed the formation of "electron bridges" along lines joining adjacent atoms. It is concluded that these observations are consistent with a partial disorder introduced in the doped crystal by the substitution of chlorine into sites normally occupied by sulfur atoms. Observed variations between corresponding x-ray intensities of the doped and undoped crystal can be similarly explained by changes in the extinction effect due to this disorder.

Electronic Structure of IV and III-V Semiconductors - See 7002

7006 "IONIC RADII," SPIN-ORBIT COUPLING AND THE GEOMETRICAL STABILITY OF INORGANIC COMPLEXES by A. D. Liehr (Bell Labs.); Bell Sys. Tech. J., Vol. 39, pp. 1617-1626, Nov. 1960

The van Santen and van Wieringen theory of "ionic radii" is briefly reviewed and extended to include spin-orbit influences. It is noted that, although for the most part spin-orbit forces have little effect upon stereo-chemical predictions made for the first transition series, noteworthy exceptions to this rule occur for octahedral complexes of Co^{++} and tetrahedral complexes of Ni^{++} and Cu^{++}. Indeed, it is found that spin-orbit coercions render the ground states of these molecules Jahn-Teller resistant. Diagrams are displayed and tables are presented to illustrate the variation of ionic radii with atomic number for the second and third transition series. Paths for future theoretical research are indicated and a closer theoretical-experimental alliance is urged.

Contribution of Free Carriers to the Polarizability of Si and Ge - See 7010

DIELECTRIC PROPERTIES

Dielectric Properties of Organic Polymer Films - See 7013

7007 ELECTRO-OPTIC KERR EFFECT AND POLARIZATION REVERSAL IN DEUTERIUM-DOPED ROCHELLE SALT by H. H. Wieder and D. A. Collins (U.S. Naval Ord. Lab.); Phys. Rev., Vol. 120, pp. 725-730, Nov. 1, 1960

An investigation of the polarization reversal as a function of nucleation and growth of domains in ferroelectric deuterium-doped Rochelle salt by means of the electro-optic Kerr effect is discussed. The results indicate that a phenomenological model based on statistical nucleation of domains in a plane including the ferroelectric axis, followed by a two-dimensional sidewise expansion of the domains, will adequately account for the experimental observations for fields larger than 50 v/cm. For lower fields, the process is controlled primarily by the nucleation of new domains due to localized stresses which hinder the displacement of domain walls.

Effect of Random Inhomogeneities on Piezoelectricity - See 7019

CARRIER PROPERTIES

7008 A DOMAIN THEORY OF CARRIER BEHAVIOR IN MOLECULAR SOLIDS by H. A. Pohl, (Princeton U.); Proc. Princeton U. Conf. Semiconduction Molecular Solids, pp. 9-23, 1960

In examining the conductivity and Hall coefficients of a series of variously heat-treated and nickel-doped pyro-polymers prepared from variously loaded ion exchange resins by pyrolysis, it was observed that the Hall mobility increases with impurity addition in these condensed molecular solids. Further analysis on a two-carrier model showed two prominent features: (1) both hole- and electron-type carriers decreased in concentration as impurity was added, and (2) high doping levels led to predominantly hole-type carriers alone being present. A theoretical interpretation of the conduction in such inhomogeneous molecular solids is suggested. It predicts a negative exponential dependence of the product of hole and electron carrier concentration upon the impurity concentration, and dependence of the product upon the sixth power of the Hall mobility. Both expectations appear to be borne out by data in this system. The interpretation suggested is based upon a 'domain' hypothesis for the carriers, the effective domain sizes being dependent upon the nature of the material between regions of high conduction. In the case of the pyro-polymer molecular solids, the latter regions are considered to be the condensed aromatic layer aggregates. An alternate interpretation based upon a barrier layer model is also considered.

Carrier Concentrations in Zn_3As_2 and Cd_3As_2 - See 7027

7009 DIRECT RECOMBINATION IN GaAs by S. Mayburg (Gen'l Tel. and Electronics Labs.); 1960 Fall Mtg. Electrochem. Soc.

Experimental evidence for direct recombination in GaAs obtained by showing a decrease in lifetime with injection level in contrast to indirect semiconductors like Ge where lifetime

stays constant or increases with injection level was presented. Simulated emissions of electrons from the conduction to the valence band with photons of energy of the band gap have also been observed. Some consequences of direct recombination on GaAs device characteristics were discussed.

Recombination at Dislocations in Plastically Deformed Te - See 6936

Relation of Traps to Noise in CdS and ZnO - See 7022

7010 THE TEMPERATURE DEPENDENCE OF THE POLARIZABILITY OF THE FREE CARRIERS IN GERMANIUM AND SILICON by M. Cardona, W. Paul and H. Brooks (Harvard U.); Helv. Phys. Acta., Vol. 33, No. 5, pp. 329-346, 1960

Measurements of the reflectivity of n- and p-type Ge and Si containing more than 10^{18} carriers/cc at 297°K and 90°K from 2 to 20 μ are reported. The contribution of the free carriers to the total electric polarizability has been determined from the reflectivity and an average effective mass for the carriers has been deduced. An increase in electron mass with both carrier concentration and temperature was found in both n-type Ge and Si. If both effects are assumed to originate from the nonparabolic character of the conduction band, then the effect of carrier concentration is too large compared with the effect of temperature, and both effects are too large to be compatible with estimates of the band gap at the zone boundary. No definite conclusions can be drawn about p-type Ge owing to transitions between branches of the degenerate valence band. For p-type Si the effective mass increases with temperature.

Measurement of Drift Mobility Using the Field-Effect Modulation of Photoconductors - See 7070

7011 HOLE MOBILITY AND CRYSTAL SIZE IN LEAD SULFIDE PHOTOCONDUCTIVE FILMS by H. E. Spencer and J. V. Morgan (Eastman Kodak); J. Appl. Phys., Vol. 31, pp. 2024-2027, Nov. 1960

A correlation between the size of the microcrystals in photoconductive lead sulfide films and hole mobility calculated from Hall, signal, and noise measurements is reported. Films composed of larger microcrystals exhibit larger mobilities. Field-effect mobility as a function of frequency has also been measured. The data indicate that the surfaces as well as the bulk of the films are p type. The lead sulfide-air interface of the films changes from exhaustion type to enhancement type as the film thickness increases.

7012 MOBILITY DOPING OF SEMICONDUCTING COMPOUNDS by A. J. Cornish (Westinghouse); 1960 Fall Mtg. Electrochem. Soc.

Doping of semiconducting compounds is normally accomplished by adjusting carrier densities. In many applications it appears advantageous to be able to control the mobilities of the carriers as well as the densities. Mobility doping, the adjustment of the mobilities of the carriers, was explained and illustrated.

Carrier Mobilities in Zn_3As_2 and Cd_3As_2 - See 7027

7013 ELECTRIC CHARGE TRANSPORT THROUGH ORGANIC POLYMER FILMS by J. J. Spokas (RCA); Proc. Princeton U. Conf. Semiconduction Molecular Solids, pp. 69-84, 1960

Polystyrene films produced by the glow discharge polymerization of styrene vapor whose thicknesses ranged from 0.1 to 4 microns have been studied with respect to their electrical resistance and capacitance at field intensities as great as 5×10^6 volts/cm. A feature of the method of measurement is the charging of one surface of the sample films with an electron beam, thereby avoiding one metal or semiconductor contact and largely circumventing the problem of small imperfections and weak spots in the films. At applied fields below 10^5 volts/cm the electrical resistivity seems to approach the highest values which have been reported; however, at fields near 4×10^6 volts/cm appreciable electric currents occur which correspond to an RC constant of ~1 second and which increase sharply with further increase of the applied potential. The static dielectric constant is independent of field to within 2-3 per cent. Significant photocurrents which are excited by visible light are observed in the discharge polymerized styrene films at high electric fields; the photoconductor gain is $\sim 10^{-3}$ for blue light. Electron beam induced currents indicate that the high field conductivity is mainly due to electrons.

7014 THEORY OF IMPURITY RESISTANCE IN METALS by J. S. Langer (Carnegie Inst. Tech.); Phys. Rev., Vol. 120, pp. 714-725, Nov. 1, 1960

A many-body technique is developed for the calculation of the d-c resistivity of a Fermi fluid in the presence of a few, randomly scattered, fixed, impurities. A certain class of graphs yields an expression for the conductivity which is similar in form to the standard classical transport coefficient; but the decay time is determined by the scattering of single-particle-like excitations at the Fermi surface by screened impurities. A propagator method similar to that used in field theory is employed throughout the paper, and the perturbation-theoretic interpretation of this method is examined in some detail.

7015 IMPURITY CONDUCTION AT LOW CONCENTRATIONS by A. Miller and E. Abrahams (Rutgers U.); Phys. Rev., Vol. 120, pp. 745-755, Nov. 1, 1960

A calculation of the conductivity of an n-type semiconductor in the region of low-temperature T and low impurity concentration n_D is presented. The model is that of phonon-induced electron hopping from donor site to donor site where a fraction K of the sites is vacant due to compensation. To the first order in the elec tric field, the solution to the steady-state and current equations is shown to be equivalent to the solution of a linear resistance network. The network resistance is evaluated and the result shows that the T dependence of the resistivity is $\rho \propto \exp(\epsilon_3/kT)$. For small K, $\epsilon_3 = (e^2/k_0)(4\pi n_D/3)^{\frac{1}{2}}(1 - 1.35\,K^{\frac{1}{2}})$, where k_0 is the dielectric constant. At higher K, ϵ_3 and ρ attain a minimum near K = 0.5. When the dependence on n_D is extracted, the agreement of the latter and of ϵ_3 with experiment is satisfactory. The magnitude of ρ is in fair agreement with experiment. The influence of excited donor states on ρ is discussed.

Piezoresistance of Antimony-Doped Ge - See 7003

Resistivity of Granular SiC - See 6948

7016 ELECTRICAL RESISTIVITY OF THE HEAVY RARE-EARTH METALS by R. V. Colvin, S. Legvold and F. H. Spedding (Iowa State U.); Phys. Rev., Vol. 120, pp. 741-745, Nov. 1, 1960

Measurements of the electrical resistivities of polycrystalline Gd, Tb, Dy, Ho, Er, Tm, and Lu between 1.3°K and room temperature are reported. The slope of the resistivity curve for Gd changes near the Curie point. The curve for Tb is very much like that for Gd but there is some evidence that two ordering temperatures exist for this metal. Dy, Ho, and Tm all show peaks in resistivity near their Néel points, while Er shows only a change in slope at its Néel point. The change from ferromagnetism to antiferromagnetism in Dy is seen as a sharp rise in the resistivity.

Resistivity of Ag_2Se - See 7077

7017 ION SIZE EFFECT AND MECHANISM OF ELECTROLYTIC RECTIFICATION by P. F. Schmidt, F. Huber and R. F. Schwarz (Philco); J. Phys. Chem. Solids, Vol. 15, pp. 270-290, Oct. 1960

Previous theories of electrolytic rectification are reviewed and it is shown that none of them is able to account for all of the phenomena observed. Experimental results are then presented which show that both the magnitude of the cathodic current at a given applied field, and the activation energies for cathodic current flow are controlled by the size of the cation in solution, and by specific adsorption under applied cathodic bias. The existence of a surface barrier, height about 1 volt, thickness about 250 A, has been proven. The proposed band scheme for anodic oxide layers thus includes a steep surface barrier at the outer oxide interface, an ohmic contact at the valve metal/oxide interface, and traps in the oxide.

7018 RECTIFICATION PHENOMENA IN POLYCRYSTALLINE PHTHALOCYANINES by F. A. Haak and J. P. Nolta, (Hughes); Proc. Princeton U. Conf. Semiconduction Molecular Solids, pp. 25-35, 1960

Observations of rectification in compressed powders of metal-free copper, nickel, and molybdenum phthalocyanines when thin slices of these materials were sandwiched between different metals are reported. The presence of a small amount of a liquid polar impurity was shown to be essential for rectification, suggesting the possibility of electrolytic formation of a rectifying film or an ionic space charge barrier at one or both of the semiconductor-metal interfaces. The highest rectification ratio observed is 500, and was obtained with copper phthalocyanine between a Pt and a Ag or Al electrode. The effects of temperature, electrode material, and electrode size on the rectification ratio are discussed.

GALVANOMAGNETIC PROPERTIES

7019 EFFECT OF RANDOM INHOMOGENEITIES ON ELECTRICAL AND GALVANOMAGNETIC MEASUREMENTS by C. Herring (Bell Labs.); J. Appl. Phys., Vol. 31, pp. 1939-1953, Nov. 1960

The effects of random inhomogeneities on piezoelectric, galvanomagnetic, and thermoelectric measurements is discussed. The scale of the inhomogeneities is supposed small compared with the dimensions of the specimen being measured, but large compared with mean free path, Debye length, etc. Formulas which are asymptotically exact in the limit of small fractional fluctuations in the local conductivity, etc., are derived for all the effects. Comparison with other approximations and application to various exactly soluble cases show that these formulas are often roughly valid for quite sizable fluctuations. For material which, if uniform, would show a high field saturation of transverse magnetoresistance, the presence of appreciable inhomogeneties in the Hall constant will cause the magnetoresistance to increase indefinitely with field. This effect is due to the current distortions arising from the large and fluctuating Hall fields. For the special case of an isolated inclusion, these distortions are shown to extend, at high fields, to distances in the direction of the magnetic field which are many times the diameter of the inclusion. Under some conditions it appears that even the random distribution of impurities in a semiconductor can give rise to perceptible fluctuations on a scale large enough for concepts of macroscopic conduction to be applicable. Applications to polycrystalline metals and semiconductors are discussed briefly.

Use of Magnetoresistance Measurements to Study the Magnetic Properties of Permalloy Films - See 7044

7020 ANOMALOUS HALL EFFECT IN $AgSbTe_2$ by R. Wolfe, J. H. Wernick and S. E. Haszko (Bell Labs.); J. Appl. Phys., Vol. 31, pp. 1959-1964, Nov. 1960

The Hall coefficient of the ternary semiconductor $AgSbTe_2$ near room temperature is positive in some specimens and negative in others, although the Seebeck coefficient is always positive. The negative Hall coefficient decreases as the temperature is lowered from 180°K to 70°K and changes sign at lower temperatures. This negative Hall coefficient is associated with the presence in the $AgSbTe_2$ of a second phase consisting of Ag_2Te. The properties of the two-phase material are interpreted in terms of the theory of the transport properties of inhomogeneous semiconductors. The lattice thermal conductivity is so low (0.0064 watts/cm°C at 290°K) that the calculated "phonon mean free path" is less than the nearest neighbor distance. The thermal conductivity of a specimen rich in $AgSbTe_2$-Ag_2Te eutectic is higher than that of either of the components. This excess thermal conductivity is attributed to circulating thermoelectric currents.

Use of Low Temperature Hall Measurements for Determining Impurity Concentrations in Si - See 6941

OTHER ELECTRICAL PROPERTIES

7021 IRREVERSIBLE THERMODYNAMICS OF A NONLINEAR R-C SYSTEM by W. Bernard (Raytheon) and H. B. Callen (U. Penn.); Phys. Rev., Vol. 118, pp. 1466-1470, June 15, 1960

A recently derived formalism of nonlinear irreversible thermodynamics is applied to a circuit containing a capacitor and a

nonlinear resistor. The solution is compared with those obtained by M. Lax and other investigators. It is shown that the fluctuation-dissipation theorem is rigorous, and that no correction factors need be introduced for nonlinear systems. The dynamical behavior of the microscopic fluctuations, from which the microscopic motion can be obtained, is also derived. Finally, a specific Markoffian model of a nonlinear R-C system, in strong interaction with a temperature reservoir, is shown to be consistent with the general analysis.

7022 EXCESS NOISE IN SEMICONDUCTORS by J. J. Brophy (Armour Res. Found.); U. S. Gov. Res. Rep., Vol. 34, pp. 639-640 (A), Nov. 18, 1960 PB 149 505

A study of random electrical noise phenomena in solids that was undertaken to determine the origin of 1/f noise in ZnO and to apply noise measurements to the problem of trapping transitions and neutral energy transport in cadmium sulfide is reported. A characteristic relaxation time of 500 μsec associated with exciton diffusion or other neutral transport in CdS was established from noise measurements. Under uniform illumination the current noise in single crystal CdS may be interpreted in terms of multiple trapping in shallow levels within 0.5 volts of the conduction band. Discrete levels at 0.36 and 0.43 volts were observed in lightly doped crystals. Noise measurements are particularly suitable for determination of frequency factors of such traps and values ranging from 10^8 to 10^{11} sec^{-1} are derived. It is possible to account semi-quantitatively for the 1/f noise present in some crystals on the basis of the exponential trap distribution determined from photoconductivity experiments and the constant frequency factor of these traps derived from low frequency noise measurements.

7023 DEPENDENCE OF SECONDARY ELECTRON EMISSION FROM MgO SINGLE CRYSTALS ON ANGLE OF INCIDENCE by A. B. Laponsky and N. R. Whetten (GE Res. Lab.); Phys. Rev., Vol. 120, pp. 801-806, Nov. 1, 1960

The influence of the angle of incidence of primary electrons on the energy distribution and total yield of secondary electrons from MgO cleaved single crystals is discussed. Charging effects have been minimized by using single pulse techniques. The relative number of low-energy secondary electrons decreases with increasing angles of incidence. The effect appears to be most marked at primary energies in the vicinity of the maximum of the yield curve. At lower and higher primary energies the dependence on angle of incidence diminishes. Under most conditions the total yield increases with increasing angles of incidence. The magnitude of the increase is influenced by the primary electron energy. At low energies a slight decrease in total yield with increasing incidence angles has been observed. A dependence of the backscattered fraction of electrons on the angle of incidence of the primaries has been observed at several primary electron energies. A number of maxima and minima occur superposed on the gross variation of total yield with angle of incidence. The angular positions of the maxima are insensitive to primary energy but show a dependence on the crystal orientation. Several models for accounting for the phenomena are discussed.

7024 SECONDARY ELECTRON EMISSION OF MgO CRYSTALS BOMBARDED BY RELATIVISTIC ELECTRONS by M. A. Pomerantz, R. A. Shatas and W. C. Schieve (Franklin Inst.); J. Appl. Phys., Vol. 31, pp. 2036-2039, Nov. 1960

Measurements of the secondary electron yield of single crystals of MgO at a primary energy of 1.3 Mev are reported. A modification of the "sandwich" technique developed earlier for investigating the secondary electron emission of metals at high primary energies was used. The value of δ for Al was measured concurrently under identical conditions. The accumulation of surface charges usually encountered with insulators is prevented by the bombardment-induced conductivity of MgO. The influence of multiple scattering and energy loss of the primary beam, as well as of δ-ray production, must be considered when the targets are relatively thick as in the present case. An empirical correction for normalizing the thick target measurements to thin target conditions was determined. The result is: $\delta_{MgO} = 0.09 \pm 0.02$ as compared with $\delta_{Al} = 0.023 \pm 0.003$.

7025 DEMBER EFFECT IN SILVER CHLORIDE by A. M. Goodman and G. Warfield (Princeton U.); Phys. Rev., Vol. 120, pp. 1142-1148, Nov. 15, 1960

An investigation of the Dember effect in silver chloride using a chopped light-a-c amplification system of measurement is described. The effect has been resolved into a self-sustaining component which reaches a steady state (for a particular wavelength and intensity of incident light) and a non-self-sustaining component which decays with time. The steady-state self-sustaining effect has been found to be of only one polarity (normal polarity) when the illuminated face of the sample is coated with silver, but of both polarities when the illuminated face is not coated. The normal or positive polarity self-sustaining effect shows up at a shorter wavelength and the inverse self-sustaining effect at longer wavelengths, both in the vicinity of the optical absorption edge. A possible explanation for this behavior based on the existence of surface states is suggested. In the coated sample, the normal polarity effect was found to exhibit a peak at a wavelength of about 0.383 μ at T = 88°K.

7026 FUSED CONTACTS TO SILICON CARBIDE by T. C. Taylor (Raytheon); Proc. Conf. Silicon Carbide, Pergamon Press, 1960, pp. 431-442

Experimental studies of some fused rectifying and non-rectifying contacts to SiC are reported. Silicon which is heavily doped with arsenic or phosphorus gives non-rectifying contacts to n-type SiC crystals when alloyed at temperatures near 1500°C. The measured behavior of these contacts includes the effects of some spreading resistance in the SiC. It is not known whether the contact impedance alone is non-rectifying, or alternatively, negligible compared to the spreading resistance. The development of a rectifying structure wherein pure aluminum is fused to n-type SiC, giving a layer of aluminum carbide between the aluminum and SiC crystal, is also reported. Electrical measurements have shown that the rectifying barrier in this structure is at or near the aluminum carbide-SiC interface. This rectifier has room temperature electrical characteristics similar to those reported elsewhere for aluminum-doped fused junctions in SiC.

ELECTRICAL PROPERTIES OF SPECIFIC MATERIALS

Electrical Properties of SiC Films - See 6960

Electrical Properties of Sintered PbSe - See 6959

Electrical Properties of Tri-Clinic Copper Tungstate, AlB, Si, Ge, I and KCl - See 6998

ELECTRICAL PROPERTIES OF SPECIFIC MATERIALS (Cont'd)

Electrical Properties of HgSe-HgTe Alloys - See 6931

7027 PHYSICAL PROPERTIES OF P-TYPE Zn_3As_2 AND N-TYPE Cd_3As_2 by W. J. Turner, A. S. Fischler, and W. E. Reese (IBM); 1960 Fall Mtg. Electrochem. Soc.

Zn_3As_2 and Cd_3As_2 are II-V semiconductors which obey normal valence rules. Both compounds are tetragonal with solid-solid phase transitions at elevated temperatures. Single crystals of both substances have been prepared. In general, p-type Zn_3As_2 has a room-temperature hole mobility of less than 30 $cm^2/v\,sec$. From Hall data the carrier concentration in undoped material was approximately 5×10^{17} cm^{-3} in the range 77° - $300^\circ K$. Selenium appears to act as a deep level compensator when added to the melt. The intrinsic optical gap of Zn_3As_2 at $300^\circ K$ is 0.93ev. Electron Hall mobilities as high as 15,000 $cm^2/v\,sec$ have been observed in n-type Cd_3As_2 with net carrier concentration of 3×10^{18} cm^{-3}. The Hall coefficient remains constant from 4° to $300^\circ K$. The room-temperature optical gap obtained from absorption measurements is 0.13ev.

7028 SEMICONDUCTION IN ALUMINUM-DOPED PYROPOLYMERS by J. P. Laherrere and H. A. Pohl, (Princeton U.); Proc. Princeton U. Conf. Semiconduction Molecular Solids, pp. 93-121, 1960

A study of the electronic behavior of aluminum-doped pyropolymers prepared by the pyrolysis of a suitably doped ion exchange resin and heat treated at 800, 1000 and $1200^\circ C$ was described. These materials are p-type semiconductors of 0.01 to 0.1 ohm-cm resistivity at room temperature. The presence of aluminum decreases the conductivity and increases the resistance-temperature coefficient. The effects are opposite to those observed in nickel-doped pyro-polymers. Hall voltage measurements placed the carrier concentration in excess of 4×10^{19} per cc. The absolute thermoelectric power of these materials, doped from 0 to 10 atom per cent, varied from 2 to 5 microvolts per degree, and increased with temperature in a manner showing the carrier concentration to increase with temperature rise and to be about 2×10^{20} per cc. The evidence to date indicates that the aluminum is present in the form of carbide-like compounds, and not as the element or the oxide.

7029 PI-ELECTRONS AND HOLE PRODUCTION IN ORGANIC MOLECULAR SOLIDS by S. Mrozowski (U. Buffalo); Proc. Princeton U. Conf. Semiconduction Molecular Solids, pp. 1-7, 1960

It is explained why all organic molecular crystals and polymers are intrinsic semiconductors with an energy gap decreasing as the size of the conjugated system increases. It is also shown how in charring, as the substance is devolatilized, the electron spin resonance is first created and why it is later destroyed by surface trapping of π electrons, which leads at the same time to π hole formation and to an extrinsic conductivity of chars, carbons and polycrystalline graphites. The mechanism of trapping and the available experimental evidence are discussed.

7030 NUCLEAR QUADRUPOLE RESONANCE IN SUPERCONDUCTING GALLIUM by R. H. Hammond and W. D. Knight (U. of Calif.); Phys. Rev., Vol. 120, pp. 762-772, Nov. 1, 1960

An investigation of the nuclear quadrupole resonance (NQR) of Ga^{69} between 0.8 and $4.2^\circ K$ is reported. (The superconducting critical temperature is $1.084^\circ K$.) Progressive saturation of the resonance is produced at increasing rf power levels of a frequency-modulated marginal oscillator. The nuclear spin-lattice relaxation rate $1/T_1$ (sec^{-1}) is approximately $\frac{1}{2}T(^\circ K)$ in the normal state. The contact part of the hyperfine interaction appears to be predominant in producing relaxation. The rf fields are assumed to obey the London law of penetration, and an average rf field is determined in the superconductor. The relaxation rate shows a maximum enhancement by a factor 1.8 at approximately $0.95\,T_c$, a result which agrees with that obtained by Slichter and Hebel, and Redfield for the nuclear magnetic resonance of aluminum, and which serves as an additional experimental justification for certain features of the Bardeen-Cooper-Schrieffer theory of superconductivity. Unsaturated signal intensities in normal and superconducting states furnish a basis for estimating the penetration depth in superconducting metal spheres: $\lambda(0) = 1200\,A$ for an average particle diameter of $2.7\,\mu$. The NQR frequency of Ga in the superconductor shifts by $(+)5 \times 10^{-5}$ of the normal frequency [the corresponding result for indium is found to be approximately $(-)10^{-2}$]. This means that the contribution of the conduction electrons to the average nuclear quadrupole coupling is modified by the rearrangement of the conduction band in the superconductor. It is demonstrated that, if the quadrupole term in the hyperfine interaction were to predominate, the spin relaxation rate in the superconductor would have a temperature dependence like that of the ultrasonic attenuation.

MAGNETIC PROPERTIES

Relation of Electrical Resistivity to Néel Point in the Heavy Rare-Earth Metals - See 7016

7031 MAGNETIZATION PROCESS OF A HELICAL SPIN CONFIGURATION by U. Enz, Sixth Conf. Magnetism and Magnetic Materials, Nov. 14-17, 1960, New York, N.Y.

The behavior of a helical spin configuration of a hexagonal crystal in an applied field was discussed for the case where the axis of the helix is identical with the hexagonal c-axis and the magnetization vector in each layer is parallel to the basal plane. In a small field applied parallel to the basal plane a slight deformation of the helix occurs, resulting in a small increase in overall magnetization. If the field surpasses a certain critical value, the helix changes abruptly into a state with high resulting magnetization. In this state the spin-directions are oscillating about the direction of the applied field, the magnetization being about 85% of the saturation value. In still higher fields, saturation is reached completely. An investigation of the properties of the hexagonal oxide $(BaSr)_2Zn_2Fe_{12}O_{22}$, which is of the Y-type was reported. The Ba-rich composition is ferrimagnetic and has a preferential plane for the magnetization at all temperatures. The Sr-rich composition has no spontaneous magnetization, but a magnetization equal to the one in the Ba-case can easily be induced by an applied field. This behavior can be explained by the assumption of a helical spin configuration. The magnetic properties of dysprosium were also discussed in terms of a helical spin configuration.

7032 NEW METHOD FOR TREATING THE ANTIFERROMAGNETIC GROUND STATE by H. L. Davis (Ohio State U.); Phys. Rev., Vol. 120, pp. 789-801, Nov. 1, 1960

A perturbation expansion for the ground-state energy of an

antiferromagnetic spin system is obtained in terms of a linked-spin-cluster expansion similar to Goldstone's linked-Feynman-diagram expansion for the interacting Fermion system. From the energy perturbation series, perturbation series for the long- and short-range order may be obtained. Using these perturbation series, the ground-state properties are calculated through seventh order and compared with the results obtained by other investigators. In all cases, the values obtained here for the ground-state energy are lower than those which have been obtained by purely variational means. The results for the long-range order are radically different from the variational results but agree qualitatively with those obtained by spin-wave theory; however, the method is free of the usual objections which are voiced to spin-wave treatments of antiferromagnetism. The present work is incomplete in that limits on the error introduced by using only a finite number of terms of the perturbation series to calculate the physical properties are not obtained. But the author feels that the merit of the present work is in the method rather than the results since it provides a consistent framework both to settle the convergence question and to treat the antiferromagnetic spin system at finite temperatures.

7033 EXCHANGE INVERSION IN $Mn_{2-x}Cr_xSb$ by W. H. Cloud, T. A. Bither and T. J. Swoboda (duPont); Sixth Conf. Magnetism and Magnetic Materials, Nov. 14-17, 1960, New York, N.Y.

The first example of a ferrimagnetic to antiferromagnetic first order phase transition with decreasing temperature has been found in $Mn_{2-x}Cr_xSb$ for $0.02 \leq x \leq 0.2$. These compounds exhibit normal Curie point behavior with a Curie temperature only slightly lower than Mn_2Sb. The magnetization increases with decreasing temperature in a manner similar to Mn_2Sb but at a critical temperature decreases to zero over about a 10° interval. The temperature T_s at which this transition takes place increases with increasing chromium content. The tetragonal crystal structure of this material is the same as that of Mn_2Sb and does not change on passing through the phase transition. Neutron diffraction studies have shown that for $T > T_s$ the magnetic structure is the ferrimagnetic structure of Mn_2Sb, but for $T < T_s$ both the Mn(I) and the Mn(II) sublattices are antiferromagnetically ordered along the tetragonal axis. The three adjacent Mn(II)-Mn(I)-Mn(II) layers remain ferrimagnetically ordered at all temperatures. Above T_s, this set of three atomic layers is ferromagnetically coupled to adjacent sets, but below T_s, it is antiferromagnetically coupled to adjacent sets. Kittel has proposed recently that ferromagnetic-antiferromagnetic transitions can arise if the sign of the molecular fields is dependent on a critical lattice dimension. This theory suggests there should be a discontinuous change in lattice dimension at T_s and that the magnitude of this change should increase as the square of the sublattice magnetization. These conclusions are in agreement with observations.

7034 OBSERVATION OF DOMAINS IN IRON WHISKERS UNDER HIGH FIELDS by C. A. Fowler, Jr., E. M. Fryer and D. Treves (Pomona Coll.); J. Appl. Phys., Vol. 31, pp. 2267-2272, Dec. 1960

The use of an instrument based on the longitudinal Kerr magneto-optic effect to observe the magnetic domain development in iron whiskers undergoing a magnetization cycle is described. It is found that domains persist at the tip of the whisker even under conditions for which the crystal is usually assumed to be saturated. Under applied fields of a few thousand oersteds these persistent domains at the tip, in all of the specimens observed, are magnetized perpendicular to the axis of the whisker and in the same sense around its lateral faces. It is proposed that these domains are caused by the high fields localized near the sharp corners and edges of the crystal.

7035 NEUTRON AND OPTICAL STUDIES OF DOMAINS IN NiO by W. L. Roth (GE Res. Lab.); J. Appl. Phys., Vol. 31, pp. 2000-2011, Nov. 1960

An investigation of antiferromagnetic domains in NiO by neutron diffraction and optical observation of single crystals is described. There are two kinds of antiferromagnetic domain walls, T (twin) and S (spin-rotation). A T wall is produced by rotation of the antiferromagnetic pattern of magnetic moments and an S wall by rotation of the direction of the magnetic moments. The T walls can be observed with polarized light, and both T- and S-type domains can be studied by neutron diffraction. Crystals with simple T-wall structures are produced by annealing at high temperature. The crystallography of the T walls can be understood in terms of a small rhombohedral deformation which accompanies the antiferromagnetic ordering. The T walls are easily displaced by the application of small mechanical stresses or magnetic fields. A crystal without T walls may still contain S walls, and these S walls also are displaced or rotated by magnetic fields.

7036 ANTIFERROMAGNETIC DOMAINS IN α-MANGANESE AND ITS ALLOYS by A. Arrott and B. R. Coles (Ford Motor); Sixth Conf. Magnetism and Magnetic Materials, Nov. 14-17, 1960, New York, N.Y.

It has been shown that under certain conditions hysteresis appears below $50^\circ K$ in the magnetic isotherms of α-Mn. The coercive forces attain the order of kilo-oersteds. This is also observed for alloys of Mn with Fe and Cr prepared in the α-phase. Field cooling can give a permanent magnetic moment which may or may not be accompanied by hysteresis. An interpretation in terms of domains was given. The driving force for domain formation can arise from disorder as a result of alloying or from imperfections induced by preparation. It was also noted that the powder pattern neutron diffraction results of Kasper and Roberts can be reinterpreted as giving evidence for spin arrangements with a periodicity incommensurate with the lattice periodicity. This incommensurateness could also lead to domain formation in the way described by Overhauser in discussing Cu-Mn and Cr.

7037 TRIANGULAR MOMENT ARRANGEMENTS IN MANGANESE SPINELS by V. L. Moruzzi (IBM); Sixth Conf. Magnetism and Magnetic Materials, Nov. 14-17, 1960, New York, N.Y.

Low temperature magnetization measurements at pulsed fields of 75 kilo-oersted for selected single crystal members of the spinel series $Mn_xFe_{3-x}O_4$ were discussed in terms of Yafet-Kittel-Lotgering triangular moment arrangements. For $x < 1$, it has been found that, within experimental error, no high field susceptibility exists. For $1 \leq x \leq 3$, high field susceptibilities ranging from 1.0×10^{-4} to 3.3×10^{-4} gauss/oersted have been observed. The results for $MnFe_2O_4$ and for Mn_3O_4 are in essential agreement with previously reported polycrystalline measurements. For Mn_3O_4, the magnetization curves at $4.2^\circ K$ depend upon orientation. Extrapolation of these curves results in an anisotropy field of approximately 150 kilo-oersted. The anomalously low spontaneous magnetization and the observed high field susceptibility values for $1 \leq x \leq 3$ are best explained by a noncollinear moment arrangement in which the B lattice moments are subdivided into two groups. The angles between

the B lattice moments have been determined from assumed ionic distributions and observed magnetic moments at 4.2°K. From these values and the high field susceptibility measurements, values of n (the AB Weiss constant) and of β (the ratio of the BB to the AB Weiss constants) have been calculated. In addition, Curie temperature measurements have been used to obtain estimates of values of α (ratio of the AA to the AB Weiss constants). αβ diagrams which qualitatively explain observed anomalies in magnetization vs. temperature curves have been constructed. From the αβ diagram for Mn_3O_4 it is expected that the vanishing of the spontaneous magnetization at 43°K represents a transition from a triangular moment arrangement to one in which the A lattice is paramagnetic and the B lattice is antiferromagnetic. Torque measurements on Mn_3O_4 crystals provide evidence for the existence of this antiferromagnetic state. At 77°K, a uniaxial torque is observed which is proportional to the square of the applied field. The amplitude of this torque decreases rapidly with increasing temperature and vanishes in the neighborhood of 100°K.

7038 SPIRAL WALLS IN THIN MAGNETIC FILMS by H. W. Fuller, H. Rubinstein and D. L. Sullivan (Laboratory for Electronics, Inc.); Sixth Conf. Magnetism and Magnetic Materials, Nov. 14-17, 1960, New York, N.Y.

Dense concentrations of walls have been observed to appear in very thin magnetic films with the application of an AC field. Some observations have shown roughly circular concentric walls around barely discernible imperfections. Particularly clear powder patterns of such walls, obtained on the thin end of a permalloy film of tapered thickness, were presented. The patterns allow the deduction of the detailed magnetization distribution which takes the form of a pair of antiparallel domains that spiral in toward the central imperfection. A mechanism for the formation of spiral walls was presented, together with confirming experimental evidence. The experiments establish the nature of the central imperfection as a region of abnormally high uniaxial anisotropy where the magnetization is constrained to lie in one direction along the easy axis while the magnetization of the surrounding regions of the film can be rotated with an applied field.

7039 INFLUENCE OF SUBSTRATES ON THIN MAGNETIC FILMS ELECTRODEPOSITED IN A MAGNETIC FIELD by M. Lauriente and F. X. McNally (Westinghouse); 1960 Fall Mtg. Electrochem. Soc.

An investigation of the influence of various substrates on the magnetic properties of thin magnetic films of nominal composition 80Ni-20Fe, electrodeposited in a magnetic field, was reported. Chemically reduced silver, copper-clad laminate, and sputtered, vacuum evaporated and fired gold were included in the study. Electron micrographs and magnetic measurements were used to explain some of the unusual magnetic characteristics which have been found.

7040 COMPOSITION AND THICKNESS EFFECTS ON MAGNETIC PROPERTIES OF ELECTRODEPOSITED THIN NICKEL-IRON FILMS by I. Wolf (GE); 1960 Fall Mtg. Electrochem. Soc.

Use of a magnetic field during deposition to align the magnetic axes in a nickel-iron film in one direction so that the film exhibits a single "easy" axis of magnetization was described. In this way an "induced" anisotropy is established. The effects of thickness (500-6000A) and composition (~60% Ni - 100% Ni) on the anisotropy field, H_k, as well as on wall coercive force, H_c, and easy direction disturb, H_c, were discussed and evidence for stress interaction with magnetization and some data on substrate roughness were given.

7041 MAGNETIC ANISOTROPIES OF Ni FILMS EVAPORATED AND MEASURED AT 10^{-8} MM Hg AND BELOW by C. D. Graham, Jr. and J. M. Lommel (GE); Sixth Conf. Magnetism and Magnetic Materials, Nov. 14-17, 1960, New York, N.Y.

The magnetic properties of thin films of Ni, about 700 A thick, which have been vapor deposited on glass substrates at normal incidence at room temperature in vacua of about 5×10^{-9} mm Hg were discussed. Measurements were made with a torque magnetometer in the vacuum system. At fields below about 50 oe, the films show a sin θ torque curve with the magnitude of the peak torque proportional to field. In this range, the films behave like permanent magnetic dipoles. From 50 to about 500 oe, the torque curve is irregular in form, and the rotational hysteresis is large. About about 500 oe, the torque is very nearly sin 2θ and is independent of field. The magnitude of the uniaxial anisotropy is about 2000 ergs/cc. The direction of the remanent magnetization of the films may be changed at will by saturating the film in a high field; the uniaxial anisotropy measured at high fields is not reflected in the properties measured in low fields. The films show magnetic annealing at room temperature, i.e., a film placed in a saturating field at room temperature gradually forgets its original anisotropy and acquires a new anisotropy parallel to the applied field. The time dependence of the anisotropy is given by exp $(-bt^{1/3})$ at room temperature. Exposing the films to air causes only slight changes in the magnetic properties. One single crystal Ni film has been prepared by sublimation onto a rock salt crystal. Normal magnetic annealing effects were not present in this case.

Properties of Fe and Ni Films Prepared by Impact Evaporation - See 6975

7042 ANNEALING OF OBLIQUE-INCIDENCE PERMALLOY FILMS by G. P. Weiss and D. O. Smith (Lincoln Lab.); Sixth Conf. Magnetism and Magnetic Materials, Nov. 14-17, 1960, New York, N.Y.

A study of the anisotropy of oblique-incidence Permalloy films made at a substrate temperature of 200°C after annealling for several hours at 300°C was reported. Before the anneal the usual two-fold magnetic axis with the easy direction perpendicular to the incident depositing beam is present. After anneal films with positive magnetostriction have the same general magnetic symmetry, while those with negative magnetostriction may have either two-fold or four-fold anisotropy but with the original easy direction now a hard direction. Application of a large magnetic field in any direction during anneal does not influence the final magnetic anisotropy. Electron diffraction shows no crystallographic texture before or after anneal. The anisotropy was measured by means of ferromagnetic resonance. A coaxial bridge permits measurement over the frequency range 50 Mc to 2100 Mc. The film is placed in a rectangular coaxial cavity which can be heated up to 500°C in a vacuum of 10^{-6} mm Hg; continuous angular orientation of the film is possible with a resolution of ±0.5°. Bridge balance is good enough to permit samples of less than 500 A thickness to be measured.

7043 ROTATABLE ANISOTROPY IN THIN PERMALLOY FILMS by R. J. Prosen, J. O. Holmen and B. E. Gran (Honeywell Res. Ctr.); Sixth Conf. Magnetism and Magnetic Materials, Nov.

14-17, 1960, New York, N.Y.

Vapor deposited permalloy films which possess a new property, called "rotatable" anisotropy, in which the direction of easy magnetization is aligned by a suitable magnetic field were described. The threshold value of this field has the following properties: 1) It is of the order of 30 oersteds and is greater than the coercive force; 2) It is isotropic in the plane of the film; 3) It is independent of temperature from 345°K to at least 78°K. The hysteresis curves are identical for any established easy axis. This easy direction loop has a remanence which is approximately one-half of the saturation value for all thicknesses studied while the hard direction loop has the low loss characteristics typical of anisotropic thin films. The time necessary to establish a new easy direction of magnetization with a given field is independent of temperature for the range 78° to 345°K. Therefore, it is concluded that a diffusion process is not involved in establishing a new easy axis. The rotatable anisotropy can be irreversibly destroyed by heating the films to temperatures above 650°K. Following this treatment the films exhibit a lower coercive force and show a rectangular, isotropic hysteresis loop for all drive fields in the plane of the films. By employing partial etch techniques, it has been found that when the surface layer, which is less than 150 A thick, is removed, the rotatable anisotropy disappears; the film then shows a hysteresis loop identical to those obtained by heating above 650°K. This is strong evidence that the origin of rotatable anisotropy lies in a thin surface layer.

7044 MAGNETORESISTANCE AND MAGNETIC SWITCHING IN PERMALLOY FILMS by R. L. Coren and H. J. Juretschke (Polytechnic Institute of Brooklyn); Sixth Conf. Magnetism and Magnetic Materials, Nov. 14-17, 1960, New York, N.Y.

The use of magnetoresistance measurements to study the magnetic properties of permalloy films was described. Resistivities parallel and transverse to the current were measured simultaneously as the applied magnetic field was varied in magnitude or direction in the film plane. The results were discussed in terms of a new representation in which the resistivity components are regarded as Cartesian coordinates. This representation is independent of the current direction relative to any magnetically preferred orientations in the film. The statistical, domain wall, switching model of Conger and Essig has been extended to include the situation in which the field and easy magnetic axis are not parallel and a switching profile which gives a unified representation of the domain wall and coherent rotational switching response of a uniaxial film to an applied field has been constructed. The incidence of moving domain walls under certain field conditions was discussed with the help of this profile and it was shown that the magnetoresistance curves may be understood in terms of the magnetic changes.

Magnetic Properties of Permalloy Films Evaporated at Grazing Incidence - See 6971

Effect of Plating Parameters on the Magnetic Properties of Co and Co-Ni Alloys - See 6994

Properties of Thin Ferrite Films - See 6974

Properties of Ferrite Thin Films Prepared by Spraying - See 6976

7045 FERROMAGNETIC RESONANCE DUE TO MAGNETIC FIELDS GENERATED BY DISPLACEMENT CURRENTS IN FERRITES by I. Bady and G. S. McCall, Jr. (USASRDL); Sixth Conf. Magnetism and Magnetic Materials, Nov. 14-17, 1960, New York, N.Y.

Observation of a novel mode of excitation of ferromagnetic resonance wherein the rf magnetic field causing the resonance is generated by a displacement current in the ferrite, was reported. When a ferrite rod is placed in the center of a rectangular waveguide parallel to the E field, a relatively large displacement current may be set up due to the relatively large dielectric constant of the ferrite (typically 9 to 13). This displacement current generates a magnetic field which is circumferential with the rod. The ratio of this magnetic field to the transverse magnetic field due to normal waveguide modes in an empty waveguide is proportional to the dielectric constant and the ratio of rod diameter to free space wavelength. For a rod with a dielectric constant of eleven and a diameter of 1/8 inch, the above ratio is approximately 1:2 at 3000 megacycles. The formula for the magnetic biasing field required to produce resonance is shown to be $H(H + 4\pi Ms) = (\omega/\gamma)^2$. An experiment is described wherein a ferrite rod is placed in a short circuited waveguide, first at a magnetic field maximum and then at an electric field maximum. The ratio of energy absorbed at ferromagnetic resonance at the two locations was measured and checked well with theoretical calculations. This phenomenon explains why ferrites with relatively high saturation magnetizations (eg, $4\pi Ms > 1500$ gauss) appear to have very large dielectric losses when measured at S band, whereas they have very low dielectric losses when measured at X band.

7046 FERROMAGNETIC RESONANCE IN PIEZOELECTRIC $Ga_{2-x}Fe_xO_3$ by A. Dymanus (Harvard U.) and I. P. Kaminow (Bell Labs.); Sixth Conf. Magnetism and Magnetic Materials, Nov. 14-17, 1960, New York, N.Y.

The growth of single crystal ferromagnetic, piezoelectric insulators with the composition $Ga_{2-x}Fe_xO_3 (0.7 < x < 1.4)$ has been reported recently by Remeika. Mrs. Wood finds the unit cell to be orthorhombic, with $c < a < b$ and a twofold axis along b (C_{2v}). Microwave resonance measurements have been made at 24, 34 and 55 kmc sec at room temperature ($x > 1$) with single crystal spheres which are rotated about each of the three principal directions. The fields for resonance curves exhibit the orthorhombic symmetry with stationary points in the three principal directions. The hard direction is along the b axis, the intermediate direction along a, and the easy direction along the c axis. The anisotropy fields are in excess of 10,000 oersteds. Measurements of anisotropy, g-value and line shape were reported for several samples and the origins of the large anisotropy were discussed.

7047 SUBLATTICE MAGNETIZATION AND RESONANCE FREQUENCY OF ANTIFERROMAGNETS WITH LARGE UNIAXIAL ANISOTROPY by B. R. Cooper (U. of Calif.); Phys. Rev., Vol. 120, pp. 1171-1175, Nov. 15, 1960

The effect of large anisotropy on the thermal behavior of the sublattice magnetization and antiferromagnetic resonance frequency is discussed. It is shown that the curves for $M(T)/M(0)$ and $\omega(T)/\omega(0)$ vs T/T_c are shifted upward from those predicted by a Brillouin function magnetization curve. The shifts are due to a combination of the effect of the large anisotropy energy with that of electron exchange correlation. Corrections to the molecular field approximation arising from pair correlations are taken into account by an extension of the Oguchi method. These corrections are expected to be roughly $1/Z$ as large as the more accurate corrections which would

arise from correlation with all Z neighbors. This expectation is supported by a comparison of the values of kT_c/J and $\bar{S}(0)$ for the Oguchi method with those obtained by the Bethe-Peierls-Weiss and spin-wave methods, respectively. The results are related to the experiments on FeF_2 where the anisotropy is comparable to the exchange energy.

7048 INFRARED ANTIFERROMAGNETIC RESONANCE IN MnO by F. Keffer, A. J. Sievers III, and M. Tinkham (U. California); Sixth Conf. Magnetism and Magnetic Materials, Nov. 14-17, 1960, New York, N.Y.

Observations of antiferromagnetic resonance in powdered MnO at 364microns at 1.5°K were reported. The resonance frequency at higher temperatures falls roughly as the square-root of the Brillouin function of spin 5/2. Fields of the order of 10^4 oersteds have no observable effect on the line at 1.5°K. All of these results give quantitative confirmation of a model in which the sublattice magnetizations are constrained to a [111] plane by magnetic dipolar interactions and are held to a preferred direction within the plane by a much weaker anisotropy. In MnO the [111] axis is thus the hard direction. Simple macroscopic theory shows that this type of anisotropy decreases with temperature as the first power of the magnetization, thereby accounting for the temperature dependence of the resonance. In this resonance mode there exists no net magnetic moment, and therefore external fields can shift the resonance frequency only by small displacements quadratic in the field strength.

7049 NONLINEAR EFFECTS OF CRYSTALLINE ANISOTROPY ON FERRIMAGNETIC RESONANCE by P. Gottlieb (Hughes Aircraft); J. Appl. Phys., Vol. 31, pp. 2059-2062, Nov. 1960

The crystalline anisotropy of a ferrimagnetic solid will cause the magnetic resonance frequency to depend upon the angle of precession. It is shown that the resonance frequency depends quadratically upon the precession amplitude to lowest order. It is also shown that the dependence of this quadratic term upon the magnetic field orientation with respect to the crystal axis is the same as dependence of the usual zero-order resonance term upon orientation of the magnetic field. It is shown that the quadratic nonlinear term can cause a foldover of the resonance line, even in a spherical sample which is usually considered to have no foldover. The necessary conditions for the onset of this foldover are discussed, and some experimental results are mentioned.

7050 SPIN-FLOPPING IN MnF_2 BY HIGH MAGNETIC FIELDS by I. S. Jacobs (GE); Sixth Conf. Magnetism and Magnetic Materials, Nov. 14-17, 1960, New York, N.Y.

The observation in MnF_2 of decoupling between the direction of antiferromagnetism and the easy axis of the crystal (i.e. "spin-flopping") at 4.2°K and 20°K by measurements of magnetization along the c-axis of a single crystal in pulsed fields to 140 koe was reported. The critical field for decoupling is 92 ± 2 koe. This is in good agreement with the values found by microwave resonance in the work of Foner and of Johnson and Nethercot. This example demonstrates that magnetization measurements in high magnetic fields can be used as an alternative tool to explore the critical interaction energies in antiferromagnets.

7051 THE NATURE OF THE LOW TEMPERATURE LINE WIDTH MAXIMUM IN YTTRIUM IRON GARNET by E. G. Spencer, R. C. LeCraw and E. H. Turner (Bell Labs.); Sixth Conf. Magnetism and Magnetic Materials, Nov. 14-17, 1960, New York, N.Y.

Two types of experiments which have been performed in order to determine the origin of the residual low temperature ferromagnetic resonance line width maximum in high purity single crystal yttrium iron garnet were described. The measured values of $\Delta H(T)$ have the general characteristics which would be shown either by (a) the presence of paramagnetic and other impurity ions which replace yttrium ions to set up a fast relaxing paramagnetic sublattice coupled to the net ferric lattice or (b) the presence of divalent ferrous ions caused by the presence of certain impurity ions or by oxygen defects. The first experiment is a measurements of the k independent line width, ΔH_{ko}, as functions of frequency and temperature through the line width maximum. The second experiment was designed to introduce the divalent ion mechanism in a single crystal sphere of high purity YIG which had previously been measured. By heat treating the sphere at greatly reduced pressures the oxygen ions were driven off, causing some of the Fe^{+++} ions to become Fe^{++}. If no phase transitions occur, it is probable that the divalent ions, being larger, are located on octahedral sites. Results of these experiments were discussed in relation to the nature of the residual line width maximum.

7052 FERRIMAGNETIC RESONANCE IN A SINGLE CRYSTAL DISC OF YTTRIUM IRON GARNET by A. W. Smith and A. Watanabe (Def. Res. Telecom. Est., Ontario); Sixth Conf. Magnetism and Magnetic Materials, Nov. 14-17, 1960, New York, N.Y.

The use of discs instead of spheres for ferrimagnetic resonance investigations was discussed. Discs have the advantage that the line width is insensitive to the surface roughness. In addition, discs can be cut close to the (110) growth faces of garnet crystals, which is usually the location of the best material, and can easily be examined for internal imperfections with an optical or infra-red microscope. Resonance measurements have been carried out on a single crystal disc of yttrium iron garnet placed in a shorted coaxial line. The d-c magnetic field was perpendicular to the plane of the disc and the frequency was 1980mc/s. The disc was 0.157cm in diameter and 0.0085cm thick, and had a (110) growth face on one side. The low power linewidth was $\Delta H = 0.70$oe. The relative susceptibility was determined as a function of rf magnetic field at the sample. The critical field for saturation was found to be $h = 9.7 \times 10^{-3}$oe by extrapolation of the $1/h_{rf}$ portion of the saturation curve. The resultant value of ΔH_K, the line width of the unstable z-directed spin wave, is 0.34oe. These results were compared with those for spheres.

7053 A NEW CHARACTERISTIC IN THE TEMPERATURE DEPENDENCE OF FERRIMAGNETIC RESONANCE LINE WIDTH IN SOME RARE EARTH DOPED YTTRIUM IRON GARNET by J. F. Dillon, Jr. (Bell Labs.); Sixth Conf. Magnetism and Magnetic Materials, Nov. 14-17, 1960, New York, N.Y.

Measurements of the ferrimagnetic resonance line width of YIG doped with each of the rare earths were reported. For the most part there is a peak in the $\Delta H(T)$ curve at some temperature between about 20° and 150°K. The position of this peak varies with the impurity, the frequency, and the crystal direction of the steady field. However, several cases have been observed in which the line width increases very rapidly with decreasing temperature down to the lowest temperature reached, about 1.5°K. This behavior occurs over a very narrow angular range. For ytterbium doped YIG, it is associated with a very mild peak

in the field for resonance. For the case of europium there appears to be no anomaly in H_{res}, though a plot of line width against angle shows an increase of about fifteen fold with a half width of perhaps 1.5°. It is suggested that this anomalous linewidth versus angle and temperature as well as the more generally encountered peak in $\Delta H(T)$ represent the excitation of transitions between sublevels of the rare earth multiplet which approach within an energy comparable with that of a photon of the exciting radiation. The temperature variation is related to the transition probability of the transitions involved, to the simple difference in population resulting from the Boltzmann distribution, and to the breadth and separation of the levels.

7054 MICROWAVE PROPERTIES AND APPLICATIONS OF GARNET MATERIALS by G. P. Rodrigue (Harvard U.); U.S. Gov. Res. Rep., Vol. 34, p. 640(A), Nov. 18, 1960 PB 146 562

The known microwave properties of the new garnet materials are summarized briefly and compared to those of the more conventional ferrites. In order to facilitate the explanation of the operation of some new types of microwave devices, recent theories of ferromagnetic resonance developed by Suhl and by Walker are outlined. Possible applications of the yttrium garnet material include low frequency conventional microwave elements, frequency doublers and detectors, a new type of microwave limiter, and the recently announced ferromagnetic amplifier. The advantages that yttrium iron garnet offer in each of these devices are briefly discussed.

7055 NON-LINEAR RESPONSE OF YIG by R. M. Hill and R. S. Bergman (Genl. Tel. and Electronics Labs.); Sixth Conf. Magnetism and Magnetic Materials, Nov. 14-17, 1960, New York, N.Y.

A study of the small, and not so small signal, second harmonic output of a single crystal YIG sphere was reported. The significant results, to date, are: 1) The crystalline magnetic anisotropy appears to be primarily responsible for the observed second harmonic. 2) At signal levels significantly above the first saturation threshold large scale (up to 20 db), coherent amplitude modulation appears on the second harmonic. A second order solution to the torque equation, including anisotropy, has been obtained which shows a term in m_z at the second harmonic which depends on K_1/M_s $(1-\cos 4\theta)$ where θ is the angle between H_z and a [100] crystal axis. The data has an 8θ dependence with minima along both [100] and [110] directions. The peak to valley ratio of second harmonic output is more than 20 db. Second harmonic is first observed at about 1 milliwatt peak power for favorable orientations. As the fundamental is increased, saturation begins at 10-100 milliwatt level. When 1 watt peak power is reached amplitude modulations begin to appear. These are coherent within a pulse and repeat from pulse to pulse. The frequencies of these modulations may be anywhere from 100 Kc to several megacycles, and may be varied by both power and magnetic field. Attempts to observe correlated variations in the absorption of the fundamental are inconclusive. However, a small one loop coil around the ferrite does detect correlated variations in M.

7056 PREPARATION AND PROPERTIES OF LOW LOSS FERRITES by A. P. Greifer, Y. Nakada and H. Lessoff (RCA); Sixth Conf. Magnetism and Magnetic Materials, Nov. 14-17, 1960, New York, N.Y.

The preparation of nickel zinc ferrites containing one to three mol percent of cobalt ferrite and small additions of molybdenum or vanadium oxides with $\mu_0 Q$ products ranging from 49,000 at 500 kc to 4,000 at 55 mc was described. The effect of stoichiometry, ferrous iron content, firing temperature and firing time on the initial permeability, μ_0, and the magnetic quality factor, Q, was discussed. The nickel ferrite-zinc ferrite system is unique in its ability to yield materials with high $\mu_0 Q$ products in this frequency range. These properties are intimately related to the perminvar characteristics these compositions possess and are interpreted in terms of the Néel-Taniguchi approach. It is believed that a necessary condition for good high frequency response is the domination of the resonance phenomena by a spin rotation mechanism in preference to a domain wall process. This is achieved in properly constituted nickel-zinc ferrites by combining a high density, a low magnetocrystalline anisotropy and a very small grain size.

Saturation Magnetization of YIG Containing Nd - See 6977

Magnetic Properties of Ultra Fine Ferrite Particles - See 6973

7057 PARAMAGNETIC BEHAVIOR OF POLYCRYSTALLINE SAMARIUM FROM 300°K TO 1400°K by S. Arajs (U.S. Steel Res. Ctr.); Phys. Rev., Vol. 120, pp. 756-759, Nov. 1, 1960

Measurements of the paramagnetic susceptibility of polycrystalline samarium metal as a function of temperature between 300 and 1400°K are reported. The high-temperature phase transformations do not produce noticeable discontinuities in the magnetic susceptibility, indicating that the interactions between the samarium ions are small at these temperatures. The experimental results are compared with the Van Vleck theory of paramagnetism. It appears that the energy levels of Sm^{+++} in metallic samarium differ more from those predicted by the Russell-Saunders coupling than has been realized before. Collective magnetic behaviors resulting from the interactions between the samarium ions are briefly discussed in the light of some recent low-temperature investigations.

7058 ELECTRON PARAMAGNETIC RESONANCE OF EUROPIUM (II) IN SINGLE CRYSTALS OF CADMIUM SULFIDE by P. B. Dorain (Brandeis U.); Phys. Rev., Vol. 120, pp. 1190-1192, Nov. 15, 1960

Paramagnetic resonance absorption measurements made with single crystals of cadmium sulfide containing europium (II) are reported. The results can be fitted to the usual spin-Hamiltonian for ^8S state. The zero field splitting is about $0.4\,cm^{-1}$. The results are compared with present theories for the crystal field splittings of ^8S.

OPTICAL PROPERTIES

7059 COLORATION OF PURE AND DOPED CALCIUM FLUORIDE CRYSTALS AT 20°C AND −190°C by W. J. Scouler and A. Smakula (MIT); Phys. Rev., Vol. 120, pp. 1154-1161, Nov. 15, 1960

It is reported that coloration of pure CaF_2 crystals with 2.5-mev electrons at room temperature results in bands at 580, 400, 335, and 225 mμ. In YF_3-doped crystals the bands are in the same spectral positions as in pure crystals. They are, however, enhanced and their intensity ratios are significantly changed, the 400-mμ band being predominant. NaF-doped crystals show an

even more drastic change: Coloration at room temperature produces bands at 605, 385, and 330 mμ and is deeper than in either pure or YF_3-doped crystals. Since the 400-mμ band is strongly enhanced by YF_3 addition which forms F^- interstitials, it is correlated to neutral fluorine atoms in interstitial positions. Similarly, the 605-mμ band in crystals doped with NaF, which creates F^- vacancies, is correlated to electrons trapped in F^- ion vacancies (F centers). The enhancement of the 385-mμ band by NaF is explained by the reduction of the activation energy required for formation of interstitials and vacancies. Of several possible correlations the 330-mμ band is probably connected with a hole trapped in a Ca^{2+} vacancy and that at 225 mμ with an electron trapped by a Ca^{2+} interstitial. The bands at 440 and 200 mμ which appear in NaF-doped crystals only must be connected with Na ions. Coloration at $-190^{\circ}C$ produces strong changes in the absorption spectrum. The primary process of coloration at low temperature cannot differ from that at room temperature but the secondary processes are strongly influenced by temperature.

7060 COLOR CENTERS IN ALKALINE EARTH FLUORIDES by D. Messner and A. Smakula (MIT); Phys. Rev., Vol. 120, pp. 1162-1166, Nov. 15, 1960

Coloration of single crystals of CaF_2, SrF_2, and BaF_2 by x-rays (150 kv) and high-energy electrons (2.5 mev) is reported. Five color-center bands in CaF_2 and SrF_2 and nine in BaF_2 have been observed in the spectral region between 0.175 and 0.8 μ. At room temperature the bands in CaF_2 are well resolved, while those in SrF_2 and BaF_2 overlap. At -190° and $-255^{\circ}C$ the bands sharpen but generally do not shift, except the 580-mμ band in CaF_2 which shifts toward longer wavelengths. Photochemical bleaching of the strongest band shows a certain influence on the others. Three bands could be correlated to the Mollwo relation with the exponent 3.85. A possible correlation of the absorption bands to certain models is discussed.

Peltier Method of Measuring Radiation Emissivity - See 7072

7061 FACTORS INFLUENCING THE LUMINESCENT EMISSION STATES OF THE RARE EARTHS by L. G. Van Uitert (Bell Labs.); J. Electrochem. Soc., Vol. 107, pp. 803-806, Oct. 1960

The number of electronic states from which luminescent emission by rare earth ions can be observed is dependent on the extent to which the host lattice perturbs their f-orbital electrons. Among others, perturbing influences may stem from the following sources: (a) coulombic affinities of the ions or molecules surrounding the rare earth ions for the electrons they share with the latter; (b) concentration effects, i.e., exchange coupling; (c) thermal effects, i.e., vibronic interactions. Results obtained on metal organic complexes, hydrates, fluorides, and tungstates are compared. The effects on emission of the rare earth ion concentration in the tungstates are compared for europium, terbium dysprosium, and erbium at room temperature, and the influences of thermally excited interactions on the emission of erbium are demonstrated.

7062 ELECTROLUMINESCENCE — A DISORDER PHENOMENON by D. W. G. Ballentyne (Harlow Res. Labs., England); J. Electrochem. Soc., Vol. 107, pp. 807-810, Oct. 1960

In general, electroluminescence is considered to occur at a junction between a semiconducting crystal and a metal or electron rich material. Experiments which indicate that electroluminescence only occurs in zinc sulfide powders containing both sphalerite and wurtzite are reported. This observation suggests that electroluminescence is a disorder phenomenon associated with stacking faults in the crystal.

7063 ELECTROLUMINESCENCE MAINTENANCE by W. A. Thornton (Westinghouse); J. Electrochem. Soc., Vol. 107, pp. 895-907, Oct. 1960

The maintenance of several electroluminescent phosphors, mainly of the ZnS: Cu, Cl type, is discussed and data which illustrate its dependence on phosphor properties, such as copper and chlorine additions, firing temperature and particle size, on conditions of operation, and on lamp construction are given. Changes in properties other than light emission and recent maintenance improvements are also described.

7064 FLUORESCENCE AND REFLECTION SPECTRA OF NaI SINGLE CRYSTALS by W. J. Van Sciver (Levinthal Electronic Prod.); Phys. Rev., Vol. 120, pp. 1193-1205, Nov. 15, 1960

The fluorescence emission and excitation, reflection, and transmission spectra of 22 different NaI crystal samples grown in crucibles of Pt or quartz under atmospheres of N_2 or H_2 or H_2 plus I_2 and in some cases containing stoichiometric excess of Na or I_2 or containing various concentrations of Tl in the range from 2.5 to 8 ev are presented.

7065 PHOSPHORESCENCE MECHANISMS. I. APPROACH AND GENERAL ANALYSIS by C. Billington (CSIRO); Phys. Rev., Vol. 120, pp. 697-701, Nov. 1, 1960

A new technique for the study of decay mechanisms in phosphors is described. When a phosphor is excited by radiation whose intensity is modulated to a depth less than 10%, the modulation of the emission intensity has negligible harmonic content. Quantitative comparisons of these two modulated signals, if of sufficient accuracy and range, result in qualitative distinctions between different basic mechanisms, and the possibility of subsequent quantitative analysis. In particular monomolecular and bimolecular processes are unequivocally distinguished.

7066 PHOSPHORESCENCE MECHANISMS. II. DESCRIPTION OF PHOSPHOROMETER by C. Billington (CSIRO); Phys. Rev., Vol. 120, pp. 702-707, Nov. 1, 1960

The functions of the phosphorometer are (i) to excite the phosphor under test with ultraviolet radiation whose intensity is modulated sinusoidally, (ii) to measure the modulation frequency, and (iii) to sample the excitation and emission intensities, and to extract from their modulated components the in-phase attenuation factor between them. The Hg arc source is current-modulated and stabilized by optical feedback over the range 3 to 30,000 cps. The average intensity of both excitation and emission is used to control the sensitivity of their respective photo-detectors so that the modulation signals are always referred to the same datum. Both signals are passed in turn through a homodyne detector whose phase is adjusted to identity with the excitation modulation. The in-phase attenuation factor which is the ratio of the homodyne outputs is determined potentiometrically with a probable error of about 0.002.

7067 PHOSPHORESCENCE MECHANISMS. III. METHOD OF ANALYSIS by C. Billington (CSIRO); Phys. Rev., Vol. 120, pp. 708-709, Nov. 1, 1960

The method of deconvolution is discussed for the case in which phosphorescence is distributed between a number of concurrent components with different rate constants. The resolution of the

method is deduced quantitatively from the known rms difference of the apparatus.

7068 PHOSPHORESCENCE MECHANISMS. IV. DECAY RATE SPECTRA OF RUBY, URANIUM GLASS, AND Mn-ACTIVATED ZINC SULFIDE by C. Billington (CSIRO); Phys. Rev., Vol. 120, pp. 710-714, Nov. 1, 1960

A study of ruby, uranium glass, and a ZnS:Mn sample by means of the phosphorometer in a program of measurement and analysis which included variation of temperature and average exciting intensity is reported. It was not possible to identify any laws of temperature dependence, but there is strong evidence that part of the phosphorescence mechanisms operating in the ZnS:Mn sample involves recombination.

Correlation Between Hole Mobility and Crystal Size in PbS Photoconductive Films - See 7011

Photocurrents Excited by Visible Light in Organic Polymer Films - See 7013

7069 MECHANISM OF PHOTOCONDUCTIVITY IN MICROCRYSTALLINE POWDERS by R. H. Bube (RCA); J. Appl. Phys., Vol. 31, pp. 2239-2254, Dec. 1960

Measurements on a variety of cadmium sulfide powder cells which show that there are four different regions encountered with variation of the applied voltage are discussed. At low voltages an ohmic region is found in which barrier breakdown does not occur. At intermediate voltages a region is found in which barrier breakdown by a Process I occurs. At still higher voltages a region is found in which barrier breakdown by another Process II occurs in addition to that associated with Process I. At very high voltages another ohmic region is found where all barrier limitations have been removed. It is proposed, on the basis of the data, that Processes I and II are associated either with tunneling of electrons through interparticle barriers or with a reduction in barrier height assisted by the localized trapping of photo-excited or field-excited holes. A model constructed along these lines is applied to a variety of observations such as current-voltage curves, photocurrent lag after periods of no applied voltage or of opposite-polarity applied voltage, the existence of a semipermanent polarized set, ac properties of powders, and the hysteresis or storage effect.

7070 FIELD-EFFECT MODULATION OF PHOTOCONDUCTANCE IN A QUASI-INTRINSIC SEMICONDUCTOR by R. R. Bockemuehl (GM); J. Appl. Phys., Vol. 31, pp. 2255-2259, Dec. 1960

The field-effect modulation of conductance in a dark-insulating photoconductor is strongly dependent on the properties of carriers of both signs. An analysis of the equilibrium space charge density resulting from electron-hole pair generation in a "depletion layer" and the resulting influence on the terminal characteristics of a photoconductive field-effect transistor is presented. The derived relationships explain the optical and frequency response behavior of the field-effect modulation of photoconductance observed in CdS and provide a method for evaluating the drift mobility of holes and other carrier properties in a quasi-intrinsic semiconductor.

Reflectivity of Ge and Se - See 7010

Faraday Effect in Ge and Si at Microwave Frequencies - See 6998

THERMAL PROPERTIES

7071 THERMAL CONDUCTIVITY OF GERMANIUM FROM 3°K TO 1020°K by G. A. Slack and C. Glassbrenner (GE Res. Lab.); Phys. Rev., Vol. 120, pp. 782-789, Nov. 1, 1960

Measurements of the thermal conductivity of germanium from 3°K to 1020°K are reported. From 3°K to 300°K a longitudinal heat flow method was used. A radial flow method employing small samples was used from 300°K to 1020°K. The advantages and special experimental techniques required in this radial method are discussed. From 3°K to 10°K the results are explained by a simple combination of boundary plus isotope scattering in which all phonon-phonon processes can be neglected. At all temperatures below 940°K the heat is carried by phonons, but at 940°K a sharp rise in the thermal conductivity indicates the presence of a second conduction mechanism which may be electron-hole pairs.

7072 MEASUREMENT OF THERMAL CONDUCTIVITY BY UTILIZATION OF THE PELTIER EFFECT. II. CORRECTION FOR WIRE RADIATION AND DETERMINATION OF SPECIMEN RADIATION EMISSIVITY by R. Simon, R. T. Bate and E. H. Lougher (Battelle Mem. Inst.); J. Appl. Phys., Vol. 31, pp. 2160-2164, Dec. 1960

The analysis in the first article on measurement of thermal conductivity by utilization of the Peltier effect [see abstract 4259] is extended to correct for radiation of heat from the lead wires. It is shown how the radiation emissivity of the semiconductor specimen can also be determined from the measured temperatures.

7073 EFFECTS OF IRRADIATION ON THE THERMAL CONDUCTIVITY OF SYNTHETIC SAPPHIRE by R. Berman, E. L. Foster, B. Schneidmesser and S. M. A. Tirmizi (Clarendon Lab., Oxford, Eng.); J. Appl. Phys., Vol. 31, pp. 2156-2159, Dec. 1960

Measurements of the thermal conductivity between 2° and 100°K on synthetic sapphire single crystals and on sintered alumina, before and after reactor and γ-ray irradiations are reported. Reactor irradiation appears to introduce two types of thermal resistivity-producing defects, one of which is dominant at low temperatures. The only effect of γ irradiation is an extra thermal resistivity at low temperatures which saturates for quite small doses. This saturation value seems to depend on the initial perfection of the crystal and is increased by reactor produced damage. At present, detailed information about the defects cannot be derived from thermal conductivity measurements alone.

7074 EFFECT OF POINT IMPERFECTIONS ON LATTICE THERMAL CONDUCTIVITY by J. Callaway (U. Calif.) and H. C. von Baeyer (U. Miami); Phys. Rev., Vol. 120, pp. 1149-1154, Nov. 15, 1960

The consequences of a simple, phenomenological, theory of lattice thermal conductivity with respect to the effect of point

imperfections are summarized. The experimental results of Berman et al. on the effect of varying the concentration of Li^6 on the conductivity of lithium fluoride are analyzed in detail.

Thermal Conductivity of $AgSbTe_2$ - See 7020

7075 INJECTION HEAT TRANSFER by V. I. Stafeev (Physico-technical Inst.); Soviet Phys.-Solid State, Vol. 2, pp. 406-412, Sept. 1960

The mechanism for the onset of the Peltier effect in a semiconductor diode with a p-n junction under various conditions of recombination is discussed. It is shown that the nature of the thermal processes is different for recombination in the space charge layer and for recombination at the contacts between a metal and the semiconductor. The transfer of heat by injected nonequilibrium carriers is considered. From the usual thermodynamic relations, the Peltier coefficient and differential thermal-emf for a diode with a through current are written. The temperature difference arising in the diode is evaluated and the possible applications of injection heat transfer for the design of cooling equipment is examined.

Effect of Random Inhomogeneities on Thermoelectric Properties - See 7019

Thermoelectric Properties of Sintered PbSe - See 6959

7076 GRADED ENERGY GAP ALLOY SEMICONDUCTOR — $GaAs_xP_{1-x}$ by R. E. Johnson and G. Towns (Texas Instr.); 1960 Fall Mtg. Electrochem. Soc.

The preparation of a graded energy gap alloy semiconductor, $GaAs_xP_{1-x}$, where x varies with position along the bar was described. For use in high-temperature thermoelectric applications, it is possible to match the composition gradient of the alloy to the thermal gradient of the element for maximum efficiency. Evaluation results at various selenium doping levels were described.

7077 THERMOELECTRIC AND CRYSTALLOGRAPHIC PROPERTIES OF Ag_2Se by J. B. Conn and R. C. Taylor (Merck, Sharp, Dohme); J. Electrochem. Soc., Vol. 107, pp. 977-982, Dec. 1960

The preparation of silver selenide by fusion techniques and its thermoelectric properties are discussed. The Seebeck coefficient, resistivity, and thermal conductivity have been measured as a function of temperature. The effect of doping with 30 different elements and compounds at different doping concentrations has been studied. The inter-relationships between the thermoelectric properties have been examined and are discussed. The crystal lattice of silver selenide has been determined, and the subcell and superstructure are elucidated.

MECHANICAL PROPERTIES

7078 MEASUREMENT OF STRESS IN VERY THIN ELECTRODEPOSITS by H. Watkins and A. J. Kolk (NCR); 1960 Fall Mtg. Electrochem. Soc.

A modified form of the Brenner-Senderoff contractometer was described. Greater sensitivity has been achieved by using jewel bearings and optical read-out. The sensitivity is sufficient to determine a 10 KSI stress in a 200 A film. This instrument has been used to study the initial growth of the plating in thin electrodeposited films of iron-nickel alloys. Electron micrographs of the films were made to help in interpreting the stress data.

7079 MECHANICAL PROPERTIES OF THIN SINGLE-CRYSTAL GOLD FILMS by A. Catlin and W. P. Walker (U. Virginia); J. Appl. Phys., Vol. 31, pp. 2135-2139, Dec. 1960

The properties of single-crystal gold films grown by vacuum deposition on heated (375°C) sodium chloride substrate blanks were described. Completely oriented films with thicknesses between 1000 and 3000 A were obtained, with the plane of the film being the {100} crystallographic plane. A small hole was drilled through the substrate with a water jet, and the mechanical properties were determined by stressing the unsupported film over this hole. The films were observed to undergo considerable plastic deformation, accompanied by the appearance and growth of mechanical twin bands as the stress was increased. X-ray diffraction studies were made to determine the twin orientation. Both the ultimate tensile stress and the elastic modulus were found to increase as the thickness of the films was reduced.

SOLID STATE DEVICES

POINT CONTACT DIODES

7080 SURFACE CURRENTS IN INVERSION LAYERS OF SEMICONDUCTORS [in German] by E. Groschwitz, E. Hofmeister and R. Ebhardt (Siemens and Halske); Arch. Elekt. Ubertragung, Vol. 14, pp. 380-396, Sept. 1960

A number of theoretical and experimental results concerning surface currents in inversion layers of semiconductors are presented and the structure of the inversion layers and the physical phenomena giving rise to structural changes are described. The current mechanism taking place in inversion layers with application of an external potential is derived theoretically by reference to the example of point contact rectifiers. Experimental results concerning the properties of the characteristic curves of formed point contact rectifiers are reported. The measured values can be interpreted satisfactorily by the surface currents which can be presented analytically. The influence on the rectification effect of the semiconductor surface and the shape of the formed zone is investigated quantitatively. It turns out that with point contact rectifiers the surface current determines in a decisive manner both the magnitude of the diode current and the shape of the characteristic curve. The investigation relates initially merely to the conditions encountered with relatively low direct voltages to prevent secondary phenomena from masking the influence of the surface effects.

Optimum Source Conductance of Crystal Mixers - See 7118

JUNCTION DIODES

Gallium Arsenide Power Rectifier - See 7091

7081 THE DESIGN OF VARACTOR DIODES by J. Hilibrand and C. F. Stocker (RCA Labs.); RCA Rev., Vol. 21, pp. 457-474, Sept. 1960

The product of diode cutoff frequency and capacitance-voltage sensitivity constitutes a figure of merit for varactor diodes which is inversely proportional to the product of the rise time and the pump power dissipation in a parametric subharmonic oscillator. It also describes the gain-bandwidth product and pump power consumption in a parametric amplifier. This figure of merit can be related in a simple manner to the parameters of the impurity distribution in the diode. Favorable diode designs embody a low-resistance base region supporting a narrow and sparsely doped junction depletion layer. Two families of practical diode doping profiles have been considered: those corresponding to alloying to outdiffused surfaces, and those whose impurity distribution can be approximated by a simple power law. Shallow alloy junctions can be improved by outdiffusion of the base wafer until the surface concentration is 30 per cent of the initial concentration. A still higher figure of merit may be obtained in a structure whose doping approximates a power law, $N = ax^b$, where N is the impurity density, x is the distance from the junction, a is a constant, and b is an arbitrary exponent (between 1 and 2 for optimum figure of merit). For higher exponents, the capacitance-voltage sensitivity decreases faster than the cutoff frequency increases. However, such superlinear structures are shown to be the most favorable for achieving high Q values for forward-bias operations. Their low depletion-layer capacitance-voltage sensitivity is compensated for by the high sensitivity of the storage capacitance.

Noise Properties of Varactor Diodes - See 7115

Silicon Carbide Varactor Diodes - See 7087

Impedance of Diffused Silicon Mesa Varactor Diodes - See 7124

7082 DEVICE AND MATERIAL CONSIDERATIONS FOR GERMANIUM TUNNEL DIODES by T. R. Selig and R. C. Thomas (GE); J. Electrochem. Soc., Vol. 107, p. 268C (A), Dec. 1960

The fabrication of low peak current, low capacitance germanium tunnel diodes with high peak-to-valley current ratios was described. Homogeneous wafers for device use are selected by four-point probe resistivity measurements based on Hall carrier concentration. Device capacitance and the peak-to-valley current ratio have been correlated with carrier concentration. Junctions are formed by alloying an appropriately doped metal to the germanium in a reducing atmosphere. The peak current is tailored with an electrolytic etch. Tunnel diodes with the following characteristics are being obtained. I_p, 1 ma ± 10%; I_p/I_v, 10:1; C, 4 μμf; -g, 0.008 mho.

7083 FAST NEUTRON BOMBARDMENT OF GERMANIUM AND SILICON ESAKI DIODES by J. W. Easley and R. R. Blair (Bell Labs.); J. Appl. Phys., Vol. 31, pp. 1772-1774, Oct. 1960

An experimental examination of the fast neutron irradiation behavior of germanium and silicon Esaki diodes is reported. The dominant change produced is an increase in the "excess" current which is proportional to integrated neutron flux. The observed increase in the vicinity of the current minimum is approximately 2.6×10^{-15} amp/fast neutron and 1.1×10^{-14} amp/fast neutron for germanium and silicon diodes respectively. Substantial changes result in the voltage-current characteristics of the diodes employed in the decade of exposure between $10^{16} - 10^{17}$ fast neutrons/cm^2 for germanium diodes and between $10^{15} - 10^{16}$ fast neutrons/cm^2 for silicon diodes. One-kilomegacycle cavity oscillators employing germanium diodes exhibit a marked reduction in power output in the decade of exposure between $10^{16} - 10^{17}$ fast neutrons/cm^2. The magnitude of the decrease is in approximate agreement with the observed bombardment reduction of diode negative conductance.

Germanium Tunnel and Backward Diodes - See 7218

Fabrication of Gallium Arsenide Tunnel Diodes - See 7150

7084 RESEARCH DIRECTED TOWARD THE STUDY, ANALYSIS AND DESIGN OF TRANSISTORS by A. W. Carlson (Transistor Applications); U. S. Gov. Res. Rep., Vol. 34, pp. 558-559 (A), Nov. 18, 1960 PB 148 556

A study of nonlinear lines having a constant series inductance and voltage dependent shunt capacitance (such as a reverse biased junction diode) is reported. Experimentally, it is found that a signal applied to such a line acting to decrease line capacitance has its slope increased as it progresses down the line. A solution for a wave traveling along a uniform loss-less distributed line having a voltage dependent shunt capacitance or a current dependent series inductance is obtained.

7085 POTENTIAL DISTRIBUTION AND CAPACITANCE OF A GRADED P-N JUNCTION by S. P. Morgan and F. M. Smits (Bell Labs.); Bell Sys. Tech. J., Vol. 39, pp. 1573-1602, Nov. 1960

For a graded p-n junction under sufficient forward bias, the usual space-charge approximation to the potential breaks down, and a numerical solution of the differential equation satisfied by the potential is required. A procedure which avoids the difficulties associated with direct numerical integration of the stiff differential equation, and which yields a pair of very close upper and lower bounds to the potential at all points is described. For a linearly graded junction, tables of bounds are given which nowhere differ by as much as 1 per cent, and which effectively bridge the gap between the space-charge case and the neutral case. The computer solutions are used to calculate the voltage dependence of the stored charge (low-frequency a-c capacitance) of a graded junction numerically, as a function of the bias voltage across the junction. The expression for the capacitance is split into two parts, one of which dominates in the neutral case and the other in the space-charge case. With properly normalized variables, it is possible to give a universal plot of small-signal a-c capacitance against applied voltage. The results differ from the usual approximate formulas by amounts ranging up to nearly 10 per cent.

7086 ANOMALOUS BARRIER CAPACITANCE IN P-N JUNCTIONS OF InSb by C. A. Lee and G. Kaminsky (Bell Labs.); J. Appl. Phys., Vol. 31, pp. 1717-1719, Oct. 1960

Reverse bias transition capacitance measurements on alloy diodes of InSb at 78°K which give values a factor of three times those calculated from normal diode theory are reported. This

result is in contrast to the reasonable agreement obtained for diodes of germanium and gallium arsenide in a comparable doping range. The experimental techniques are critically reviewed and an attempt is made to assess the implications of the results.

7087 ELECTRICAL PROPERTIES OF ALLOYED P-N JUNCTIONS IN SILICON CARBIDE by T. E. Kharlamova and G. F. Kholuyanov (Leningrad Electrotechnical Inst.); Soviet Phys.-Solid State, Vol. 2, pp. 397-402, Sept. 1960

An investigation of the current-voltage characteristics of silicon carbide p-n junctions in the temperature range from 20 to 500°C is reported. The junctions were obtained by alloying an aluminum-silicon alloy in a hydrogen atmosphere to n-type crystals of silicon carbide with a resistivity of 2 to 2.5 ohm-cm. On the basis of measurements of the dependence of the recombination radiation intensity on the voltage, laws governing the increase of the diffusion component of the current as a function of the voltage increase in the forward direction have been found. The diffusion length of holes is estimated from the time constant of the recombination radiation decay. It is shown that the leakage affects the current-voltage curves of p-n junctions. In the entire range of the investigated voltages the growth of the inverse current with the voltage was greater than linear. At high inverse voltages, phenomena which indicate that avalanche breakdown takes place along the periphery of a p-n junction and in the vicinity of defects have been observed. The capacitance of the p-n junctions and its dependence on the voltage and the temperature have been measured. The possibility of using p-n junctions in silicon carbide as non-linear capacitors is discussed.

7088 STUDIES OF MICROPLASMAS AND HIGH-FIELD EFFECTS ON SILICON (Stanford U.); U.S. Gov. Res. Rep., Vol. 34, p. 643(A), Nov. 18, 1960 PB 149 411

Methods of producing a p-n junction device for obtaining high internal fields perpendicular to a silicon surface are discussed. This device will ultimately be used to study microplasmas and high field effects in silicon. The work has proceeded in three steps. The first step was to achieve a reproducible diffusion process. The next step was the construction of the device itself. Essentially, the device is a guard ring diode with a very shallow junction which under reverse bias will, hopefully, avalanche uniformly over the junction area. In the avalanche condition the device emits light in the region of breakdown, the glow being produced by hot hole-hot electron recombination in the high fields present. The devices constructed experienced avalanche breakdown in isolated spots rather than uniform breakdown over the junction area. The attempt to correlate these breakdown spots with surface imperfections led to the discovery that surface imperfections introduced during the construction of the device were directly related to the breakdown phenomenon. Attempts to understand the nature of the surface imperfections constitute the present stage of the research.

7089 UNIFORM AVALANCHE EFFECT IN SILICON THREE-LAYER DIODES by A. Goetzberger (Shockley); J. Appl. Phys., Vol. 31, pp. 2260-2261, Dec. 1960

Utilization of the interaction of current gain and avalanche multiplication in three-layer diodes to produce a uniform avalanche effect, indicated by uniform light emission over the area of a junction is described. Proof that the effect is caused by the three-layer action is furnished by removing the emitter layer, which changes the light emission to the usually observed microplasma pattern.

7090 THIN FILM EVAPORATION TECHNIQUES by I. Berman (AF Cambridge Res. Ctr.); U.S. Gov. Res. Rep., Vol. 34, p. 639(A), Nov. 18, 1960 PB 148 969

The fabrication of p-n junctions by evaporating aluminum onto n-type silicon held at a fixed temperature is described. The properties of these junctions have been measured by metallographic techniques.

Fabrication of Junctions by Epitaxial Deposition of SiC Films - See 6960

Rectifying Barrier at an AlC-SiC Interface - See 7026

7091 A GALLIUM ARSENIDE POWER RECTIFIER by L. D. Armstrong and P. Kuznetzoff (RCA); 1960 Electron Dev. Mtg.

The fabrication and electrical characteristics of a GaAs rectifier which can operate at 400°C with a 10a forward current and reverse breakdowns of 40 - 100v were described. The units are fabricated by diffusion of manganese into GaAs having a pre-diffusion carrier concentration of about $3 \times 10^{16}/cm^3$. The diffusion techniques and evaluation were described and conversion problems were reviewed. The details of mounting rectifiers for 400°C operation, including a review of possible brazing alloys, were given. Contacts can be made to both n- and p-type material with a newly developed gold-silver-germanium alloy. Heavy nickel plating must be used with the p-type material. A typical ceramic insulated design for use at 400°C was briefly described. The photo-resist and silicon dioxide masking procedures used in the fabrication of the device were explained and new techniques dealing with the alignment of subsequent patterns were covered. Fixtures and jigs for this part of the process were detailed.

7092 METHOD OF EVALUATING SILICON MONOCRYSTALS FOR THE FABRICATION OF DIFFUSED JUNCTION DEVICES by A. Ertel (Int'l Tel. and Tel.); 1960 Fall Mtg. Electrochem. Soc.

During the manufacture of silicon diffused junction devices, such as rectifiers and zener voltage regulators, changes in resistivity during high-temperature diffusion operations along with initial crystal imperfections may result in devices having reverse voltage characteristics other than those desired. A method of predetermining the quality of devices which may be expected from a given monocrystal was described. Characterization is made immediately after diffusion and prior to device fabrication. Some typical evaluations were discussed in detail.

7093 THERMOCOUPLE FURNACE FOR DEVICE FABRICATION by M. T. Minamoto (Air Force Cambridge Res. Ctr.); Proc. Conf. Silicon Carbide, 1960, pp. 443-446

A furnace for the fabrication of silicon carbide devices is described. The furnace consists primarily of a graphite crucible supported by a polycrystalline SiC rod, commercially available as heating elements. The interface of the crucible base and the support rod form the hot junction of a thermocouple, which measures directly the temperature at the base of the crucible. The thermocouple (C-SiC) produces an e.m.f. of approximately 300 V/°C which is essentially linear and stable up to 1800°C. Details of the furnace including the preparation of the junction

and methods of thermal and electrical insulation are given.

Use of the Peltier Effect for Cooling Diodes - See 7075

JUNCTION TRANSISTORS

7094 A STUDY OF THE CHARGE CONTROL PARAMETERS OF TRANSISTORS by J. J. Sparkes (Brit. Telecommun. Res.); Proc. IRE, Vol. 48, pp. 1696-1705, Oct. 1960

The present status of the concept of charge control of transistor action is considered, the most significant performance parameters for circuit design purposes are defined, and methods of measuring them are surveyed. These parameters are the collector time constant τ_c, the saturation time constant τ_s, the "on demand current gain" β_s, the collector capacitance charge Q_v and the dc current gain β. The manner in which these parameters may be expected to vary with dc current level is analyzed, as far as possible, for homogeneous base transistors, and is considered qualitatively for graded base types. A distinction is drawn between the technique of charge analysis of transistor action, and the concept of charge control of transistor performance. It is pointed out that only devices whose performance is determined by charges which are under the control of external circuitry can be regarded as charge controlled devices. This distinction strictly speaking excludes from the class of charge controlled devices those exhibiting the "wiggle" effect or possessing carrier storage in the collector region during operation in saturation. Although charge parameters can still be used for such devices, other parameters may be desirable as additions or alternatives.

Parametric Amplifier Transistor Operating in an Up-Conversion Mode - See 7137

7095 NON-LINEAR DISTORTION AND SMALL-SIGNAL PARAMETERS OF ALLOYED JUNCTION TRANSISTORS by N. I. Meyer (Teleteknisk Forkningslab.); Danish Science Press Ltd., Copenhagen, 1960, 269 pp.

Non-linear distortion in almost-linear networks with special reference to transistors, and the variation of transistor small-signal parameters with the d-c operating point are discussed. The first subject includes a treatment of non-linear distortion in some almost-linear complex two-poles, the results being subsequently extended to the treatment of alloyed junction transistors in the low and medium frequency range. Analytical expressions are developed for the second and third harmonic distortion factors (k_2 and k_3) as functions of the h-parameters and their derivatives, the load and generator impedances, and the frequency. The second subject includes a theoretical and experimental investigation of the complex h-parameters as functions of emitter current and collector voltage at low and medium frequencies. The theoretical expressions are based on the Webster-Misawa-Rittner theories, but they have been modified, e.g., by the introduction of the space-charge recombination effect. The theory has been checked by manufacturing transistors with known values of the important device parameters. The modified theory seems to explain a discrepancy previously found by the author between the theoretical and experimental results for the variation of h_{12} with emitter current.

A computer program for calculating k_2 and k_3 has been set up on the basis of the above mentioned results. In this way, k_2 and k_3 can be calculated for 100 different working conditions in less than 8 minutes. The calculated results are in good agreement with corresponding measured values. The theoretical results have been used as the basis for the design of a three-stage carrier-frequency amplifier. Using the common-base configuration in a push-pull coupling, it turned out to be possible to fulfill the CCIF requirements on k_2 and k_3 without the use of external feedback circuits at power levels up to 4 dbm.

7096 GENERALIZED PADÉ APPROXIMATION by J. L. Stewart (U. Arizona); Proc. IRE, Vol. 48, pp. 2003-2008, Dec. 1960

Approximation by minimizing the magnitude of the complex error phasor in the steady state is considered and relationships to conventional magnitude-only and phase-only methods are discussed. The particular case of the Taylor approximation about zero frequency is shown to be equivalent to the Taylor approximation in terms of the complex variable. Generalized examples are given which relate to rational approximations for transistor alpha, resistance-capacitance transmission lines, and the Z transform.

7097 INVESTIGATION OF PHYSICAL LIMITATIONS ON CURRENT GAIN (BETA) AND RESEARCH ON IMPROVED SILICON CONTACTS by L. L. Maissel and J. P. Spratt (Philco); U.S. Gov. Res. Rep., Vol. 34, p. 577(A), Nov. 18, 1960 PB 148 553

The factors which limit the grounded emitter current gain (β) of a transistor, and research on improved contacts for silicon are discussed. Theoretical analysis of β limitations suggested a technique for evaluating the relative importance of the factors known to affect current gain. Attempts to apply this technique experimentally yielded anomalous results. These discrepancies, as yet unexplained, indicate that it is not possible to produce high-gain and/or high-frequency devices by biasing transistors near punch-through voltage. The first step in the study of improved silicon contacts was to determine the possibility of developing a microalloy structure for silicon. When experiments showed that such a device, while possible, would not be adaptable to large-scale production, this work was discontinued. Attention was then turned toward a silver-antimony contact. A method of jet-plating silver onto silicon was developed. The effect of silver alloying on lifetime was investigated; no adverse effect was noted. The use of diffusion from a plated contact as a method of producing a good injecting contact of small area was studied. It was concluded that this method does not yield usable contacts.

7098 THE RF TRANSCONDUCTANCE OF THE HF-ALLOYED AND DRIFT TRANSISTOR AS A FUNCTION OF THE FREQUENCY AND OPERATING POINT AND ITS DERIVATION [in German] by W. Minner (Telefunken); Arch. Elekt. Uebertragung, Vol. 14, pp. 411-420, Sept. 1960

The RF transconductance of a transistor depends on frequency and cannot be derived from the characteristic showing the collector d-c current as a function of the base-emitter d-c voltage. In this paper an empirical equation is given, which permits the calculation of the RF transconductance as a function of the base-emitter d-c voltage U_{BE} up to a frequency nearly twice the α-cutoff frequency. The constants of this equation can be taken from the measurement of the transconductance as a function of U_{BE} at a single frequency in the vicinity of the

α-cutoff frequency. The differentiation of this equation with respect to U_{BE} gives the higher derivatives of the transconductance needed for calculation of the conversion transconductance and the collector short circuit current at combination frequencies of higher order. It is shown that the time constant associated with the base-emitter region is dominant for an alloyed transistor whereas the time constant associated with the collector-base region is dominant for a drift transistor. The theoretically predicted results have been verified experimentally.

7099 THE OPERATION OF JUNCTION TRANSISTORS AT HIGH CURRENTS AND IN SATURATION by C. A. Mead (Cal. Inst. Tech.); Solid-State Electronics, Vol. 1, pp. 211-224, July 1960

The lumped-model characterization for junction transistors is extended to current ranges where the transistor operation may no longer be considered linear. A number of effects which contribute to the nonlinear behavior are considered. In all cases it is shown that the self-bias cutoff effect plays an important part in the deterioration of performance at high currents. In alloy transistors, both normally and inversely biased, an exact solution for the form of the current gain as a function of collector current is given for the case where the injected density is small compared with the equilibrium base majority-carrier density. This solution is shown to be applicable to normally biased diffused-base units. A decrease in current gain is predicted due to the self-bias effect. The sources of lateral base current are bulk recombination and injection into the emitter, the relative amount being immaterial since both are proportional to the injected density. In the small-area alloy devices, it is seen that the injected density becomes large compared with the base majority-carrier density before the transistor performance is appreciably degraded. In such cases the lateral base current is seen to be normally dominated by non-unity emitter efficiency. In all cases, surface recombination is assumed to be the dominant source of total base current, and the first-order correction to the linear theory is shown to exhibit a $1/(1 + Ki_c)$ dependence. At higher currents all cases follow the observed $1/i_c$ proportionality. The effect of non-linear phenomena on saturation voltage is considered in some detail. The saturation voltage is shown to increase with drive current, again emphasizing the importance of avoiding large overdrive currents. The use of alloy transistors as low-level signal switches is discussed, indicating the necessity for high values of β and low values of K.

Resorption Time of Excess Charge Carriers in a Transistor Base - See 7148

7100 UNIFORMITY OF JUNCTIONS IN DIFFUSED SILICON DEVICES by L. E. Miller (Bell Labs.); Properties of Elemental and Compound Semicon. (Interscience); pp. 303-321

Solid state diffusion techniques have expanded the attainable uniformity in semiconductor junctions by an order of magnitude. The technique of beveling and staining has greatly facilitated the study of junction uniformity in silicon. The effects of surface roughness, surface erosion, nonuniformity of source concentration, problems related to the oxide mask process, surface melting, and localized preferential diffusion in silicon are reviewed.

Double Diffused Si Transistors - See 6949

Evaluation of Silicon Crystals for the Fabrication of Diffused Transistors - See 7092

Silicon Epitaxial Transistors - See 7219

7101 USE OF SILICON CARBIDE IN HIGH TEMPERATURE TRANSISTORS by H. -C. Chang, C. Z. Le May and L. F. Wallace (Westinghouse); Proc. Conf. Silicon Carbide, Pergamon Press, 1960, pp. 496-507

Theoretical analyses of bipolar and unipolar SiC transistors for 500°C operation are presented. Experience with Si and III-V compounds is applied to hexagonal SiC crystals, based on recent data for this compound. Fundamental techniques, such as fusion, diffusion, etching, and ohmic contacts, are studied with emphasis on the control of junction perfection, depth, and separation.

7102 TRANSISTOR STRUCTURE by W. R. Runyan (Texas Instr.); U.S. Pat. 2,948,835, Issued Aug. 9, 1960

A technique for dissipating heat from a junction transistor arrangement useful in non-grounded emitter or collector circuits is described. The junction bar is mounted in the usual manner on three leads which extend either through the base of the header or through the wall of the can. Either the emitter or collector, preferably the former, is connected to the header by means of a material such as intrinsic silicon which has good thermal conductivity and sufficiently high electrical resistivity to isolate electrically the emitter (or collector) from the header.

High Gain Cascaded Transistor Functional Units - See 7104

FIELD EFFECT TRANSISTORS

Effect of Electron-Hole Pair Generation on the Characteristics of a Photoconductive Field-Effect Transistor - See 7070

FUNCTIONAL UNITS

7103 A CATEGORIZATION OF THE SOLID-STATE DEVICE ASPECTS OF MICROSYSTEMS ELECTRONICS by I. A. Lesk, N. Holonyak, Jr., R. W. Aldrich and J. W. Brouillette (GE); Proc. IRE, Vol. 48, pp. 1833-1841, Nov. 1960

The contribution of solid-state electronic devices to microsystems electronics is discussed and it is pointed out that there is considerable confusion in this field at the present time. Dividing the field of solid-state devices into four categories into which may be placed all device approaches to microsystems electronics (and, incidentally, solid-state components in general) makes it easier to assess the merit of each new contribution by comparison with existing components. These four categories are basic, complex, integrated, and array. The construction details and operating principles, as well as the electrical characteristics, of a new device must be specified in order for it to be properly categorized. Some new examples of complex and integrated devices are presented to emphasize their differences.

Minimization of Power Dissipation in Functional Units - See 7121

7104 HIGH GAIN SILICON TRANSISTORS by H. W. Henkels and T. P. Nowalk (Westinghouse); Semicon. Prod., Vol. 3, pp. 39-42, Sept. 1960

The fabrication of silicon transistors with extremely high gain by cascading transistors within single crystal elements is described. The units represent the first steps in the achievement of multifunction devices in monolithic blocks of semiconductors, i.e., the initial stages in the development of the molecular engineering concept. Two examples of such devices are given. The first device is a one watt silicon transistor with current gain from 1000 to 500. The former value holds at one ampere; the latter value at about 2.5 amperes. Saturation resistance is 0.4ohm. The second device has a current gain of between 400 and 600 at currents from 5 to 2 amperes. Collector-to-emitter voltage breakdown is 85 volts; the saturation resistance is about 0.5 ohm. The properties of both devices are described together with the types of high gain units that can be readily achieved with the new techniques.

GALVANOMAGNETIC DEVICES

7105 A HALL EFFECT MULTIPLIER FOR USE AT RADIO FREQUENCIES by E. Cohen (Assoc. Elec. Ind.); Electronic Engrg., Vol. 32, pp. 558-559, Sept. 1960

The design of an indium arsenide Hall effect multiplier is considered. It is shown that the determining factor in high frequency operation is carrier break-through caused by inductive pick-up in the Hall circuit (in the absence of a magnetic field) due to carrier current flowing in the plate. This may be minimized by certain circuit configurations and, in conjunction with plug-in type of broad band transformers, lead to carrier break-through greater than 50db below maximum Hall signal.

Indium Arsenide Hall Generators - See 7220

7106 CORBINO DISK by D. A. Kleinman and A. L. Schawlow (Bell Labs.); J. Appl. Phys., Vol. 31, pp. 2176-2187, Dec. 1960

When a disk with concentric inner and outer electrical contacts is placed in a magnetic field parallel to its axis, and current is made to flow through the disk, the lines of current flow have a spiral shape. This spiral current flow produces its own magnetic field, which interferes constructively or destructively with the applied field, depending upon whether the carriers spiral inward or outward, respectively. For ordinary conductors and ordinary currents the effect of the self-field of the current is very small. However, the effect should be large in materials of very high mobility such as has been recently reported for bismuth at 4.2°K. In this paper the theory of the effect is given for the case in which the mean free path of the carriers is small compared to the inner radius of the disk. The analysis shows that the disk behaves as a rectifier. The easy direction of flow corresponds to outward spiraling of the carriers, which at large currents results in the expulsion of the magnetic field from the disk. In the hard direction of flow the magnetic field at the center of the disk may be several orders of magnitude larger than the applied field. It is suggested that the corbino disk may be a useful rectifier in applications requiring extremely low impedance. It may also be a useful voltage regulator in a very low-voltage high-current power supply. A device consisting of the disk and a coil to provide the magnetic field is discussed in some detail. The static characteristics when the coil is connected through a suitable resistance in parallel with the disk exhibits a negative resistance. This negative resistance is useful in a-c operation if a condenser is also connected in series with the coil. The equations and boundary conditions which determine the electrical properties of the disk in the time-dependent case are formulated.

OTHER CONDUCTIVE DEVICES

7107 TITANIUM THIN FILM RESISTANCE FOR MICROSYSTEMS ELECTRONICS (Lockheed); 1960 Fall Mtg. Electrochem. Soc.

Chemical processes for the fabrication of a stable thin film resistance material are described. Titanium is deposited on a ceramic substrate using a fused-salt technique and then electrochemically processed to produce a thin film with stable resistance values up to 2000 ohms per square and useful from -65° to 250°C. The resistance is monitored during the conversion process so that exact values may be made. The dependency of resistance characteristics on the process control parameters is discussed.

7108 CONCERNING THE DYNAMIC CURRENT-VOLTAGE CHARACTERISTICS OF SILICON CARBIDE RESISTORS by V. V. Pasynkov, G. F. Kholuyanov and L. K. Chirkin (Leningrad Electrotechnical Inst.); Soviet Phys.-Solid State, Vol. 2, pp. 403-405, Sept. 1960

The dynamic current-voltage curves of low-voltage nonlinear silicon carbide resistors at low current densities are discussed. These curves differ essentially from the dynamic current-voltage characteristics of resistors operating under the conditions of Vilit arresters. The hysteresis of the current-voltage curves is due to the process of charging and discharging of the capacity of a nonlinear resistor and is not connected with micro-heating of contacts between silicon carbide crystals. The capacitance of nonlinear resistors made of green and black silicon carbide is independent of the frequency in the range 50kc - 25Mc and of the d-c bias voltage.

7109 A NEW SEMICONDUCTOR MICROWAVE MODULATOR by H. Jacobs, F. A. Brand, M. Benanti, J. D. Meindl (USAS RDL) and R. Benjamin (Monmouth Coll.); IRE Trans., Vol. MTT-8, pp. 553-559, Sept. 1960

A new semiconductor device is proposed for use as an amplitude modulator for microwave transmission. The principle of action depends upon the increase of absorption with an increase of conductivity caused by the injection of excess minority carriers. Experiments conducted at 9600Mc indicate little or no phase and frequency modulation. The mechanism of the modulation action and the device design are discussed.

PHOTODEVICES

Power Amplifiers Based on Electro-Optical Effects - See 7145

Electro-Optical Switch and Potentiometer (Raysistor) - See 7221

Diffused Si Photovoltaic Devices - See 6949

7110 A TWO-COLOR INPUT, TWO-COLOR OUTPUT IMAGE INTENSIFIER PANEL by F. H. Nicoll and A. Sussman (RCA); Proc. IRE, Vol. 48, pp. 1842-1846, Nov. 1960

The design and construction of a two-color input, two-color output image intensifier panel are described. The solid-state panel is so constructed that it can be independently excited by either a visible image or a near-infrared image on the input. The visible input image excites one of the colors in the output image while the infrared input image excites the other color of the output image. The characteristics of the panels are given in terms of input and output light levels, spectral response and gain. Photographs which show the output image for visible input only, infrared only, and the two combined are given.

THERMAL DEVICES

7111 THERMISTORS, THEIR THEORY, MANUFACTURE AND APPLICATION by R. W. A. Scarr and R. A. Setterington (Std. Telephones Cables); Proc. IEE, Vol. 107B, pp. 395-409, Sept. 1960

The theory of the operation of thermistors is described, the reason for their negative temperature coefficient of resistance is explained, and the expressions which govern their parameters are developed. Methods of manufacture of the various forms of thermistors are outlined in general terms, and numerous applications of the device are described and discussed. Guidance is given on the approach to circuit problems, and the possibilities of exploiting some of the device's interesting and unusual properties are indicated. It is pointed out that the thermistor can now be used in many fields as an adequate alternative to components of more specialized application.

MAGNETIC DEVICES

Device Applications of Yttrium Garnets - See 7054

7112 OPERATION OF THE FIELD DISPLACEMENT ISOLATOR IN RECTANGULAR WAVEGUIDE by R. L. Comstock and C. E. Ray (Bell Labs.); IRE Trans., Vol. MTT-8, pp. 605-611, Nov. 1960

A field displacement isolator in WR-159 rectangular waveguide consisting of a full height ferrite slab having a resistive film on one face is treated analytically. The resultant transcendental equation was programmed for a computer and values of the propagation constant found in the frequency range 5.90 to 6.45 kMc for various film resistivities. Two TE modes are found to exist whose relative behavior depends on the resistivity of the film. Reasonably close experimental verification of the results was obtained for the total attenuation and for the predicted E-field distributions by E-field probe tests. Additional attenuation above that predicted by the theory for a single mode is observed as a result of an interference at the end of the ferrite. A partial height ferrite slab isolator was subjected to E-field probe tests. The field distributions were found to be similar to the full height case. Here, also, additional attenuation is obtained at some frequencies as a result of an interference.

YIG Resonance Isolators - See 7115

S Band Ferrite Circulators - See 7222

7113 BROAD-BAND RIDGE WAVEGUIDE FERRITE DEVICES by E. S. Grimes, Jr., D. D. Bartholomew, D. C. Scott and S. C. Sloan (Sperry Microwave); IRE Trans., Vol. MTT-8, pp. 489-492, Sept. 1960

The design and development of a medium CW power level, 1.57:1 bandwidth, quadruply-ridged circular waveguide Faraday rotator and two high CW power, 2:1 bandwidth, double ridge rectangular waveguide isolators are discussed. The rotator is designed in quadruply-ridged circular waveguide with a ferrite configuration somewhat different from that proposed by other investigators. It can be made to exhibit broadband rotation and large rotation per unit length of ferrite section, and may be used in most medium CW power level applications. Forty-five degree rotation is achieved from 7.0 kMc to 4.0 kMc in DR-37 waveguide and from 3.8 kMc to 7.6 kMc in D-34 waveguide respectively. The reverse to forward wave attenuation ratio exceeds 10.0 db to 1.0 db for both isolators.

Ferromagnetic Thin Film Made of Gyralloy 1 - See 7190

7114 FINE WIRE FERRITE LIMITERS by E. Stern (GE); Sixth Conf. Magnetism and Magnetic Materials, Nov. 14-17, 1960, New York, N.Y.

Use of the subsidiary resonance observed in a ferrite at high microwave magnetic field intensities for limiting purposes was discussed. The limiter threshold power is related to the oersteds of magnetic field intensity produced in the ferrite per watt of power input. The circumferential field about a wire is directly proportional to the current and inversely proportional to the wire diameter. Thus a fine wire imbedded in a ferrite will produce intense microwave fields at low microwave power levels provided the wire is properly matched to the microwave structure. The response of a ferrite limiter to a microwave pulse characteristically exhibits a leakage spike whose duration is inversely proportional to ΔH_K, the spin linewidth, and a plateau whose power level is proportional to ΔH_K^2. Thus, low threshold power levels normally can be achieved at the expense of long spike duration. The fine wire technique was analyzed for limiter applications and it was shown that threshold power levels less than a watt can be achieved in a ferrite with wide spin linewidths. A particular structure has been designed, built and evaluated. It is found that a threshold power level less than one watt can be achieved with material producing spike duration times of less than 20 nanoseconds. In addition, the experimental results show that the spike decreases rapidly with increasing power. This effect is thought to be related to the excitation of spin waves of progressively broader linewidths with increasing input power.

Fine-Grained Ferrite for Transducer Heads - See 7171

7115 MICROWAVE SOLID-STATE DEVICES (Bell Labs.); U.S. Gov. Res. Rep., Vol. 34, p. 564(A), Nov. 18, 1960 PB 149 016

A study of slow-wave structures to be used in traveling wave masers for a frequency of 2390 Mc is reported. Resonance isolators have been operated using yttrium iron garnet at liquid helium temperature and at the magnetic field called for by the ruby maser operation. On the basis of these results, the development of a ruby traveling wave maser for this frequency has been initiated. A theory of high power performance of traveling wave masers has been developed. It suggests a novel utilization of traveling wave masers as energy storage and conversion elements. Low-temperature noise measurements on a diffused germanium varactor diode have been obtained for amplification in the degenerate mode at a frequency of 6 kMc/sec. Excess noise temperature is determined as a function of the diode operating temperature in the range from near liquid nitrogen temperature to room temperature. Harmonic generation at relatively high-power levels has been achieved using diffused-silicon-junction diodes. The diodes used are "gradual grade" units, in the sense that their impurity gradients are substantially less than those of the silicon varactor diodes, although they are designed to minimize series resistance to ensure maximum cut-off frequency.

OTHER SOLID STATE DEVICES

Ferroelectric Memory Cells - See 7193

Fabrication of Thin Film Cryotrons - See 7192

7116 NANOSECOND RESPONSE AND ATTENUATION CHARACTERISTICS OF A SUPERCONDUCTIVE COAXIAL LINE by N. S. Nahman and G. M. Gooch (U. Kansas); Proc. IRE, Vol. 48, pp. 1852-1856, Nov. 1960

A miniature superconducting coaxial line which transmits nanosecond (nsec) pulses without any measurable change in rise time is described. Data in regard to the temperature dependence of the bandwidth over the range 293°K to 4.2°K are presented. The investigation is confined to ten and hundred foot lengths of cable.

7117 INTERCARDIAC CATHETER TIP PIEZORESISTIVE PRESSURE GAUGE by M. Traite, W. Welkowitz and R. Downs (Gulton Ind.); Rev. Sci. Instr., Vol. 31, pp. 987-991, Sept. 1960

A pressure gauge that can be encased in a small-bore plastic catheter is described. The small size permits insertion directly into the heart. The unit uses a two-section piezoresistive element, operated as a cantilever. The sensitivity of the gauge is 0.16 mv/v/psi, and the frequency response is flat from 0 to 400 cps.

SOLID STATE DEVICE MEASUREMENTS

Measurement of Diode Impedance - See 7124

7118 A NOTE ON THE OPTIMUM SOURCE CONDUCTANCE OF CRYSTAL MIXERS by R. J. Mohr (Microwave Dynamics), and S. Okwit (Airborne Instr. Lab.); IRE Trans., Vol. MTT-8, pp. 622-627, Nov. 1960

An accurate and convenient technique for measuring the match of a crystal mixer is described. Use is made of the fact that with a proper RF drive level, the fundamental conductance of a mixer crystal may be made equal to the optimum source conductance of the crystal for mixer operation. The required drive level depends on certain crystal parameters and on the image frequency termination of the mixer. Design curves are given which simplify the determination of the proper RF drive level for a wide range of crystal parameters and their condition of image frequency termination.

BASIC SOLID STATE DEVICE CIRCUITS

GENERAL (Network Theory, Miniaturization, etc.)

7119 THE NODE SYSTEM OF EQUATIONS by W. C. Peterson (No. Carolina State Coll.); and J. J. LaRue (U. Michigan); J. Franklin Inst., Vol. 270, pp. 175-189, Sept. 1960

The minimum number of simultaneous equations and unknowns required to describe the behavior of an electrical network is in many cases obtained by considering the independent node voltages to be the unknown variables. However, the usual techniques for writing node equations are not applicable to networks containing ideal voltage sources not incident to the reference node. The node system of equations for general networks with ideal current and voltage sources arbitrarily located is derived on the basis of a particular type of cut-set or segregate matrix, and a novel method for writing the node equations of such networks by inspection is presented. The application to networks containing vacuum tubes, transistors and magnetic coupling is illustrated.

7120 ON THE SYNTHESIS OF ACTIVE NETWORKS WITH ONE NEGATIVE IMPEDANCE CONVERTER by R. T. Chien (IBM Res. Ctr.); Proc. 1960 Natl. Electronics Conf., pp. 405-411

The Linvill configuration is used to synthesize second-order, non-positive-real, driving-point functions. Synthesis is accomplished by the use of a surplus factor. With the arbitrariness of the surplus factor, one is able to control the driving-point function. The existence of the solution in all cases is demonstrated and the minimum number of elements property of the solution is proved. It is shown that only five elements are required besides the NIC. RC networks are used in some cases

and RL networks are used in the remaining cases. The method used is extended to realize all three functions. Necessary and sufficient conditions are found for three functions to be a realizable set. The synthesis itself is carried out in the same manner as in the previous case.

Categorization of the Solid-State Device Aspects of Microsystems Electronics - See 7103

7121 OPTIMUM STABILIZATION NETWORKS FOR FUNCTIONAL ELECTRONIC BLOCKS by J. D. Meindl and O. Pitzalis (USASRDL); Proc. 1960 Natl. Electronics Conf., pp. 576-590

The problem of optimizing the design of the stabilization network of a functional block capable of performing as an audio, tuned, or video amplifier, harmonic oscillator, modulator, mixer, detector, and the like is considered. The active element may be a single bipolar transistor or several connected directly in tandem The functional device design procedure differs widely from the conventional and utilizes, as the broad optimizing criterion, the minimization of power dissipation in the functional block. The results show that with optimum designs, 3 to 1 reductions in power dissipation are commonplace with 10 to 1 and larger reductions possible. The design procedure includes the important effects in semiconductor blocks of temperature variation for all passive elements, as well as the supply voltage. The results show that well-stabilized transistor operation is possible for resistive networks whose temperature variation is 50 percent over a 130°C temperature range. Both transistor and resistor manufacturing tolerances are considered quantitatively. Experimental data which support the design theory are presented.

7122 PRACTICAL CONSIDERATIONS IN THIN CIRCUIT MICROELECTRONICS by J. M. Blank, I. A. Lesk, and J. J. Suran (GE); Proc. 1960 Natl. Electronics Conf., pp. 438-443

The practical objectives of micro-systems electronics are considered; they include size reduction, more efficient power utilization, increased reliability and reduced cost. Also, any practical approach should have sufficient versatility for a wide variety of applications. It is concluded that the thin circuit (2D, modular, substrate) approach offers more promise in satisfying all these objectives than any other presently proposed scheme, since it allows a high degree of freedom in circuit design, the use of pretested components with close parameter control, and the use of different techniques for producing a wide variety of conductors, resistors and capacitors in place on the substrate. The substrate is a thin wafer of any practical shape. The circuit components are laid down in an order determined by the processes used. For example, if anodized capacitors are made on the substrate, only those other materials that will not be affected by the anodizing process may be present at that time. High value resistors and capacitors, as well as inductors, may be made and attached to the circuit separately. Active components (i.e., transistors, diodes) are separately packaged in thin, miniature enclosures. The application of thin circuit techniques to some logic functions, and their design, construction, and operation, are discussed.

7123 DISTRIBUTED PARAMETER CIRCUITS AND MICROSYSTEM ELECTRONICS by P. S. Castro and W. W. Happ (Lockheed); Proc. 1960 Natl. Electronics Conf., pp. 448-460

A basic three-layer resistance-capacitance distributed-parameter microminiature structure is analyzed and the results are expressed in terms of indefinite admittance and impedance matrices. The indefinite matrix formulation allows a systematic derivation of the network functions of all possible one-ports and two-ports obtainable from this basic network; thirteen non-redundant one-ports and 21 non-redundant two-ports exist. The resulting network properties are discussed in terms of an RC half-section for the one-ports and coupling, decoupling and frequency selective networks for the two-ports. Plots of the attenuation and phase characteristics of these networks are made and compared with those of lumped parameter networks.

Titanium Thin Film Resistance for Microsystems Electronics - See 7107

Microsystems Bandpass Amplifier - See 7131

7124 MICROWAVE SOLID-STATE DEVICES (Bell Labs.); U.S. Gov. Res. Rep., Vol. 34, p. 564(A), Nov. 18, 1960 PB 149 017

Starting with a four terminal network representation, the impedance transformation from the semiconductor region of a mesa diode to a transmission line is discussed. It is shown that, under certain assumptions, the transformation between measured reflection coefficient and device impedance can be formulated in a simple way, and may be arrived at through a series of operations on a Smith chart. Proper use of impedance standards can determine the transformation. Experiments (conducted at a single frequency only) indicate validity of the assumptions, one of which is the appropriateness of the impedance concept itself. Using these measurement techniques, the impedance of a considerable number of diffused silicon mesa varactor diodes has been evaluated. The experimental results, obtained using diffused silicon from a single run with a fixed impurity gradient, indicate a dependence of Q (measured at 1 kMc per sec.) on the area of the diffused junction. This is attributed to the presence of an equivalent series resistance, some of which must be attributed to losses near the active region of the device. The magnitude of this series component is enough to begin limiting the cut-off frequency obtainable with diffused wafers when the junction capacity sizeably exceeds two or three pf. Possible reasons for these losses are discussed.

7125 TRANSIENT PHENOMENA IN THE CONNECTING OF A QUICK-ACTING SHORT-CIRCUITER [in Czech.] by J. Klier (CKD); Elektrotech. Obzor., Vol. 49, pp. 605-608, Nov. 1960

A short-circuiter for protecting semiconductor rectifiers against considerable overload and against short-circuit is described. This apparatus short-circuits the secondary winding of a transformer. The current flowing through the primary and secondary windings of the transformer after connection of the contacts of the quick-acting short-circuiter consists of two components, i.e., a stabilized and a transient component. It is the transient components that increase the stress of the transformer and all parts of the circuit. The circumstances on which the magnitude of the transient components depends and the conditions under which they attain their maximum value are considered. It is further shown how these components depend on the fortuitousness of the instant at which the quick-acting short-circuiter connects its contacts and upon the load of the transformer prior to short-circuiting.

7126 THE USE OF THE SILICON RESISTOR IN THE D.C. STABILIZATION OF TRANSISTOR CIRCUITS by D. H. Mehrtens and J. T. Zakrzewski (E.M.I. Electronics Ltd.); Electronic

Engrg., Vol. 32, pp. 624-629, Oct. 1960

A new method of stabilizing the d-c operating point of transistors, using the silicon resistor, is introduced and its application to both small-signal and power transistors is expounded. Practical evidence is given to show that it is possible with this method to obtain constant collector current over the whole operating temperature range of transistors in the great majority of cases.

AMPLIFIERS

7127 SEMICONDUCTOR GAIN CONTROL TECHNIQUES by J. S. Brown (GE); Proc. 1960 Natl. Electronics Conf., pp. 541-548

Common methods of reducing transistor gain utilize a reduction of the emitter current or collector voltage or both. In many applications these methods cause distortion because the transistor's signal handling capability is reduced when the gain is reduced, and this occurs when the signal is large. Also, the resulting impedance changes may cause detuning. Consequently other techniques have been developed in recent times. Several of these techniques are discussed with particular attention to considerations necessary to utilize the potentials of the methods fully. The relationship between the gain control circuits and the rest of the amplifier is also discussed.

7128 AN IMPROVED METHOD OF GAIN CONTROL FOR TRANSISTOR I.F. AMPLIFIERS by A. L. Hopper (Bell Labs.); Proc. 1960 Natl. Electronics Conf., pp. 152-156

An improved circuit for the gain control of transistor IF amplifiers is described in which the emitter circuit of a grounded base stage is shunted by a diode connected between the control voltage and a constant current source. The transistor stages are coupled by matched double tuned parallel-to-series transformers. This combination permits gain reduction by lowering emitter current without the usual compression at high input levels and band shape distortion due to effects of impedance mismatch. The design of AGC circuitry is simplified since little or no d-c gain is required and an inherent threshold is provided.

Non-Linear Distortion in Almost-Linear Networks - See 7095

7129 CALCULATION OF THE DISTORTION AND CURRENT EFFECTS IN TRANSISTOR AMPLIFIER STAGES ON THE BASIS OF EQUIVALENT CIRCUIT DIAGRAM [in German] by J. S. Vogel and M. J. O. Strutt (ETH); Arch. Elekt. Uebertragung, Vol. 14, pp. 397-404, Sept. 1960

Approximations for the input and transfer characteristics of a transistor by a sum of exponential functions which permit the evaluation of non-linear distortion effects such as the generation of harmonics, modulation rise, distortion of modulation and cross-modulation of junction transistors are described. The calculations are carried out in the low frequency range for various permissible values and are then applied to two-stage amplifier circuits. The extension of the theory, necessary to evaluate distortion at high frequencies, is indicated.

Transistor D-C Galvanometer Driver Amplifier - See 7203

D-C Amplifier Misalignment - See 7194

7130 DESIGN OF TRANSISTOR VIDEO AMPLIFIERS by H. Hodara (Hallicrafters), E. E. Waller (Armour Res. Found.), and S. A. Yefsky (Cook Electric); Proc. 1960 Natl. Electronics Conf., pp. 549-569

A systematic design procedure for transistor video amplifiers is developed. The premises on which the design procedure is based are, 1) The establishment of a suitable equivalent circuit for the frequency ranges of interest, based on the low-frequency T circuit; 2) The use of a gain-bandwidth trading technique analogous to that used in vacuum tube video amplifier practice; 3) The use of reactive compensating networks to increase the resulting gain-bandwidth product. It is shown that the iterative stage possesses inherent gain-bandwidth trading properties, and that additional flexibility in using this property is achieved with emitter degeneration. A design parameter m is introduced in the use of reactive compensating networks. A set of universal curves is presented showing stage responses as a function of m and other circuit and transistor parameters. Input and output stage requirements are also considered.

Design of Video Current Amplifiers - See 7165

7131 A MICROSYSTEMS BANDPASS AMPLIFIER by W. D. Fuller and P. S. Castro (Lockheed); Proc. 1960 Natl. Electronics Conf., pp. 139-151

The design and fabrication of physically-small electronic circuits and subsystems based upon materials integration, distributed parameter networks and techniques of vacuum deposition are discussed. One of the important parts of the fabrication process is termed "dynamic testing" as it is accomplished during the fabrication process and is a measurement of the operation of the total circuit being fabricated. Frequency selective networks have been synthesized from a thin film structure consisting of alternate layers of resistive and dielectric materials. Eight particular RC distributed parameter frequency selective networks have been synthesized and analyzed with respect to their impedance levels, shape of the selective characteristic, and the RC products for a specified frequency. The theory of feedback amplifiers using these distributed networks was then investigated, leading to the design of an IF bandpass amplifier. The morphology of this amplifier is based on a one-inch square substrate of barium titanate with a dielectric constant of 1700. The patterns of resistive and conductive materials are deposited in a sequential process. The active elements are added to the substrate after the deposition of the conductive material. During the deposition of the resistive material, the gain, center frequency and bandwidth of the amplifier stage are dynamically monitored.

Carrier-Frequency Transistor Amplifier - See 7095

Regenerative Pulse Amplifier - See 7168

7132 ANALYSIS OF THE STABILITY OF TUNED TRANSISTOR AMPLIFIERS by Iu. L. Simonov; Radio Engrg. Electronics, Vol. 5, No. 3, pp. 105-117, 1960

The stability of tuned transistor amplifiers is analyzed by the method of input admittance. The stability conditions are derived with relationships for the limiting stable gain of tuned amplifiers with various numbers of stages.

7133 PARAMETRIC AMPLIFICATION by M. O. Thurston

(Ohio State U.); U.S. Gov. Res. Rep., Vol. 34, p. 577(A), Nov. 18, 1960 PB 149 166

The capabilities and limitations of parametric amplifiers of the non-linear capacitance type are discussed. The dependence of junction capacitance on bias voltage for various special impurity distributions near the junction has been calculated theoretically. It is found possible to obtain a moderately large rate of change of capacitance with voltage at a reverse bias voltage large enough to make the capacitance itself small. The implications of this design for high-frequency, high-sensitivity amplifiers are considered. Diodes embodying this idea have been constructed and initial tests have been made. In support of the work on diode characteristics it was found necessary to extend the theory of parametric amplifiers. The results obtained permit the performance of a parametric amplifier to be related to the capacitance characteristic of the diode, even at moderately high signal level. Experimental frequency multipliers and parametric amplifiers have been constructed and tested at various frequencies from audio to 23 kMc.

7134 OPTIMUM NOISE AND GAIN-BANDWIDTH PERFORMANCE FOR A PRACTICAL ONE-PORT PARAMETRIC AMPLIFIER by J. C. Greene and E. W. Sard (Airborne Instr. Lab.); Proc. IRE, Vol. 48, pp. 1583-1590, Sept. 1960

A practical one-port parametric amplifier is analyzed to determine the conditions under which minimum effective noise temperature and maximum gain-bandwidth product can be obtained. The analysis considers the effects of resistive loss and stray parasitic reactance in the junction diode that provides the essential nonlinear reactance. It is shown that the conditions necessary for minimum noise temperature are compatible with those necessary for maximum gain-bandwidth product only if the diode has a high self-resonant frequency (the frequency at which the average diode capacitance resonates with the diode lead inductance). It is also shown that minimum noise temperature is always achieved when the diode loss alone is used as the idler circuit loading (regardless of the temperature of any additional idler loading), that there is a characteristic figure of merit for the diode, and that there is an optimum pump frequency. Based on the equations derived, universal curves that enable an optimum amplifier to be designed for specified signal frequency and diode characteristics are given. In conclusion, it is shown that if junction diode parametric amplifiers operated at room temperature are to challenge seriously the low-noise performance of the maser at microwave frequencies, a substantial improvement in the diode figure of merit is required.

7135 SYMMETRICAL MATRIX ANALYSIS OF PARAMETRIC AMPLIFIERS AND CONVERTERS by S. Deutsch (Polytech. Inst. Brooklyn); Proc. IRE, Vol. 48, pp. 1595-1602, Sept. 1960

It is shown that the parametric amplifier and frequency converter can be described by four equations whose coefficients form a matrix that is symmetrical. Because of this symmetry, the calculations for gain, bandwidth, and noise figure yield simple and manageable results. By regarding the matrix as a nodal admittance array, an equivalent conductance circuit is constructed. The derived expressions show that, for low noise figure, the idle-frequency should be much higher than the signal-frequency. This is also the requirement for wide bandwidth. Numerical examples of amplifier and converter design are given.

7136 SOME LIMITATIONS ON PARAMETRIC AMPLIFIER NOISE PERFORMANCE by R. D. Weglein (Hughes Aircraft); IRE Trans., Vol. MTT-8, pp. 538-544, Sept. 1960

Two practical limitations which set an upper bound to the performance of solid-state parametric amplifiers are discussed: First, for a given diode Q and junction geometry, there exists a noninfinite idler frequency, which determines the lowest radar noise temperature. Second, because of its extreme noisiness the reverse-breakdown current limits the maximum capacitance swing at both extremes and consequently the minimum noise performance. It is suggested that in certain cases refrigeration may be a partial remedy to both limitations.

Figure of Merit for Varactor Diodes - See 7081

7137 PARAMETRIC AMPLIFICATION PROPERTIES IN TRANSISTORS by R. Zuleeg (Hughes Aircraft) and V. W. Vodicka (Gen. Telephone); Proc. IRE, Vol. 48, pp. 1785-1786(L), Oct. 1960

A parametric amplifier transistor operating in an up-conversion mode which gives 72 db conversion gain at 450 mc with a signal-to-noise ratio of 21 db at 20 kc bandwidth and 1 μv input is reported. Maximum oscillation frequency is 600 mc. Parametric-amplifier transistors can be made with larger dimensions for a given frequency to provide higher power handling capability. The variable reactance properties necessary for parametric amplification have been designed into experimental germanium transistors. At a particular frequency, the input impedance can be made real for a specific current (current tuning). With feedback operation and current tuning in the new mode, 66 db conversion gain was obtained at 350 mc compared to normal gain of 5 db. Extension of the useful frequency range of transistors to 5 - 10 kmc is likely in the near future.

7138 COUPLED-CAVITY TRAVELING-WAVE PARAMETRIC AMPLIFIERS: PART I - ANALYSIS by M. R. Currie (Hughes Res. Labs.), and R. W. Gould (Calif. Inst. Tech.); Proc. IRE, Vol. 48, pp. 1960-1973, Dec. 1960

A general class of traveling-wave parametric amplifiers based on coupled-cavity filter circuits is described. This type of amplifier which is particularly suited to microwave frequencies, incorporates new features that overcome some severe difficulties associated with other circuit structures. Traveling-wave diode-type amplifiers having relatively wide bandwidths and great simplicity at S band have resulted from this approach. An analysis is presented which provides detailed information on operating characteristics, including the effects of terminal impedances, reflected waves, circuit loss, etc., and also leads to a simple physical picture of the cumulative interaction mechanism in terms of coupled-mode concepts. Gain bandwidth considerations are discussed in terms of a fundamental "interaction-impedance" parameter. Representative calculated curves show that unilateral gains of 12 to 15 db over relatively wide bandwidths are attainable with as few as 4 to 6 diodes. Methods of increasing the gain through use of ferrites and special circuit techniques are proposed.

7139 COUPLED-CAVITY TRAVELING-WAVE PARAMETRIC AMPLIFIERS: PART II - EXPERIMENTS by K. P. Grabowski and R. D. Weglein (Hughes Res. Labs.); Proc. IRE, Vol. 48, pp. 1973-1987, Dec. 1960

The filter-circuit approach to broadband traveling-wave parametric amplification at microwave frequencies is described from an experimental point of view. The experiment revolves around

a series of inductively coupled microwave cavities, each loaded with one variable-capacitance semiconductor diode. Gain-bandwidth products of 2000 Mc with a 350-Mc bandwidth at S band have been obtained by using commercially available diodes. Noise temperatures of 130°K have been measured. A qualitative prediction of the gain-frequency behavior is given and the experimental arrangement is set forth in some detail. It consists of a series of these coupled cavities with separate pump power distribution at each diode. Through this flexibility in pump phase shift and amplitude, a variety of advantages is achieved. The effects of the many variables on the performance of the amplifier are described. Several methods of achieving short-circuit stability of this amplifier are outlined. These are: 1) nonuniform pump phase shift between sections, 2) nonreciprocal loss with ferrites, and 3) nonreciprocal loss with upper pass bands. The experimental behavior of each method is shown, and the noise performance to date is briefly discussed.

7140 TUNABLE PARAMETRIC AMPLIFIER FOR THE 350-1200 MC FREQUENCY RANGE by N. C. Gittinger (GE); Proc. 1960 Natl. Electronics Conf., pp. 462-471

The design and construction of a continuously tunable parametric amplifier for the 350-1200 Mc frequency range are described. The amplifier is of the negative resistance type, utilizing a fixed pump frequency and separate, independently adjustable signal and idler cavities. The theoretical effect of the pump to idler frequency ratio, the degree of antenna and second stage coupling, and the use of isolators and circulators on the noise figure and the gain-bandwidth product of the amplifier are discussed. The measured performance of the amplifier is compared with the theory. The effect of ambient temperature and pump signal variations on the performance and stability of the amplifier is discussed. The critical stability and incidental modulation requirements of the pump source are pointed out.

7141 A NOTE ON THE DESIGN OF COMMON-EMITTER DISTRIBUTED AMPLIFIERS by C. W. McMullen (Northwestern U.); Proc. 1960 Natl. Electronics Conf., pp. 570-574

In designing a common-emitter distributed amplifier, the important parameters of the transistor are its transconductance, its input and output capacities, and its input and output conductances. An analytical and experimental study has shown how these parameters can be controlled in order to achieve an optimum amplifier design. A summary of the most significant results of this study are given.

7142 DESIGNING SHUNT-PEAKED TRANSISTOR AMPLIFIERS by R. S. Pepper and D. O. Pederson (Univ. of Calif.); Electronics, Vol. 33, pp. 68-70, Dec. 2, 1960

Design equations and examples for two methods of designing shunt-peaked transistor amplifiers are presented. The pole-zero cancellation method and the maximally flat magnitude method equations are developed and circuit design examples for each case are worked out. Agreement between calculated and experimental results is within a few percent. A table of symbols and definitions and one of transistor parameters are given.

7143 EXACT THEORY AND SYNTHESIS OF A CLASS OF TUNNEL DIODE AMPLIFIERS by L. I. Smilen and D. C. Youla (Brooklyn Polytechnic Inst.); Proc. 1960 Natl. Electronics Conf., pp. 376-404

The design of a practical negative resistance amplifier which uses a single tunnel diode in conjunction with a lossless, reciprocal two-port equalizer is described and two configurations of this class of amplifiers are considered. The Transmission amplifier has the lossy generator and load terminating opposite ports of a lossless two-port and the diode across either port. In the Reflection amplifier, the generator and load are in shunt across one port and the diode is across the second port, of the equalizer. A gain-bandwidth restriction exists for any tunnel device because of the presence of its parasitic capacitance. The limitation on the transducer power gain function for each configuration is given in the form of an integral inequality. Using these relations the maximum flat gain attainable over a band of frequencies is derived. Exact expressions for the Butterworth and Tchebycheff responses of the Transmission amplifiers are given. These characteristics are not realizable with a Reflection amplifier since the rate of falloff of its response cannot exceed 6 db/octave. However, it is capable of closely approximating a Butterworth response over a wide band of frequencies. A precise theory for these transducers, which derives their sensitivity behaviors, noise figures and stability performances, has been developed. Straightforward synthesis procedures for the realization of the Transmission amplifiers to give Butterworth and Tchebycheff responses are given. The Reflection amplifier is synthesized to have a Butterworth equalizer. In each case the matching network is a lossless ladder. The synthesis is simplified by a set of general design formulas and curves. Each synthesis procedure is illustrated by a design problem.

7144 SYSTEMS USING TRANSISTORS AND TRANSDUCTORS by D. A. Ramsay (GE Ltd.); Electronic Engrg., Vol. 32, pp. 476-479, Aug. 1960; pp. 540-544, Sept. 1960; pp. 640-643, Oct. 1960

Transistors are limited in voltage and power level and are sensitive to temperature variation. Transductors (saturable reactors) do not have these particular limitations and for some applications these two devices have complementary properties so that their combination provides advantages over the use of one or the other alone. In particular, a transistor control element can be incorporated with transductors to provide amplifiers which are not limited in output power or voltage. Also, highly efficient power amplifiers can be formed with circuits analogous to those of magnetic amplifiers, but in which the output transductor elements are replaced by switching transistors or by controlled silicon rectifiers; in these circuits transductors can be very suitable as control elements. Especially in conjunction with switching transistors, the useful properties of transductors can be exploited to provide small, robust and highly efficient systems.

7145 POWER AMPLIFIERS BASED ON ELECTRO-OPTICAL EFFECTS; A SURVEY by G. Diemer and J. G. Van Santen (N. V. Philips); Philips Res. Rep., Vol. 15, pp. 368-389, Aug. 1960

Electro-optical effects (such as electro-luminescence, photoconduction and combinations thereof) as well as devices based on these effects are discussed from the point of view of power amplification. Special features arise from the change in nature of the power (electric to radiation or vice versa) and from energy transport by quantum radiation. A survey of applications along these lines is given.

OSCILLATORS

7146 A PHASE STABILIZED VLF OSCILLATOR by R. M. Truesdell (Collins Radio); Proc. 1960 Natl. Electronics Conf., pp. 735-743

Design and construction considerations for a step-tuned, very low frequency stabilized master oscillator having a long term frequency stability of one part in 10^8 for a period of one day are discussed. Design considerations necessary to produce a short term jitter of not greater than ±3 degrees are also discussed. The loop bandwidth requirements of this system must necessarily be limited to approximately 30 cps in order to minimize 100 cps spectrum point modulation of the 49 to 64.9 kc output. Compromise methods to reduce sidebands and at the same time minimize envelope phase shift around the loop are presented. A unique 100 cps step-tuned master oscillator used in the system is discussed. Use of a transistor stage, operating as a reactance multiplier, for automatic phase control of the master oscillator module is described. Other special features of the system include a high stability modular frequency standard, an automatic full-control phase-lock indicator, an AGC-controlled output amplifier and a remote-controlled autopositioner for 100 cps stepping. The system is designed for rack mounting and utilizes both modular and card cage construction.

7147 INVESTIGATION OF A TRANSISTOR LC-OSCILLATOR by M. I. Kontorovich, S. G. Pellikan, and V. N. Frolov; Radio Engrg. Electronics, Vol. 5, No. 3, pp. 118-132, 1960

A non-linear theory for a junction transistor oscillator is presented. Relations defining the amplitude and frequency of oscillation are derived. Recommendations are made for the design of oscillator circuits and theoretical conclusions are compared with experimental results.

7148 THE INFLUENCE OF TRANSISTOR SATURATION UPON THE MULTIVIBRATOR OPERATION by V. A. Kuz'min and B. N. Vinogradoso (M. V. Lomonosov Moscow State U.); Radio Engrg. Electronics, Vol. 5, No. 3, pp. 190-198, 1960

A method, applicable to various pulse circuits, for calculating the resorption time of excess charge carriers in a transistor base is presented. The effects of saturation on the rise time and duration of pulses in a junction transistor multivibrator are studied theoretically and experimentally.

7149 CALCULATION OF PULSE DURATION IN A TRANSISTOR BLOCKING OSCILLATOR by V. A. Kuz'min (M. V. Lomonosov Moscow State U.); Radio Engrg. Electronics, Vol. 5, No. 3, pp. 199-206, 1960

The pulse duration for a common emitter transistor blocking oscillator is calculated theoretically. Experimental verification of the results obtained has been carried out.

7150 ESAKI DIODE OSCILLATORS FROM 3 TO 40 KMC by R. Trambarulo and C. A. Burrus (Bell Labs.); Proc. IRE, Vol. 48, pp. 1776-1777 (L), Oct. 1960

The properties of gallium arsenide Esaki junction diode oscillators with fundamental power to 40 kMc and harmonic output to 63 kMc are discussed. The maximum fundamental power measured was 3.5 μw at 37 kMc, using diodes having peak currents in the 300-700 μa range. The junctions are formed by alloying tin to zinc-diffused gallium arsenide, and aluminum to germanium doped with arsenic. Impurity concentration in the germanium is approximately 6×10^{19} and resistivity is 0.0015 ohm-cm. Peak currents from less than 100 μa to more than 30 ma were obtained with peak-to-valley current ratios greater than 2:1 and commonly 6:1. Results indicate that gallium arsenide diodes have a lower barrier capacitance than germanium units of the same negative resistance.

7151 TRANSISTOR BETA-PHASE-SHIFT OSCILLATOR by A. R. Saha (Jadavpur U., Calcutta); J. Electronics Control, Vol. 9, pp. 113-125, Aug. 1960

A junction-transistor oscillator circuit which makes use of the internal phase-shift of a transistor and only a single C-R section as the external phase-shifting network is described. Advantage is taken of the low-input impedance of a common emitter junction transistor. Analytic expressions for the frequency of oscillation and minimum voltage feedback factor for sustained oscillations have been deduced. Calculated values of frequency and minimum voltage feedback factor are shown to compare favorably with the experimental values. A range of oscillation frequency extending to several times the cut-off value of the transistor is shown to be obtainable.

SWITCHING CIRCUITS

7152 TRANSISTOR TRIGGER CIRCUIT STABILIZATION by H. Mann (Bell Labs.); U.S. Pat. 2,964,655, Issued Dec. 13, 1960

A technique for preventing the triggering point of a two-stage regenerative amplitude comparison circuit from drifting with temperature is described. One Zener diode is connected to fix the maximum collector voltage of the first stage when the first stage is conducting, and a second Zener diode is connected to fix the maximum voltage drop between the collector electrode of the first stage and the base electrode of the second. As the temperature rises, the breakdown voltage of each diode increases by approximately the same amount. The increase in potential of the collector electrode of the first transistor is offset by an increase in breakdown voltage in the second diode, and a subsequent increase in the potential at the base of the second transistor.

7153 A CASCODE TRIGGER CIRCUIT USING A PNP AND NPN TRANSISTOR by P. Arnoldt (W. G. A. Whitworth Aircraft Ltd.); Electronic Engrg., Vol. 32, pp. 620-623, Oct. 1960

A monostable trigger circuit employing a pnp and an npn transistor in a cascode arrangement is described. The circuit, when preceded by a diode pump integrator, forms a frequency dividing stage. Optimum conditions to ensure the safest operation with temperature variations are derived. Practical values for a stage reliably dividing by 10 over a temperature range of 5° to 50°C with input pulses of 100 kc/s are given. The output pulse of such a stage is suitable for driving the input of a subsequent stage. The trigger circuit can also be employed to generate sawtooth waveforms or operate as a time modulator.

Tunnel Diode Trigger Circuits - See 7179

7154 HIGH-CURRENT SOLID-STATE SWITCHES by C. H. Price, Jr. (Northeastern U.); Electronics, Vol. 33, pp. 72-73, Sept. 16, 1960

A high-current transistor switch with a saturation resistance of

0.0296 ohms which delivers 610w to the load is described. A hybrid multivibrator, using pnp transistors and a unijunction transistor as a timer and trigger, produces an unsymmetrical output. A cascaded emitter follower provides isolation between the multivibrator and driver stages. The output transistor is reverse biased to prevent thermal runaway. The driving pulse is coupled by Zener avalanche breakdown saturating the output transistor and providing a large current pulse.

Electro-Optical Switch - See 7221

SIGNAL CONVERTERS

7155 CIRCUIT PROPERTIES OF A DOUBLE-SIDEBAND, DOUBLY-PUMPED NONLINEAR REACTANCE MODULATOR by D. K. Adams (U. Michigan); Proc. 1960 Natl. Electronics Conf., pp. 480-486

A circuit is considered in which a lossless nonlinear capacitance couples the frequencies ω_0, ω_1, ω_2, ω_3 and $2\omega_0$; where $\omega_2 = \omega_0 + \omega_1$ and $\omega_3 = \omega_0 - \omega_1$. Both ω_0 and $2\omega_0$ are taken as pump frequencies, and are assumed to be phase locked. The method of approach is a small-signal analysis. Arbitrarily large unilateral conversion gains are shown to be possible between any two of the three frequencies: ω_1, ω_2, and ω_3. Particular attention is given to a case providing: 1) simultaneous unilateral conversion gain between ω_1 and ω_3 and between ω_2 and ω_3, and 2) gain-independent, conjugately-matched terminal admittances at ω_1 and ω_2. It is shown that noise figures, gain-bandwidth products, and parameter sensitivities compare favorably with conventional nonlinear reactance circuits, even when the latter employ circulators. Also, effects of losses internal to the nonlinear capacitance are included by perturbation.

Semiconductor Diode Modulator for D-C Current Measurement - See 7202

Semiconductor Microwave Carrier Injection Modulator - See 7109

7156 TUNNEL DIODE CONVERTERS by C. S. Kim and J. E. Sparks (GE); Proc. 1960 Natl. Electronics Conf., pp. 791-800

The circuit requirements for tunnel diode converter operation are considered. Two classes of self-oscillating converters are compared. One type contains two tuned circuits and operates on the fundamental of the oscillation frequency. The other type, which has three tuned circuits, utilizes the oscillator harmonics. The independent tuning capability of the harmonic converter makes it easier to discriminate against the noise contribution of the image frequency band. A generalized analysis of tunnel diode converters is presented using a three-port equivalent circuit as a model. Expressions for available gain, normalized bandwidth, and noise figure are obtained.

Symmetrical Matrix Analysis of Parametric Converters - See 7135

7157 LARGE SIGNAL ANALYSIS OF A PARAMETRIC HARMONIC GENERATOR by K. M. Johnson (Hughes Aircraft); IRE Trans., Vol. MTT-8, pp. 525-532, Sept. 1960

Large signal analysis of a harmonic generator using a semiconductor diode reveals a larger possible efficiency than a similar small signal analysis. As higher harmonic numbers are reached, large signal analysis becomes increasingly more important in predicting the maximum conversion efficiency. It is shown that there exists an optimum value for the diode bias voltage and an optimum coupling of the load and generator to the diode, and that the diode operating voltage should almost drive the diode into conduction. An expression for the maximum conversion efficiency for any harmonic is derived, and it is shown that the conversion loss increases with increasing harmonic number, approximately 2.9 db per n for large harmonic numbers in a typical case.

Harmonic Generation with "Gradual Grade" Diffused Si Junction Diodes - See 7115

7158 REGENERATIVE FRACTIONAL FREQUENCY GENERATORS by S. Plotkin and O. Lumpkin (Hoffman Electronics); Proc. IRE, Vol. 48, pp. 1988-1997, Dec. 1960

A new regenerative frequency divider circuit which offers several advantages over other available circuits is presented. These advantages are large lock-in or "stability" range, ability to produce either relatively constant output or amplitude modulated output, circuit simplicity and the fact that it is self-starting. An approximate nonlinear analysis which provides a reasonable prediction of the operation is given. This analysis is a quasi-linear, semigraphical technique which clearly shows the dependence upon diode characteristics and transistor input impedance. Results are also given for harmonic generation giving a fractional frequency output and not merely a subharmonic.

Frequency Divider Using a Transistor Cascode Trigger Circuit - See 7153

WAVEFORM GENERATORS

7159 GENERATOR DELIVERS CONSTANT CURRENT OR VOLTAGE PULSES by L. A. Rosenthal (Rutgers U.); Electronics, Vol. 33, pp. 82-84, Sept. 16, 1960

A pulse generator which provides a 0 - 10v constant voltage pulse or a 0 - 10amp constant current pulse with time duration of 100-1000 μsec is described. A thyratron provides pulse width timing and base current drive to a pulse shaping transistor connected as an emitter follower. The transistor is saturated, placing a regulated voltage across the emitter resistor. An inductor across the base circuit reduces storage time to 10μsec. The shaped pulse is direct coupled to a linear output transistor connected as an emitter follower. For a constant voltage output, a low impedance load is placed in the emitter. For constant current, one ohm is used in the emitter and the load placed in the collector. Internal resistance is 295 ohms in the constant current mode and 0.1 ohm in the constant voltage mode. The generator is useful in the study of electrothermal parameters.

7160 HIGH-POWER PULSE GENERATION USING SEMICONDUCTORS AND MAGNETIC CORES by E. M. Lassiter, P. R. Johannessen and R. H. Spencer (MIT); Commun. and Electronics, No. 51, pp. 511-517, Nov. 1960

An experimental magnetic pulse generator which can be used as a radar modulator is described. The generator utilizes a p-n-p-n silicon controlled rectifier as an electronic switch in the charging circuit. In the discharge network saturable inductors operate as high-power switching devices and, together with the capacitors, reduce the duration of the current pulse from a long duration at the charging circuit to a short duration at the output. The circuit operates at a repetition rate of 5 kc and produces an average power output of 300 w. The peak power and pulse width at the output are approximately 40 kw and 1.5 μsec, respectively. The efficiency of the circuit, not considering the bias circuit, is approximately 70%.

Sawtooth Waveform Generator - See 7153

APPLICATIONS OF SOLID STATE DEVICES

MEDICAL

7161 A TRANSISTOR CARDIOTACHOMETER FOR CONTINUOUS MEASUREMENTS ON WORKING PERSONS by G. A. Harten and A. K. Koroncai (N. V. Philips); Philips Tech. Rev., Vol. 21, No. 10, pp. 304-308, 1959/1960

Investigations into the physiological aspects of work call for a means of continuously measuring the heart rate of persons engaged on their normal work, where it is evidently not feasible to take the pulse in the normal way. In the apparatus described the individual heart beats are converted into electrical pulses by arranging for a beam of light transmitted through the lobe of the ear to fall on a phototransistor. Each pulse causes a miniature transistorized transmitter to transmit a note of 3000 c/s on a carrier of 10-15 Mc/s. Together with aerial and Ni-Cd batteries, this part of the equipment weighs about 3 lbs, and is carried on the back. The transmitted signals are picked up by a conventional radio receiver and either counted directly or applied to a recording count-rate meter (range 1-3 c/s; time constant ~5 sec). Rapid changes in heart rate can be faithfully recorded by means of a special circuit that supplies pulses whose amplitude is a measure of the time between two heart beats.

Intercardiac Catheter Tip Piezo-Resistive Pressure Gauge - See 7117

7162 TRANSISTORIZED RATEMETER DESIGN by J. F. Marvin, W. D. Miller and M. K. Loken (U. Minnesota Hospitals); Rev. Sci. Instr., Vol. 31, pp. 1238-1240, Nov. 1960

A transistorized ratemeter featuring lower power requirements, smaller space consumption, superior reliability and durability together with the stability of vacuum tube circuits in a-c operation which has been developed to make practicable multiple channel in vivo counting systems for use in x-ray or operating rooms is described.

7163 MINIATURE SEMICONDUCTOR DOSE RATE METER by C. H. Hertz and R. Gremmelmaier (U. Lund and Siemens); Acta Radiol., Vol. 54, pp. 69-80, July 1960

A small roentgen dose rate meter which utilizes the photoeffect in a GaAs p-n junction to make measurements inside body cavities is described. Because of the special geometry of the probe element its energy dependence in the conventional roentgen therapy range is reduced and is quite satisfactory inside a water phantom. The length of the cylindrical probe is 10 to 25 mm, its diameter 2.5 mm, and its sensitivity about 3×10^{-9} A per r/min.

MILITARY

7164 PROJECTILE TELEMETRY WITH MICROWAVES by W. M. Kendrick and L. A. Peters (Aberdeen Proving Ground); Electronics, Vol. 33, pp. 68-71, Sept. 16, 1960

Determining projectile acceleration during firing by modulating a 24,000 Mc beam at a frequency dependent upon projectile acceleration is described. An externally generated microwave beam is transmitted along the gun barrel and amplitude modulated by a transducer system in the projectile. A portion of the beam is transmitted through a ferrite rod in the projectile with a rotation approaching 45° maximum and reflected back through the rod with additional rotation, the amount dependent upon the strength of an applied alternating magnetic field. The rotated portion and the portion simply reflected from the projectile form a resultant whose amplitude depends on the amount of rotation in the ferrite. A variable capacitance gage controls a Clapp oscillator which feeds a mesa transistor amplifier to provide the alternating magnetic field. The gage produces an oscillator frequency shift of 2 kc per 1000 psi with a range of 10,000 psi and an initial capacitance of 20 pf.

TELEVISION

7165 TRANSISTORS IN VIDEO EQUIPMENT by P. B. Helsdon (Marconi's Wireless Tel.); J. Soc. Mot. Pict. TV Engrs., Vol. 69, pp. 404-405, June 1960; J. Brit. IRE, Vol. 9, pp. 753-768, Dec. 1959

The principles involved in the design of video current amplifiers for television using transistors are discussed in terms of the hybrid-pi equivalent circuit. The importance of the current gain bandwidth factor is emphasized and a design philosophy which exploits an unconventional concept of gain-bandwidth is presented. An investigation of noise with regard to camera head amplifier design gives the transistor parameters and circuit conditions necessary for maximum signal-to-noise ratio. Experimental confirmation shows transistors to be comparable with vacuum tubes in this application.

7166 A TRANSISTORIZED HORIZONTAL SWEEP CIRCUIT AND A TRANSISTORIZED HIGH VOLTAGE GENERATOR FOR A TELEVISION SET by D. J. Herick, H. Pelzl, and P. A. van

TELEVISION (Cont'd)

Berkum (Zenith); Proc. 1960 Natl. Electronics Conf., pp. 713-728

A transistorized horizontal deflection circuit and a high voltage generator for a portable television set are described. The peak magnetic energy in the yoke equals 536 microjoules and is enough to scan a 72° diagonal angle, 1-1/8" neck diameter tube with a high voltage of 9 kv. If the high voltage current equals 375 microamperes, the total power dissipation is 11.15 w. The efficiency of the high voltage generator, which can also be used separately, exceeds 50%.

TELEPHONY

7167 THE E6 NEGATIVE IMPEDANCE REPEATER by A. L. Bonner, J. L. Garrison and W. J. Kopp (Bell Labs.); Bell Sys. Tech. J., Vol. 39, pp. 1445-1504, Nov. 1960

A low-cost, transistorized, voice-frequency two-way repeater for use in the exchange area plant, including use in trunks between local offices and between local and toll offices is described. It permits both types of trunks to be operated at low net loss, while meeting the impedance requirements placed on trunks between local and toll offices. These features are possible because of a unique method of repeater design, in which the impedance-matching function and the gain function are allocated to separate portions of the repeater and are separately adjustable. The impedance-matching function is accomplished by means of a line building-out network, which permits any cable pair associated with the repeater to be built out and made to match the impedance of the toll office. The gain unit presents the same image impedance, which is essentially independent of gain adjustment. Changes in gain are controlled by two resistive, adjustable networks — one in the series-connected negative impedance converter, and the other in the shunt-connected converter. In previous designs of negative impedance repeaters, complex impedance networks were required for adjustment of both gain and impedance match. The E6 repeater also incorporates novel mechanical features, with transistorization resulting in low power drain and less heat dissipation in the telephone central office. Power is derived from the existing 48-volt central office battery.

7168 A TRANSISTORIZED PULSE CODE REPEATER by G. R. Partridge (Raytheon); Semicon. Prod., Vol. 3, pp. 31-35, Sept. 1960

A pulse amplifier, or repeater, for regenerating a train of pulses in a PCM cable system is described. The repeater operates at 1152 kc, uses about 400 milliwatts of power, and has 26 transistors. The repeater amplifies traffic in each direction in a 24 channel system, and includes fault locating facilities and a loading coil for a voice frequency order wire. Satisfactory operation is obtained over a temperature range from -55 to +65 degrees Centigrade. Problems found in the preamplifier and retiming portions of the repeaters are discussed and the output amplifiers and fault locating system are described.

RADAR

Magnetic Pulse Generator for a Radar Modulator - See 7160

Pulse Amplitude Interpolation Computer for Doppler Radar - See 7195

Solid State Radar Transponder - See 7223

MICROWAVES

7169 THE GENERATION OF MICROWAVE ELECTROMAGNETIC RADIATION IN MAGNETIC MATERIALS by J. H. Rowen and F. G. Eggers (Bell Labs.); Sixth Conf. Magnetism and Magnetic Materials, Nov. 14-17, 1960, New York, N.Y.

The generation of microwave electromagnetic energy in a single crystal YIG by direct conversion of low frequency input signals was described. Through a novel means of excitation an effective driving field can be achieved at the harmonic frequency with an amplitude which is determined by the magnitude of the anisotropy energy so that the amplitude of even the high order harmonics is still quite large. On the basis of quite conservative assumptions it is shown that the amount of power radiated at the harmonic frequency is ultimately limited by the level of the spin wave breakdown and that power outputs of the order of several watts or more per cubic centimeter are theoretically possible. In the experimental verification of this principle a spherical sample 0.035" in diameter was excited by a driving frequency of 9.2 Mc, and output signals in the S-band range were observed. The output signals exhibited the proper dependence on static magnetic field and were estimated to be approximately 10^{-8} watts in amplitude. While this amplitude is far below the level predicted above, it is still quite large enough to provide unmistakable verification of the principle and to suggest that further experimental refinements may result in significant output. In order to generate signals in the millimeter range one must employ materials having higher anisotropy, and it is suggested that ultimately antiferromagnetic resonance excited by an analogous technique can be employed.

RECORDING AND REPRODUCTION

7170 A TRANSISTORIZED PORTABLE MAGNETIC FILM RECORDING CHANNEL by C. E. Hittle, M. Rettinger and K. Singer (RCA), J. Soc. Mot. Pict. TV Engrs., Vol. 69, pp. 593-598, Sept. 1960

A portable, magnetic film recording channel, designed with a transistorized mixer and recorder plus some accessories, is described. The mixer provides for switching, equalizing, and mixing of up to four microphones. Two independent vu meters indicate recording and magnetic playback levels. Optional accessories consist of microphone impedance matching transformers, precision gain controls, and transistorized compressor. A high-gain transistorized playback amplifier and bias oscillator are located in the recorder.

7171 DURABLE HIGH-RESOLUTION FERRITE TRANSDUCER HEADS EMPLOYING BONDING GLASS SPACERS by S.

Duinker (N. V. Philips); Philips Res. Rep. Vol. 15, pp. 342-367, Aug. 1960

The magnetic and mechanical properties of a very dense, homogeneous and fine-grained ferrite are discussed with reference to its application as a material for making transducer heads for magnetic recording and reproducing for which it was specially developed as a substitute for laminated metallic alloys. The technique of producing transducer gaps by preparing ultra-thin (i.e., from less than one micron onwards), well-bonding and stress-free glass layers between polished ferrite surfaces is described, and the excellent qualities of such gaps as regards their optically and magnetically measured length and their wear-resistance are discussed. Several novel single- and multiple-track head constructions are outlined which, compared to existing assembling methods, are characterized by reduced production costs. This is because the expensive mechanical operations (polishing and gap preparation) can be confined to the most vital parts of the head (i.e., the frontal part containing the gap) and can be done for a large number of heads simultaneously in a prefabrication stage.

COMPUTERS

7172 DESIGN OF A HIGH SPEED PARALLEL SOLID STATE DIGITAL COMPUTER by I. C. Hinckfuss, R. J. Keith and I. J. Macaulay (Weapons Res. Est.); Proc. IRE, Aust., Vol. 21, pp. 581-590, Sept. 1960

The design of a surface barrier transistor digital computer is discussed. The logical operations of the parallel arithmetic unit (adder, multiplier, divider and square-rooter), the control unit and the immediate access magnetic core store of 1024 32-bit words is described. Anticipated operation times are: addition, $<8\,\mu$sec, multiplication $<40\,\mu$sec, division $\sim 40\,\mu$sec and square root $<80\,\mu$sec. Several ideas which, while using the same circuit techniques, will yield faster computation times are discussed. However, these ideas all imply much greater complexity in the computer logic.

7173 TRANSISTORIZED BUILDING BLOCKS FOR DATA INSTRUMENTATION by J. A. Cunningham and R. L. Hill (NBS); U.S. Gov. Res. Rep., Vol. 34, p. 611 (A), Nov. 18, 1960 PB 161 569

A number of modular transistorized digital circuits that have been used in automatizing data recording and preliminary processing tasks encountered in scientific operations are described. These versatile building blocks can be connected together systematically to form digital circuits that accept raw data from experimental equipment and transpose these data into a form suitable for input to a high-speed electronic computer. These blocks can be used where: (1) data are produced in large volumes; (2) data taking is extremely fast, extremely slow, or extremely precise; (3) a need exists to minimize human error, tedium and eyestrain; or (4) computation is extensive. Five major packages and 8 special-purpose packages are described.

7174 A THEOREM FOR DERIVING MAJORITY-LOGIC NETWORKS WITHIN AN AUGMENTED BOOLEAN ALGEBRA by R. Lindaman (Rem. Rand); IRE Trans., Vol. EC-9, pp. 338-342, Sept. 1960

Recent developments in computer technology have produced devices (parametrons, Esaki diodes) that act logically as binary majority-decision elements. Conventional design techniques fail to utilize fully the logical properties of these devices. The resulting designs are extravagant with respect to the number of components used and the operating time required. This paper reviews the conventional technique briefly and proposes an alternative method that produces more nearly minimal designs.

7175 STATIC SWITCHING by G. T. Ohlsen (Assoc. Elec. Ind. Ltd.); Electronic Engrg., Vol. 32, pp. 609-613, Oct. 1960

The purposes and advantages of static switching and its derivation from digital computer techniques are outlined. A comparison of existing techniques is made and a complete system employing transistor NOR units as the logic element is described, together with the treatment and solution of a simple problem.

7176 THE ELLIOTT SHEFFER STROKE STATIC SWITCHING SYSTEM by P. Kellett (Elliott Automation Ltd.); Electronic Engrg., Vol. 32, pp. 534-539, Sept. 1960

A system in which interconnections between a number of logic elements, all of the same type (the Sheffer Stroke), permit any logical configuration or switching sequence is described. The simple rules which restrain the interconnections are stated. A number of basic interconnections of general use are described and the 'Sheffer Stroke', the 'nor' and the better known 'and', 'or', 'not' logic elements are compared. Available power switches which may be controlled by the output of a logic element are described. Provision is made for connecting the loads in a matrix with considerable economy.

7177 IMPROVEMENTS TO CURRENT SWITCHING by F. K. Buelow (IBM); IRE Trans., Vol. EC-9, pp. 415-418, Dec. 1960

The use of diode switching circuits in conjunction with emitter followers and current switching circuits to evolve a new set of system building blocks is discussed. These blocks exhibit typical delays under five millimicroseconds. Diodes cost less and are physically smaller than transistors; therefore, this new system is cheaper and faster than an all-current switching system and permits at least a fivefold increase in packaging density.

7178 TUNNEL DIODE LOGIC CIRCUITS by R. H. Bergman (RCA); IRE Trans., Vol. EC-9, pp. 430-438, Dec. 1960

The switching properties of a monostable type of tunnel diode logic circuit are analyzed and found to depend upon the negative resistance-capacitance time constant of the unit. The basic function performed by the circuit is a thresholding operation from which a set of logical building blocks is derived. Compatible dynamic and bistable storage schemes are discussed. Of major importance is the effect of diode variations upon the logical gains and delays of the circuits. These properties have been tabulated for tunnel diodes with 5 per cent tolerances on knee current and voltage. Experimental circuits using diodes with a time constant of 1.4 nanoseconds have given a nominal switching time of 7.5 nanoseconds.

7179 ESAKI DIODE LOGIC CIRCUITS by G. W. Neff, S. A. Butler and D. L. Critchlow (IBM); IRE Trans., Vol. EC-9, pp. 423-429, Dec. 1960

A variety of digital computer circuits which utilize the properties of tunnel diodes is described. In particular, shift registers,

triggers, and counters are presented. The following shift registers are described: 1) A register which consists of one Esaki diode and one conventional diode per stage. Shifting is accomplished with a two-phase square-wave drive. The Esaki diode provides memory and power gain, and the conventional diode provides a unilateral flow of information. 2) A register which combines Esaki diodes with square-loop ferromagnetic cores. Again the Esaki diode provides memory and power gain. Upon application of a single-phase drive, the cores perform a gating operation depending upon the state of the diodes. 3) With the use of Esaki diode-transistor combinations, high-speed circuits are obtained which depend upon the Esaki diodes primarily for memory and the transistors for power gain and unilateral flow of information. The flip-flop and counter circuits are the following: 1) A binary counter using Esaki diodes with magnetic cores; 2) high-speed flip-flops using Esaki diode-transistor combinations.

7180 CALCULATED WAVEFORMS FOR TUNNEL DIODE LOCKED PAIR by H. R. Kaupp and D. R. Crosby (RCA); Proc. 1960 Eastern Joint Computer Conf., pp. 233-240

An introductory analysis of the tunnel diode locked pair circuit is presented. The characteristics of the tunnel diode, together with the simplicity of the locked pair circuit, makes it a major contender for use as a high speed computer element. High speed and high gain are the main advantages of the locked pair; the three phase power supply and lack of a simple means for logical inversion are its main disadvantages. The basic circuit consists of two tunnel diodes in series, the node common to the tunnel diodes being both the input and output terminal. As a computer element, the locked pair functions in much the same manner as the phase locking harmonic oscillator (PLO). Like the PLO, the locked pair overcomes the difficulty of coincident input and output terminals by using a three phase voltage source. The feasibility of using a digital computer to solve nonlinear circuit problems is also demonstrated. A digital computer makes possible an exact solution by doing away with relatively ineffectual linear approximation techniques. Furthermore, the stray parameters associated with laboratory work at high frequencies are excluded, thereby disclosing the true nature of the circuit.

Tunnel Diodes and Backward Diodes Designed for Use in Computer Logic Circuits - See 7218

7181 SIMPLIFIED DESIGN OF TRL GATING by J. S. Raskin (Hughes Aircraft); Proc. 1960 Natl. Electronics Conf., pp. 701-712

Previous methods of Transistor Resistor Logic gate design required the choice of an input resistor which allowed a compromise between crosstalk and fan-out. It is shown how the input resistor may be calculated in terms of the transistor parameters, power supply voltages, power dissipation per gate, fan-in, and fan-out. An analysis of the approach illustrates that the relationship of fan-in versus fan-out has been optimized. Two design equations are derived: 1) Optimum fan-in versus fan-out; 2) Input resistor as a function of transistor parameters, optimum fan-in and fan-out (found by number 1), and power supply voltages. With these equations, guesswork is eliminated and optimum solution is assured.

7182 SYSTEM APPLICATION OF HYBRID LOGIC CIRCUITRY by J. T. Lynch and J. J. Karew (Burroughs); IRE Trans., Vol. EC-9, pp. 418-423, Dec. 1960

The "Hybrid Transistor Diode Logic" (HTDL) circuit technique which employs either diodes or emitter follower transistors as gates and buffers to maximize the circuit performance rating is described. The HTDL technique combines the advantages of lumped and distributed gain circuits. The cascading of diodes and emitter followers in logical gate matrices can be analyzed as the transmission of binary signals through a video system of a given bandwidth. The HTDL technique optimizes the use of the transistor through nonsaturating, low-impedance circuitry. This optimum use of 200 - 500 megacycle gain-bandwidth transistors is primarily limited by present-day packaging techniques and their inductive and capacitive loading effects upon the circuits. The development of macromodule packaging techniques, using 200 - 500 Mc transistors, in HTDL circuitry, would permit system speeds (synchronous clock rates) to exceed 50 Mc.

7183 IMPULSE SELECTION FOR CORE LOGIC by R. H. Tancrell (Lincoln Lab.); Sixth Conf. Magnetism and Magnetic Materials, Nov. 14-17, 1960, New York, N.Y.

A new magnetic phenomenon observed with low coercive force ferrite cores which shows promise of meeting the various requirements for computer logic was described. Basically this magnetic property utilizes two thresholds of the magnetic material. One of the thresholds is time dependent, being a function of the width of an applied current pulse. The other threshold is related to the d-c coercive force of the saturated core, which can be changed electrically. With these properties, circuit possibilities can be achieved which in previous magnetic devices were performed by means of turns ratios on cores or by geometry configurations. Selection of a core is achieved by applying to the core an impulse of high current which lowers its coercive force. A low amplitude current, which is otherwise below the d-c coercive force, can then continue the switching process. In a logic scheme, the switching output of one core can be used directly to supply the current pulse to initiate switching in a receiver core. Most of the energy required to switch the receiver is supplied by a low amplitude current from an external generator. By this means 'flux gain' is achieved. Control of the information flow can be obtained by connecting cores in the proper configuration with single turn windings.

GaAs Tunnel Diode Decade Scaler - See 7224

7184 A BINARY COUNTER AND ACCUMULATOR USING TRANSISTORS AND MAGNETIC CORES by H. R. Irons (Nav. Ord. Lab.); U.S. Gov. Res. Rep., Vol. 34, p. 576(A), Nov. 18, 1960 PB 147 565

Binary devices which employ a transistor-magnetic core combination as a fundamental building block for digital circuits are described. These devices are capable of high operating speeds and yet require very little power at low operating speeds. For example, a five stage binary counter has a total power consumption of 40 micro watts when operated at a counting rate of 100 pulses per second. The same counter is capable of operation at rates as high as 2×10^6 pulses per second. Good reliability is indicated by the fact that a counter has been operated successfully over a temperature range of -65°F to 160°F with a supply voltage of -2.0 volts to -4.5 volts.

7185 READ-OUT SYSTEMS FOR TRANSISTOR SCALERS by T. G. Benbow (Atomic Weapons Res. Estab.); Electronic Engrg.,

Vol. 32, pp. 774-776, Dec. 1960

Three types of read-out display using a meter movement, filament lamp, and neon lamps are considered for use with transistor operated scalers and practical circuits are shown for the preferred system of switched neon lamps.

Digital Arithmetic Unit - See 7225

7186 A PARALLEL ARITHMETIC UNIT USING A SATURATED-TRANSISTOR FAST-CARRY CIRCUIT by T. Kilburn, D. B. G. Edwards and D. Aspinall (Manchester U.); Proc. IEE, Vol. 107B, pp. 573-584, Nov. 1960

A transistor switch technique which is of particular importance in applications where a large number of switches have to be connected in series and where the propagation time of information through these switches has to be a minimum is described. Its use has been demonstrated in parallel addition with an addition time over 24 digits of 200 mμsec. It is shown how the technique can be used in conjunction with more conventional logical circuits to provide a simple arithmetic unit.

7187 HIGH-SPEED TRANSISTORIZED ADDER FOR A DIGITAL COMPUTER by F. Salter (Argonne Natl. Lab.); IRE Trans., Vol. EC-9, pp. 461-464, Dec. 1960

An adder that has been developed for the Floating Indexed Point Arithmetic Unit, FLIP, to be used in conjunction with GEORGE, the existing computer built at Argonne National Laboratory, is described. The logic of the high-speed adder and the special circuits required are presented. The adder is parallel and its high speed is made possible by reducing the carry propagation time. Each bit of the adder contributes one transistor to make up a tall AND gate which reduces the carry propagation time to 0.2 μsec. Using this high-speed carry propagation and rather common RCTL transistor circuitry, it is possible to complete an addition in less than 0.25 μsec.

7188 A DIGITAL COMPUTER STORE WITH VERY SHORT READ TIME by T. Kilburn and R. D. Grimsdale (U. Manchester); Proc. IEE, Vol. 107B, pp. 567-572, Nov. 1960

The operating principles and the construction of storage units with a very short read access time are described. One form of the store which has been constructed has a capacity of 200,000 bits of permanent information and another has been built with a capacity of 100,000 bits, the whole contents of which may be changed in under one minute. The technique employed permits the construction of very large stores at low cost. Each digit cell is formed, basically by two sets of windings which form the primary and secondary of a transformer and the two binary states are determined by the presence or absence of a piece of linear ferrite material coupling the windings. The access time is largely determined by the physical size of the store and the speed of operation of the associated circuits; a time of 100 mμsec is typical.

7189 FERRITE-CORE MEMORY SYSTEMS WITH RAPID CYCLE TIMES by D. B. G. Edwards, M. J. Lanigan and T. Kilburn (Manchester U.); Proc. IEE, Vol. 107B, pp. 585-598, Nov. 1960

Improvements in storage systems using currently available square-loop ferrite cores are considered. These enable the normal cycle time of 6-10 μsec to be reduced to less than 2 μsec. Effort has been concentrated on the word-selected two-core-per-digit arrangement, and the most promising techniques are those which involve partial-flux switching. A system suitable for a store of 1024 words of 52 digits with a cycle time of about 1.6 μsec is developed. In a smaller store of 100 words a cycle time of approximately 0.6 μsec is feasible.

7190 A COMPUTER STORAGE MATRIX USING FERROMAGNETIC THIN FILMS by E. M. Bradley (Int. Computers and Tabulators Ltd.); J. Brit. IRE, Vol. 20, pp. 765-784, Oct. 1960

A new method for selecting a magnetic film storage element from a matrix of elements which exploits the coherent rotational mode of reversal is described. It is shown that, by using a film made of a newly developed alloy "Gyralloy I," the reproducibility problems previously encountered can be solved. It is shown that the use of aluminum as substrate for the film enables the signal to noise ratio to be increased to an acceptable level even for very large stores; the drive power requirements are shown to be correspondingly reduced. Details of the performance and construction of a storage device which contains 50 words each of 50 bits are given.

7191 HIGH SPEED THIN MAGNETIC FILM MEMORIES by R. Bogusch and E. A. Fisch (GE); Proc. 1960 Natl. Electronics Conf., pp. 840-845

The development of high-speed thin magnetic film memories is described. A brief description of the properties of the film is given, along with a discussion of the phenomenon of rotational switching. The transistorized driving and sensing circuitry is also described.

7192 SUPERCONDUCTING DEVICES AND CIRCUITS by D. R. Young (IBM); Electronics, Vol. 33, pp. 84-87, Oct. 14, 1960

High speed switching and storage capabilities of superconducting computer circuits with thin film cryotrons is described. Control is obtained by operating the cryotron close to the critical temperature (where the resistance abruptly falls to zero) and applying a magnetic field to force the superconductor into the normal state. Mounting the cryotron on an insulated superconducting shield plane reduces the inductance and increases the speed to 2×10^{-7} second. Current gain is obtained by using a gate film that is wider than the control film. The film thickness must be at least comparable to the magnetic field penetration depth to provide current gain. The films are deposited in a high-vacuum system by evaporation. A 5/8 x 2 in substrate holds 32 cryotrons.

7193 FERROELECTRIC MEMORY CELLS by R. A. Fotland (Horizons); U.S. Gov. Res. Rep., Vol. 34, p. 570(A), Nov. 18, 1960 PB 148 816

Techniques for obtaining 20 micron films of sodium niobate and barium-lead titanate ceramics are described. Inferences derived from the switching voltage-film thickness curves indicate that the sodium niobate crystallites are surrounded by a 10^{-6} cm parelectric skin. Switching voltages as low as 20 volts have been utilized with switching pulse lengths of 50 mμsec. A 15 megacycle read-out voltage functions effectively. The second-harmonic phase of an output current provides a nondestructive read-out. Ten by ten matrices have been examined with a static address and found to possess good uniformity. Coincidence switching is effective due to the high loop squareness when operating in the second-harmonic output mode. Indications which show the feasibility of large matrix sizes are presented.

7194 DC AMPLIFIER MISALIGNMENT IN COMPUTING SYSTEMS by R. L. Konigsberg (Johns Hopkins U.); IRE Trans., Vol. EC-9, pp. 352-358, Sept. 1960

The concept of the equivalent input circuit representation for d-c offset is generalized for the four amplifier types with finite input impedances, and the conditions under which the use of each equivalent circuit is justified are given. In each case, two offset generators which are characteristic of the amplifier alone — independent of driving source impedance and load impedance termination — are defined. Because of this independence, the offset generators are referred to as "characteristic misalignment generators." When the amplifier is connected into a system, a knowledge of these generators permits calculation of the effect of amplifier offset on system performance.

7195 A DIGITAL-ANALOG PULSE AMPLITUDE INTERPOLATION COMPUTER by J. D. Schmidt, B. K. Eriksen and F. H. Schlereth (GE); Proc. 1960 Natl. Electronic Conf., pp. 600-610

A transistorized computer circuit which automatically interpolates between two inputs of different amplitudes and adds or subtracts this quantity to a third input is described. This function is very useful in computing Doppler frequency in certain radar systems. A bipolar interpolation of the form $N_F = K A/A + B$ is performed where N_F is the interpolated quantity, K an arbitrary constant, and A and B are the two inputs. The processing of the information is done by a hybrid digital-analog system with the interpolation being performed by an analog circuit and the addition or subtraction being performed digitally. The hybrid system gave an accuracy of 0.3% in this application and resulted in a considerable saving in circuit complexity over a straight digital or analog system.

POWER

7196 TRANSISTOR D-C REGULATORS by F. Allen and H. J. Reed (Diamond Ord. Fuze Labs.); U.S. Gov. Res. Rep., Vol. 34, p. 568 (A), Nov. 18, 1960 PB 148 224

Modifications and extensions of a basic series-type regulator circuit utilized in the design of three d-c regulators for electrochemical power supplies are described. Expressions for the regulated output voltage and the output resistance are given in terms of the supply voltage and circuit parameters. The performance of the experimental circuits is in reasonable agreement with the calculated values obtained from the stability equations.

7197 STABILIZED VOLTAGE SUPPLIES USING TRANSISTORS by J. S. Bell and P. G. Wright (Smiths Aircraft Instr.); Electronic Engrg., Vol. 32, pp. 758-761, Dec. 1960

Two methods of obtaining ±300v stabilized supplies from a common low voltage source are described. The first circuit described is of a novel type and the design given is based upon initial investigations only, there being considerable scope for further improvements in design. The second type, which has been extensively investigated, follows the more usual form of series stabilizer, modified to use transistors throughout. Neither circuit is restricted solely to double voltage supplies. The first type requires minor modifications to accommodate single positive or negative outputs while the second design already consists of two identical stabilizers fed from a common convertor.

7198 SOLID-STATE D-C SWITCHED REGULATORS by A. A. Sorenson (Space Technology Lab.); Electronics, Vol. 33, pp. 121-123, Nov. 25, 1960

A switched voltage regulator with 90% efficiency and capable of 50w output is described. The output voltage is varied by altering the relative periods for which a switching transistor is opened and closed. The transistor is switched by an oscillator circuit composed of the transistor, a four-layer diode and an RC network. An LC filter on the output provides a low ripple content. A diode permits the energy stored in the inductor to be delivered to the load when the switch is open. Design equations are developed and circuits providing ±1% and ±0.5% regulation for a -15%, +30% input voltage variation are presented.

7199 LOW-COST TRANSISTOR OVERLOAD SAFETY CIRCUIT by K. Redmond (Amperex Elect.); Electronics, Vol. 33, p. 102, Oct. 14, 1960

An inexpensive transistor overload safety circuit using rejected transistors and diodes is described. A p-n-p transistor is placed across the supply voltage and held at cutoff by a series resistor and diode in the base-emitter circuit. A voltage higher than the proper line voltage turns on the transistor and a current surge is provided to open the fuse. Rejected power transistors can be used in this application. By placing a large resistor in series with the supply line, the circuit serves as a voltage regulator. An increase in voltage above a preset level will cause current to flow through the transistor and drop the excess voltage across it.

Corbino Disk Voltage Regulators - See 7106

7200 A TRANSISTOR REGULATED POWER SUPPLY FOR A HIGH CURRENT MAGNET by K. C. Brog (Case Inst. Tech.); U.S. Gov. Res. Rep., Vol. 34, p. 565 (A), Nov. 18, 1960

Current regulation of a high current electromagnet utilizing power transistors in series is described. A sampling voltage, obtained from a sensing resistor in series with the magnet, is compared with a reference voltage; the error signal is sufficiently amplified and fed back to the series transistors through a two-stage transistor driver. Magnetic fields from 845 gauss to 8550 gauss with field regulation of a few parts per million over this range have been obtained.

7201 DEVELOPMENT OF POWER TRANSISTOR CIRCUITRY by R. R. Smyth (Technical Operations); U.S. Gov. Res. Rep., Vol. 34, p. 582 (A), Nov. 18, 1960 PB 149 014

The use of a simple transistor push-pull oscillator circuit as a d-c to d-c power converter is discussed. The transistors act essentially as switches alternately connecting the supply battery across each half of a transformer primary. As a result the transistor dissipation is very low and the circuit efficiency high. Because of the importance of transistor dissipation in determining the maximum power output, considerable attention is given to the problem of determining optimum conditions. The problem of regulating the output voltages has also received considerable attention. Three practical circuits have been developed. Satisfactory regulation of a single output for both supply voltage and load current changes has been obtained with a circuit employing saturable reactors in the output circuit.

POWER (Cont'd)

Transistor High Voltage Generator for a Television Set - See 7166

CONTROL

Electro-Optical Relay - See 7221

Systems Using Transistors and Transductors as Control Elements - See 7144

INSTRUMENTATION

7202 A HIGH SENSITIVITY SEMICONDUCTOR DIODE MODULATOR FOR D-C CURRENT MEASUREMENT by H. E. De Bolt (Avco); IRE Trans., Vol. NS-7, pp. 1-4, Dec. 1960

A semiconductor diode modulator capable of measuring d-c currents down to 10^{-10} to 10^{-11} ampères is described. This modulator requires only one diode although a second is normally installed for balance purposes in high sensitivity measurements. The modulator utilizes pulse techniques instead of sine waves, which makes possible the high sensitivity. The circuit details of the modulator and design criteria are discussed.

7203 THE DESIGN AND EVALUATION OF A SIX CHANNEL, D-C COUPLED, TRANSISTORIZED GALVANOMETER DRIVER AMPLIFIER WITH CURRENT LIMITERS by W. M. Crouch (Arnold Engrg. Dev. Ctr.); U.S. Gov. Res. Rep., Vol. 34, p. 563(A), Nov. 18, 1960 PB 148 099

A d-c amplifier designed to drive recording galvanometers and to work in conjunction with analog magnetic tape systems is described. This amplifier has an input impedance compatible with the tape systems, unity or greater voltage gain, very low output impedance, and a frequency response which allow its use with all existing recording galvanometers. The unit has built-in current limiters which allow its use with low frequency, low current galvanometers without subjecting the galvanometer to the possibility of being overdriven from random signals or noise. The amplifier has been tested for gain, frequency response, drift, phase shift, distortion, common mode rejection, input and output impedance, linearity, output noise level, line voltage interaction, and cross talk.

7204 NEW LOOK AT WAVE ANALYZER DESIGN by J. R. Petrak (Hewlett-Packard); Electronics, Vol. 33, pp. 68-70, Sept. 23, 1960

A junction transistor wave analyzer with fixed selectivity from 0-50 kc and a linear dial calibration is discussed. Actual linear-frequency versus dial-rotation is achieved by a special capacitor. The drive mechanism gives an equivalent dial scale over 50 feet in length. A conventional afc system alters local oscillator frequency to correct for detuning of incoming signal. A frequency restorer circuit combines the local oscillator frequency with the IF frequency and a low-pass filter provides the difference frequency as an external signal when the analyzer is tuned to the frequency component of the input signal under measurement. The preamplifier has a distortion figure better than 90 db down and an input impedance of 100 k ohms. Silicon diodes provide overload protection. A lowpass filter with a 50 kc passband, 60 db down at 100 kc and higher, rejects input frequencies in the IF amplifier passband to prevent erroneous readings.

7205 DETECTORS FOR MICROWAVE SPECTROMETERS by M. W. Long (Georgia Inst. Tech.); Rev. Sci. Instr., Vol. 31, pp. 1286-1289, Dec. 1960

The sensitivity of detectors used in sample modulated microwave spectrometers is investigated. Characteristics of crystal diodes and barretters as functions of microwave power are compared with an ideal detector operating at room temperature. A spectrograph which was used to measure a $CFCl_3$ line having a calculated absorption coefficient of 3.9×10^{-11} cm^{-1} is described. The relationship between recorder deflection and absorption coefficient is discussed.

7206 AN AUTOMATIC DEW-POINT HYGROMETER USING PELTIER COOLING by P. Gerthsen, J. A. A. Gilsing and M. van Tol (N. V. Philips); Philips Tech. Rev., Vol. 21, No. 7, pp. 196-200, 1959/1960

The most accurate method of measuring the humidity of a gas is to determine the dew point. The cooling required for this purpose can be obtained by utilizing the Peltier effect of a combination of certain semiconductors. A dew-point hygrometer based on this principle is described. In this apparatus a silver reflector (5 mm thick, surface area 75 mm^2) is cooled to below the dew point. A beam of light is directed from this reflector on to a cadmium sulphide photoresistor. When the reflector mists over, the beam is diffusely reflected; the photoresistor therefore receives less light and the photocurrent decreases. The latter controls the current through the Peltier element. The control loop thus formed is in equilibrium when the temperature of the reflector is equal to the dew point. The error in the measurement is less than $\frac{1}{2}^{\circ}$C.

7207 ON THE USE OF 2N504 TRANSISTORS IN THE AVALANCHE MODE FOR NUCLEAR INSTRUMENTATION by R. Fullwood (U. Penn.); Rev. Sci. Instr., Vol. 31, pp. 1186-1189, Nov. 1960

The operation of transistors in the avalanche mode as fast discriminators on photomultiplier tubes and as the pulse generating element in pulse generators is described. They exhibit the property of a fast rise time ($\lesssim 1$ nsec) and sharp discriminating characteristics but have the disadvantage of a long recovery time (~ 80 nsec).

7208 HEAVY PARTICLE DETECTOR WITH SILICON N-P JUNCTION [in French] by G. Ansel, P. Baruch and O. Smulkowski (Ecole Normale Supérieure); Nuc. Instr. Methods, Vol. 8, pp. 92-105, July 1960

The use of silicon n-p junctions to detect heavy charged particles produced by nuclear reactions inside an accelerator vacuum chamber at room temperature is discussed. The response to particle energy dissipated in the barrier is linear. The width of resolved peaks at half maximum is independent of incident particle energy and is equivalent to 40 kev for α particles and 30 kev for protons and deuterons. The rise time of the signal due to particles stopped in the barrier is of the order of 1 μsec while that due to particles traversing it has a slow component; this allows their distinction electronically. The detectors are insensitive to γ rays and neutrons.

7209 FAST-NEUTRON DETECTION AND SPECTROSCOPY USING A SOLID STATE DETECTOR by T. A. Love and R. B. Murray (Oak Ridge Natl. Lab.); Bull. Am. Phys. Soc., Ser. II, Vol. 5, pp. 416-417 (A), Nov. 25, 1960

A neutron sensitive counter constructed by depositing a thin layer of Li^6F between two silicon surface-barrier counters was described. Neutrons are detected by observing the $\alpha + T$ charged particles resulting from the $Li^6(n, \alpha)T$ reaction; pulses from the two counters are added and the sum pulse is amplified and recorded. Since the sandwich geometry permits simultaneous detection of both reaction products, the magnitude of the sum pulse is proportional to the energy of the incoming neutron plus the reaction Q value. Pulse-height spectra from slow neutrons and from monoenergetic fast neutrons, in the energy region 0.6 to 15 Mev, have been recorded from several counters of this type using sensitive areas of about 0.7 cm^2, with a Li^6F layer of order 150 $\mu g/cm^2$ thick. In all cases a well defined neutron peak was observed in the pulse-height spectra. The full width at half-maximum of the fast-neutron peak was about 300 kev approximately independent of neutron energy.

CdS and ZnS Crystal Counters - See 6967

7210 FAST TRANSISTORIZED TIME-TO-PULSE-HEIGHT CONVERTER by G. Culligan and N. H. Lipman (CERN); Rev. Sci. Instr., Vol. 31, pp. 1209-1214, Nov. 1960

A transistorized time-to-pulse-height converter which has a timebase range of 0 to 15 nsec, and a stability of 10^{-10} sec is described. The circuit has been used for the mass analysis of particle beams by time-of-flight. Time resolutions of 10^{-9} sec were obtained using conventional scintillation counters. The circuit has a short dead time (3×10^{-7} sec), contains a gating facility, but is of simple design. It has been in use at CERN for the previous six months, and functions satisfactorily under experimental conditions.

7211 EIGHT-LEVEL PULSE-HEIGHT ANALYZER FOR SPACE PHYSICS APPLICATIONS by U. D. Desai, R. L. Van Allen and G. Porreca (Goddard Space Flight Ctr.); Trans. 1960 Natl. Symposium on Space Electronics and Telemetry, paper 4-4, 10 pp.

A scintillation spectrometer for the study of low-energy particles in space is discussed. The spectrometer consists of a cesium iodide scintillation crystal, a photomultiplier with high-voltage power supply, and a transistorized eight-level pulse-height analyzer. The pulse-height analyzer is of the threshold-integral type. Each discriminating level is maintained accurate to ±5% over a temperature range of $-10^{\circ}C$ to $+50^{\circ}C$. Since the spectrometer was designed for a spacecraft with digital telemetry, several special features were required in order that the two systems be compatible.

Transistorized Ratemeter Design - See 7162

7212 USES OF SEMICONDUCTOR DETECTORS IN HEALTH PHYSICS MONITORING by A. R. Jones (Atomic Energy of Canada); Nucleonics, Vol. 18, pp. 86, 88, 90-91, Oct. 1960

The characteristics required of semiconductor junction detectors to be used in monitoring alpha particles, beta and gamma rays, and neutrons are discussed and some instruments which have been developed or are presently being developed are described. At present alpha and neutron monitors are feasible and gamma and beta monitors require further development. Some needed device and material improvements are pointed out.

7213 A TRANSISTORIZED RADIATION MONITOR by M. van Tol and F. Bregman (N. V. Philips); Philips Tech. Rev., Vol. 21, No. 7, pp. 201-206, 1959/1960

A portable radiation monitor in which the readings are insensitive to the transistor characteristics is described. A method of arriving at a (non-linear) scale that covers the whole range between zero radiation (zero deflection) and an infinitely high radiation level (full-scale deflection) is also discussed. Readings are sufficiently accurate (less than 10% error for a deflection error equivalent to 1% of the scale length) over a part of the scale extending from 0.1 to 0.9 of the scale length. The radiation-level reading at the upper limit of this range is a good 40 times higher than that at the lower limit. The instrument can easily be adjusted to bring any given radiation level within the usable range. The calibration procedure is particularly straightforward.

Miniature Dose Rate Meter - See 7163

7214 A REACTOR SAFETY SYSTEM USING TRANSISTORS AND SILICON CONTROLLED RECTIFIERS by W. M. Trenholme (GE); IRE Trans., Vol. NS-7, pp. 14-19, Dec. 1960

An all-semiconductor reactor safety system which consists of a d-c amplifier, an adjustable trip level bistable circuit, a diode logic circuit, and a power switching circuit is described. The d-c amplifier is a simple emitter follower transistor stage. Three transistors are used in the bistable circuit, two in a Schmitt-trigger arrangement and one as an output drive. The diode logic circuit uses a combination of OR and AND gates to give 2-out-of 3 coincidence of the bistable circuit outputs. A unijunction transistor and two silicon controlled rectifiers are the active elements in the power switching circuit. These components are particularly well suited for the on-off control needed in reactors and the circuitry is reasonably fail-safe.

7215 SENSITIVE CAPACITANCE INTRUDER ALARM by S. M. Bagno (Walter Kidde); Electronics, Vol. 33, pp. 65-67, Sept. 16, 1960

A semiconductor alarm system in which the body capacitance of an intruder sets off an alarm is described. The alarm system can sense a change of 10 pf in 8000. An oscillator feeds 20 kc to a bridge circuit containing the capacitance to ground of the protected cabinet. The bridge output is amplified and converted to a dc voltage by a phase-sensitive detector, further amplified and used to bias a p-n-p and an n-p-n transistor with a relay connected in series between the transistor collectors. The bridge is normally balanced and the relay is energized. The body capacitance of an intruder unbalances the bridge and decreases the relay current, sounding an alarm. Low-pass filters eliminate RF pickup and the detector cancels out effects other than direct changes in capacitance. A rate circuit makes the phase detector insensitive to ambient weather conditions.

NEW PRODUCTS

7216 YTTRIUM-GADOLINIUM GARNETS (Sperry Microwave

Electronics Co., Clearwater, Florida)

A series of yttrium and yttrium-gadolinium garnets for use in the frequency range from 350 to 3,000 Mc is announced. Five different compositions are available in bar form. The garnets can be used at temperatures of -65°C to 125°C and at power levels from a few milliwatts to megawatts.

7217 SEMICONDUCTOR SLICER (Will Corp. Box 1050, Rochester 3, N. Y.)

A machine which can slice semiconductor samples as thin as 0.005" is announced. The sample is automatically advanced at a constant speed through a perfectly balanced, diamond-edged wheel rotating at 6500 rpm.

7218 TUNNEL AND BACKWARD DIODES (Transitron Electronic Corp., 168 Albion St., Wakefield, Mass.)

A series of germanium tunnel diodes with peak current of 1 ma and 5 ma and two complementary germanium backward diodes are announced. The backward diodes are designed for use with the tunnel diodes in logic circuits and other computer applications. The backward diodes can also be utilized in low level rectifier and detector circuits. The leakage current of the backward diodes is specified at 400 mv and the forward voltage at 15 percent of the tunnel diode's peak current. The low shunt capacitance of the backward diode permits several to be driven from one tunnel diode with little reduction in speed.

7219 EPITAXIAL TRANSISTOR (Rheem Semiconductor Corp., 350 Ellis St., Mountain View, Calif.)

The RT 409 silicon transistor which is fabricated by epitaxial deposition techniques is announced. The use of this fabrication technique results in devices which have almost no collector series resistance and low storage and turn-off times. The device has a collector breakdown voltage of 60 v and a typical collector to emitter saturation voltage at 150 ma of 0.35 v.

7220 HALL GENERATOR (Westinghouse Electric Corp., Semiconductor Dept., Youngwood, Pa.)

The type 803 indium arsenide Hall generator is announced. The device, which is essentially a multiplier that produces a voltage output proportional to the product of the current passing through it and the magnetic field perpendicular to it, has several instrument applications. It can also be used as an analog computer element. Some typical parameters of the generator are maximum control current at 25°C, 500 ma; minimum Hall constant, 100; flux density range, 0-10 kilogauss; frequency response flat to 1 Mc; and load resistance for maximum linearity, ~10 ohms.

7221 RAYSISTOR (Raytheon Co., Industrial Components Div., 55 Chapel St., Newton 58, Mass.)

The Raysistor, a four terminal electro-optical device designed to replace relays, switches, and potentiometers for low-noise commutation, switching, and controlling circuits, is announced. The device consists of a signal circuit employing a photoconductive semiconductor and a control circuit consisting of a light source. When a voltage is applied to the two terminals of the control circuit, the light source is excited and the resistance of the semiconductor is decreased by a factor of about 10^6. An ac or dc signal can then flow through the signal circuit. There is no electrical connection between the control and signal circuits. The device is capable of one billion operations and can be clip-mounted in any position.

7222 FERRITE CIRCULATORS (Melabs, Inc., 3300 Hillview, Stanford Industrial Park, Palo Alto, Calif.)

Two circulators designed primarily for telemetry applications in the S band are announced. The HS-1 operates in the 2200-2300 Mc frequency range and the HS-2 operates in the 2700-2900 Mc frequency range. The units weigh 4 or 7 ounces, depending on the connectors used, are 2.5 inches in diameter, and 1 inch in height. Both devices exhibit a minimum isolation of 20 db, a maximum insertion loss of 0.3 db, and can handle an average power of 1 watt over a wide temperature range.

7223 RADAR TRANSPONDER (Motorola, Inc., Military Electronics Div., 8201 E. McDowell Rd., Phoenix, Arizona)

The SST-102 radar transponder, a general purpose superheterodyne pulse transponder intended for use with precision C-Band tracking radars is announced. It features an all-solid state modulator switch, ferrite circulator and employs high frequency mesa transistors. The SST-102 occupies approximately 200 cubic inches, and weighs only 8.8 pounds, including a self-contained secondary power supply. Transmitter and receiver are tunable over the 5400-5900 Mc frequency band from convenient exterior controls. Code selection, delay settings and service test points are also accessible from the exterior. The transponder is specifically designed for ease of maintenance. Designed for use with chain radars, the SST-102 has both fast recovery time and a wide dynamic range. Special electronic circuitry incorporated precludes semiconductor switch "lock-on". Performance is not degraded by antenna mismatch and high sensitivity is maintained throughout the frequency range without readjustment.

7224 GaAs TUNNEL DIODE DECADE SCALER (Philco Corp., Tioga and "C" Streets, Philadelphia 34 Pa.)

High-speed decade scalers using gallium arsenide tunnel diodes in series are announced. With double-pulse resolution for switching between intermediate states of less than 14 nsec, the device utilizes the property of series-connected tunnel diodes that voltage is a multi-valued function of current. Upon initial application of source current, the stack of diodes maintains its lowest voltage. Each pulse of proper amplitude applied to the input terminal boosts stack voltage to the next higher level. A transistor reset circuit is biased to operate when the highest stack level is reached. GaAs tunnel diodes are utilized because of their intrinsically higher voltage swings, their peak-to-valley ratios of greater than ten to one, and switching times of less than a nanosecond. The tunnel diode scaler features extremely high switching and reset speeds and a significant reduction in the space, weight and power requirements of beam-switching tubes or cascaded transistor binaries used in similar applications.

7225 DIGITAL ARITHMETIC CENTER (Clary Corp., 408 Junipero St., San Gabriel, Calif.)

The model DAC-2500 digital arithmetic center, a solid state unit which performs the arithmetic and memory functions needed for process control, instrumentation and test systems, is announced. Flexible input, output and control circuits allow a wide range of peripheral equipment to be easily connected to the unit.

SUBJECT INDEX

A

Abrasions, Surface Damage of III-V Intermetallic Compounds Due to 6983
Accumulators Using Transistors and Magnetic Cores 7184
Adder, Transistor 7187
Alarm, Capacitance Intruder 7215
Alkali Halides at Low Temperatures, Mechanism for Coloration of 6933
Alkaline Earth Fluorides, Color Centers in 7059, 7060
Aluminum Boride,
  Electrical Properties of 6998
  Energy Gap of 6998
  Semiconducting Properties of 6998
Amplifiers,
  DC: Misalignment of 7194
  Electro-Optical: Power 7145
  Microsystems: Bandpass 7131
  Parametric:
    Capabilities and Limitations of 7133
    Coupled-Cavity Traveling Wave 7138, 7139
    Design of Varactor Diodes for 7081
    Limitations on Noise Performance of 7136
    Optimum Noise and Gain-Bandwidth Performance of 7134
    Symmetrical Matrix Analysis of 7135
    Tunable 7140
  Transistor:
    Automatic Gain Control 7127, 7128
    Carrier Frequency 7095
    DC Galvanometer Driver 7203
    Design of Distributed 7141
    Design of Shunt-Peaked 7142
    Distortion in 7129
    Negative Impedance Repeater 7167
    Offset in DC 7194
    Regenerative Pulse 7168
    Stability of Tuned 7132
    Video 7130
    Video Current 7165
  Tunnel Diode: Theory and Synthesis of 7143
Anisotropy:
  in Thin Permalloy Films, Rotatable 7043
  of Evaporated Nickel Films, Magnetic 7041
  of Oblique-Incidence Permalloy Films 7042
Annealing of Oblique-Incidence Permalloy Films 7042
Antiferromagnetic:
  Domains:
    in α-Manganese and its Alloys 7036
    in Nickel Oxide, Study of 7035
  Ground State, Theory of the 7032
  Resonance in Manganese Oxide, Infrared 7048
Antiferromagnets with Large Uniaxial Anisotropy, Sublattice Magnetization and Resonance Frequency of 7047
Antimony in Germanium, Valley-Orbit Splitting of 7003
Arithmetic Unit,
  Digital 7225
  Transistor 7186
Avalanche Effect in Silicon Three-Layer Diodes 7089

B

Bands in Cubic Lattices, D 7001
Barium Fluoride, Surface Energy of 6999
Barium-Lead Titanate:
  Ceramic Ferroelectric Memory Cells 7193
  Films, Preparation of Ferroelectric 6978
Binary Counter Using Transistors and Magnetic Cores 7184
Blocking Oscillators, Calculation of Pulse Duration in Transistor 7149
Bombardment Effects in Tunnel Diodes 7083
Breakdown Strength of Potassium Chloride Crystals 6998
Bridgman Method, Growth of Single Crystal HgSe-HgTe by the 6931

C

Cadmium Arsenide, Electrical Properties of 7027
Cadmium Ions in Silver Chloride, Diffusion of 6950
Cadmium Sulfide,
  Electron Paramagnetic Resonance of Europium in Single Crystals of 7058
  Relation of Traps to Noise in 7022
Cadmium Sulfide:
  Crystals,
    Distribution of Electrons in 7005
    Growth of 6961, 6967
  Crystals for Use as Detectors in Crystal Counters, Properties of 6967
  Powder Cells, Mechanism of Photoconductivity in 7069
  Type Crystals by Grain Growth, Growth of 6962
Calcium Carbonate, Surface Energy of 6999
Calcium Fluoride, Surface Energy of 6999
Calcium Fluoride Crystals, Coloration of 7059
Capacitance Intruder Alarm 7215
Cardiotachometer, Transistor 7161
Carrier:
  Behavior in Molecular Solids, Domain Theory of 7008
  Concentrations in Zinc Arsenide and Cadmium Arsenide 7027
  Mobilities in Zinc Arsenide and Cadmium Arsenide 7027
Carriers in Germanium and Silicon, Polarizability of Free 7010
Cascode Transistor Trigger Circuits 7153
Catalysis at a Semiconductor Surface 6980
Cesium Chloride Crystals, Growth of 6966
Charge:
  Control Parameters of Transistors 7094
  Transport Through Organic Polymer Films 7013
Chlorine Ions in Silver Chloride, Diffusion of 6950
Circulators for Telemetry Applications, Ferrite 7222
Cluster Formation in Crystal Lattices, Determination of 6945
Cobalt, Effect of Plating Parameters on the Structure and Magnetic Properties of 6994
Cobalt-Molybdenum Alloys, Electrodeposition of 6996
Cobalt-Nickel:
  Alloys, Effect of Plating Parameters on the Structure and Magnetic Properties of 6994
  Alloys from a Pyrophosphate Bath, Electrodeposition of 6995
Colloids in Potassium Chloride, Electron Microscope Studies of 6981
Color Centers:
  in Alkaline Earth Fluorides 7059, 7060
  into Potassium Chloride Single Crystals, Diffusion of 6934
Coloration of Alkali Halides at Low Temperatures, Mechanism for 6933
Compound Semiconductors, Analysis of Impurities in 6944
Computer,
  Digital-Analog Pulse Amplitude Interpolation 7195
  Surface Barrier Transistor 7172
Computer:
  Circuits - See also Logic Circuits
  Elements, Tunnel Diode Locked Pair 7180
  for Doppler Radar, Pulse Amplitude Interpolation 7195
  Logic:
    Circuits, Tunnel Diodes and Backward Diodes Designed for Use in 7218
    Networks, Theory of 7174
  Memories, High Speed Thin Magnetic Film 7191
  Storage Matrix Using Ferromagnetic Thin Films 7190
  Store with Very Short Read Time 7188
Computing Systems, DC Amplifier Misalignment in 7194
Conduction at Low Concentrations, Impurity 7015
Conductivity of Organic Polymer Films 7013
Contacts, Improved Silicon 7097
Contacts to Silicon Carbide, Fused 7026
Contractometer 7078
Control Elements, Systems Using Transistors and Transductors as 7144
Controlled Rectifier Reactor Safety System 7214
Converters,
  Parametric: Symmetrical Matrix Analysis of 7135
  Transistor:
    DC to DC Power 7201
    Time-To-Pulse-Height 7210
  Tunnel Diode 7156
Cooling of Junction Devices, Peltier 7075
Copper Tungstate,
  Crystal Structure of Tri-Clinic 6998
  Electrical Properties of 6998
Copper Whiskers by the Hydrogen Reduction of Cuprous Iodide Vapor, Growth of 6970
Corbino Disk, Theory of the 7106
Corbino Disk Voltage Regulators 7106
Counters, Tunnel Diode 7179
Cryotron Switching and Storage Devices 7192
Cryotrons, Fabrication of Thin Film 7192
Crystal:
  Counters, Cadmium Sulfide and Zinc Sulfide 6967
  Growth, Role of Dislocations in 6937
  Perfection, Determination of 6945
  Puller, Synthesis and Crystal Pulling of Gallium Arsenide in a Magnetic 6956
  Size in Lead Sulfide Photoconductive Films 7011
  Structure of:
    Silver Selenide 7077
    Tri-Clinic Copper Tungstate 6998
Crystallographic Properties of Silver Selenide 7077
Cuprous Iodide Vapor, Mechanism of Hydrogen Reduction of 6970
Cuprous Oxide, Diffusion of Silver into 6951
Current Regulator, Transistor 7200
Czochralski Method, Growth of Single Crystal Iron Ferrites by the 6971

D

Data Instrumentation, Transistor Building Blocks for 7173
Dember Effect in Silver Chloride 7025
Dendrites,
  Growth:
    and Evaluation of Silicon 6964
    Steps on the Surfaces of 6963
Deposition of:
  Gold on Various Base Metals, Electroless 6992
  Iron-Nickel Films, Influence of Thiourea on the 6993
  Metals on Silicon, Mechanisms of Electroless 6991
Detectors:
  for Microwave Spectrometers 7205
  in Health Physics Monitoring, Use of Semiconductor 7212
Diamond, Surface States of 7004
Dielectric Properties of Organic Polymer Films 7013
Diffusion-Limited Scaling Reactions, Theory of 6979
Diffusion of:
  Boron in Silicon, Modified Closed Box System for the 6949
  Color Centers into Potassium Chloride Single Crystals 6934
  Ions in Silver Chloride Single Crystals 6950
  Nitrogen into Silicon Carbide Grains 6948
  Silver into Cuprous Oxide 6951
Digital-Analog Pulse Amplitude Interpolation Computer 7195
Diode:
  Current Switching Circuits 7177
  Impedance, Measurement of 7124
Diodes,
  Junction:
    Analysis of Reverse Bias 7084

Anomalous Barrier Capacitance of Indium Antimonide 7086
Backward 7218
Breakdown in Silicon 7088
Capacitance of Graded 7085
Current-Voltage Characteristics of Silicon Carbide 7087
Evaluation of Silicon Single Crystals for 7092
Fabrication:
by Epitaxial Deposition of SiC Films 6960
by Thin Film Evaporation Techniques 7090
of Silicon Carbide 7093
Gallium Arsenide:
Power 7091
Tunnel 7150
Guard Ring 7088
Impedance of Diffused Silicon Mesa Varactor 7124
Neutron Bombardment of Tunnel 7083
Noise Properties of Varactor 7115
Peltier Effect in 7075
Potential Distribution in Graded 7085
Protection of 7125
Rectifying Barrier at an AlC-SiC Interface 7026
Silicon Carbide Varactor 7087
Tunnel 7082, 7218
Uniform Avalanche Effect in Silicon Three-Layer 7089
Varactor 7081
Point Contact: Surface Currents in Inversion Layers of 7080
Use of the Peltier Effect for Cooling 7075
Dislocation:
-Etch Pit Relation in Silicon Carbide 6937
Etch Pits in Tellurium 6936
Theory, Implications of the Dangling Bond Model for 7000
Dislocations, Frictional Stress on Moving 6939
Dislocations in:
Germanium 6935
Graphite, Electron Optical Study of Basal 6938
Plastically Deformed Tellurium, Recombination at 6936
Silicon Carbide 6989
the Growth of Silicon Carbide Crystals, Role of 6937
the Spinel Structure 6932
Zinc Sulfide Single Crystals 6967
Disorder Phenomenon, Theory of Electroluminescence as a 7062
Dissolution, Effect of Cold Work on 6983
Dissolution of:
Germanium, Orientation-Dependent 6984
Quartz by Gallium 6928
Distortion in:
Almost-Linear Networks, Non-Linear 7095
Transistor Amplifier Stages, Calculation of the 7129
Distributed:
Amplifiers, Design of Transistor 7141
Parameter Microminiature Structures 7123
Domain Theory of Carrier Behavior in Molecular Solids 7008
Domains in:
α-Manganese and its Alloys, Antiferromagnetic 7036
Iron Whiskers Under High Fields, Observation of 7034
Nickel Oxide, Neutron and Optical Studies of 7035
Doping:
of Semiconducting Compounds, Mobility 7012
Problems, Application of Statistical Techniques to 6947
Dose Rate Meters, Miniature 7163
Drift Mobility Using the Field Effect Modulation of Photoconductors, Measurement of 7070
Dysprosium, Electrical Resistivity of Polycrystalline 7016

E

Electrodeposited:
Cobalt and Cobalt-Nickel Alloys, Effect of Plating Parameters on the Structure of 6994
Films of Fe-Ni Alloys, Initial Growth of Plating in Thin 7078
Thin:
Magnetic Films, Influence of Substrates on 7039
Nickel-Iron Films, Effects of Composition and Thickness on the Magnetic Properties of 7040
Electrodeposition of:
Cobalt-Molybdenum Alloys 6996
Nickel-Cobalt Alloys from the Pyrophosphate Bath 6995
Thin Magnetic Films in a Magnetic Field 7039
Electrodeposits, Measurement of Stress in Very Thin 7078
Electroless Deposition of:
Gold on Various Base Metals 6992
Metals on Silicon, Mechanisms of 6991
Electroluminescence, Theory of 7062
Electroluminescent Phosphors, Maintenance of 7063
Electrolytic Rectification, Theory of 7017
Electron:
Bombardment, Production of Color Centers in Alkaline Earth Fluorides by 7059, 7060
Density Maps of Cadmium Sulfide Crystal Structure 7005
Emission from Magnesium Oxide Single Crystals, Secondary 7023, 7024
Electronic Structure of Group IV and III-V Semiconductors 7002
Electro-Optical:
Power Amplifiers 7145
Switches 7221
Electrostrictive Effect in Rutile Single Crystals 6998
Emission Spectrographic Method of Impurity Analysis 6940
Emissivity, Peltier Method of Measuring Radiation 7072
Energy Gap:
Alloy-$GaAs_xP_{1-x}$, Preparation of a Graded 7076
of Aluminum Boride 6998
of Cadmium Arsenide 7027
of Iodine 6998
of Zinc Arsenide 7027
with Size of the Conjugated System in Organic Molecular Solids, Variation of the 7029
Epitaxial:
Growth onto Silicon Carbide Seeds 6960
Junction Transistors 7219
Erbium, Electrical Resistivity of Polycrystalline 7016
Etch:
Pit-Dislocation Relation in Silicon Carbide 6937
Pits in Tellurium, Dislocation 6936
Rate of Germanium in a Specific Solution 6986
Etching, Detection of Dislocations and Precipitated Phases by 6935
Etching of:
Germanium, Orientation-Dependent 6984
Germanium and Silicon,
Comparison of 6985
Mechanism of Chemical 6987
Silicon, Liquid-Solid Interface Reactions During 6988
Silicon Carbide 6989, 6990
Etching Rate of Germanium and Silicon, Method for Monitoring the 6982
Europium in Single Crystals of Cadmium Sulfide, Electron Paramagnetic Resonance of 7058
Exchange Inversion in $Mn_{2-x}Cr_xSb$ 7033

F

Faraday:
Effect at Microwave Frequencies in Germanium and Silicon 6998
Rotator, Quadruply-Ridged Circular Waveguide 7113
Ferrimagnetic:
Resonance, Nonlinear Effects of Crystalline Anisotropy on 7049
Resonance:
in a Single Crystal Disc of Yttrium Iron Garnet 7052
Line Width in Some Rare Earth Doped Yttrium Iron Garnet 7053
to Antiferromagnetic Phase Transition in $Mn_{2-x}Cr_xSb$ 7033
Ferrite:
Circulators for Telemetry Applications 7222
-Core Memory Systems with Rapid Cycle Times 7189
Devices, Broad-Band Ridge Waveguide 7113
Films, Preparation and Properties of 6974, 697
Limiters, Fine Wire 7114
Particles, Growth of 6972
Transducer Heads 7171
Ferrites,
Ferromagnetic Resonance Due to Magnetic Field Generated by Displacement Currents in 7045
Preparation and Properties of Low Loss 7056
Ferrites by the Czochralski Method, Growth of Single Crystal Iron 6971
Ferroelectric:
Deuterium-Doped Rochelle Salt, Electro-Optic Kerr Effect and Polarization Reversal in 7007
Films, Preparation of 6978
Memory Cells 7193
Ferromagnetic:
Resonance:
Due to Magnetic Fields Generated by Displacement Current in Ferrites 7045
in Piezoelectric $Ga_{2-x}Fe_xO_3$ 7046
Line Width Maximum in Yttrium Iron Garnet 7051
Thin Film Computer Storage Matrix 7190
Ferromagnetism to Antiferromagnetism in Dysprosium Change from 7016
Field Effect Modulation of Photoconductors, Measurement of Drift Mobility Using th 7070
Films,
Annealing of Oblique-Incidence Permalloy 704
Crystallographic Orientation of Evaporated Tin Telluride 6953
Electric Charge Transport Through Organic Polymer 7013
Electrical Properties of Silicon Carbide 6960
Hole Mobility and Crystal Size in Lead Sulfide Photoconductive 7011
Influence of Thiourea on the Deposition of Iron-Nickel 6993
Magnetic Anisotropies of Evaporated Nickel 70
Magnetoresistance and Magnetic Switching in Permalloy 7044
Mechanical Properties of Thin Single Crystal Ga 7079
Photocurrents Excited by Visible Light in Organi Polymer 7013
Films:
by Evaporation, Formation of Phosphor 6968
Evaporated at Grazing Incidence, Permalloy 6971, 6973
Grown by Vacuum Deposition, Structure of Sing Crystal Gold 7079
Float Zoning of Silicon, Shape of Melt-Crystal Interfaces During 6958
Fluorescence of Sodium Iodide Single Crystals 706
Frequency Dividers, Regenerative Transistor 7153, 7158
Functional:
Electronic Blocks, Optimum Stabilization Netwo for 7121

Units,
High Gain Cascaded Transistor 7104
Minimization of Power Dissipation in 7121
Furnace for Silicon Carbide Device Fabrication, Thermocouple 7093
Fused Contacts to Silicon Carbide 7026

G

Gadolinium, Electrical Resistivity of Polycrystalline 7016
Gain Control:
for Transistor IF Amplifiers, Automatic 7128
Techniques, Semiconductor 7127
Gallium,
Dissolution of Quartz by 6928
Nuclear Quadrupole Resonance in Superconducting 7030
Gallium and Quartz, Reactions between 6928
Gallium Arsenic Phosphide, Preparation of a Graded Energy Gap Alloy- 7076
Gallium Arsenide, Direct Recombination in 7009
Gallium Arsenide:
in a Magnetic Crystal Puller, Synthesis and Crystal Pulling of 6956
Power Rectifiers 7091
Tunnel Diode:
Decade Scaler 7224
Oscillators 7150
Tunnel Diodes, Fabrication of 7150
Gallium Iron Oxide, Ferromagnetic Resonance in Piezoelectric 7046
Gallium Phosphide, Crystallization of 6965
Galvanomagnetic Properties, Effect of Random Inhomogeneities on 7019
Galvanometer Driver Amplifier, Transistor DC 7203
Garnets, Microwave Properties and Applications of 7054
Garnets for Microwave Applications 7216
Germanium,
Electrical Properties of 6998
Faraday Effect at Microwave Frequencies in 6998
Mechanism of Chemical Etching of 6987
Method for Monitoring the Chemical Etching Rate of 6982
Orientation-Dependent Dissolution of 6984
Piezoresistance of Antimony Doped 7003
Polarizability of Free Carriers in 7010
Reflectivity of 7010
Structural Defects in 6935
Thermal Conductivity of 7071
Valley-Orbit Splitting of Antimony in 7003
Germanium:
and Silicon, Comparison of the Etch Rate of 6985
Dendrites, Growth Steps on the Surface of 6963
in a Specific Solution, Etch Rate of 6986
Single Crystals Using a Silicon Nitride Receptacle, Horizontal Growth of 6955
Gold, Electroless Deposition of Gold on 6992
Gold Films Grown by Vacuum Deposition, Structure and Mechanical Properties of Single Crystal 7079
Grain Growth, Growth of Large Cadmium Sulfide Type Crystals by 6962
Graphite,
Electron Optical Study of Basal Dislocations in 6938
Surface States of 7004
Growth:
from the Melt, Cellular Interface Morphology During 6957
of Cadmium Sulfide Crystals from the Vapor Phase 6961
of Copper Whiskers by the Hydrogen Reduction of Cuprous Iodide Vapor 6970
of Fine Ferrite Particles 6972
of Germanium Single Crystals, Horizontal 6955
of HgSe-HgTe Single Crystals by the Bridgman Method 6931
of Large Cadmium Sulfide Type Crystals by Grain Growth 6962
of Silicon Carbide Single Crystals, Role of Dislo-
of Silver Selenide by Fusion Techniques 7077
of Single Crystal Iron Ferrites by the Czochralski Method 6971
onto Silicon Carbide Seeds, Epitaxial and Single Crystal 6960
Steps on the Surfaces of Dendrites 6963

H

Hall:
Effect, Identification of Impurities Using the 6941
Effect:
in Silver Antimony Telluride, Anomalous 7020
Multiplier for Use at Radio Frequencies 7105
Generator, Indium Arsenide 7220
Mobility in Molecular Solids 7008
Harmonic:
Generation with "Gradual Grade" Diffused Silicon Junction Diodes 7115
Generators, Large Signal Analysis of Parametric 7157
Health Physics Monitoring, Use of Semiconductor Detectors in 7212
Helical Spin Configuration, Magnetization Process of a 7031
Holmium, Electrical Resistivity of Polycrystalline 7016
Hydrogen Reduction of Cuprous Iodide Vapor, Mechanism of 6970
Hygrometers Using Peltier Cooling, Automatic Dew-Point 7206

I

Image Intensifier Panel, Two Color Input-Two Color Output 7110
Impedance:
of Diodes, Measurement of the 7124
Transformation from a Mesa Diode to a Transmission Line 7124
Imperfections on Lattice Thermal Conductivity, Effect of Point 7074
Impulse Selection for Ferrite Core Logic 7183
Impurities,
Analysis of 6940
Hall Effect Identification of 6941
Impurities:
by Neutron Activation Analysis, Detection of 6942
in Compound Semiconductors, Analysis of 6944
in Silicon Carbide by Neutron Activation Analysis, Determination of 6943
Impurity:
Conduction at Low Concentrations 7015
Resistance in Metals, Theory of 7014
Indium Antimonide, Theory of the Oxidation of 6979
Indium Arsenide:
Hall Effect Multiplier for Use at Radio Frequencies 7105
Hall Generator 7220
Infrared Antiferromagnetic Resonance in Manganese Oxide 7048
Inhomogeneities on Electrical and Galvanomagnetic Properties, Effect of Random 7019
Injection Heat Transfer 7075
Instrumentation, Transistor Building Blocks for Data 7173
Intercardiac Catheter Tip Piezoresistive Pressure Gauge 7117
Interface During Growth from the Melt, Microscopic Shape of a Solid-Liquid 6957
Interfaces During Float Zoning of Silicon, Shape of Melt-Crystal 6958
Intermetallic:
Compound Dendrites, Growth Steps on the Surface of 6963
Compounds,
Filled and Empty Dangling Bonds in III-V 7000
Surface Characteristics of III-V 6983
Intruder Alarm, Capacitance 7215
Inversion Layers on Semiconductors, Surface Currents in 7080
Iodine, Electrical Properties of 6998
Ionic Radii, Theory of 7006
Iron Films by Impact Evaporation, Preparation of 6975
Iron-Nickel Alloys, Initial Growth of Plating in Thin Electrodeposited Films of 7078
Iron-Nickel-Cobalt Alloys, Electroless Deposition of Gold on 6992
Iron-Nickel Films, Influence of Thiourea on the Deposition of 6993
Iron Whiskers Under High Fields, Observation of Domains in 7034
Isolator in Rectangular Waveguide, Operation of the Field Displacement 7112
Isolators,
Double Ridge Rectangular Waveguide 7113
Yttrium Iron Garnet Resonance 7115

J

Junctions in Diffused Silicon Devices, Uniformity of 7100

K

Kerr:
Effect in Deuterium-Doped Rochelle Salt, Electro-Optic 7007
Magneto-Optic Effect to the Observation of Magnetic Domain Development, Application of the 7034

L

Lattices, D Bands in Cubic 7001
Lead Selenide, Electrical Properties of Sintered 6959
Lead Sulfide Photoconductive Films, Hole Mobility and Crystal Size in 7011
Limiters, Fine Wire Ferrite 7114
Lithium Fluoride,
Surface Energy of 6999
Thermal Conductivity of 7074
Logic, Impulse Selection for Ferrite Core 7183
Logic:
Circuits,
Elliott Sheffer Stroke Static Switching 7176
Transistor Static Switching 7175
Tunnel:
Diode 7178, 7179
Diodes and Backward Diodes Designed for Use in Computer 7218
Circuitry, Transistor-Diode 7182
Gates, Design of Transistor Resistor 7181
Networks Within an Augmented Boolean Algebra, Theorem for Deriving Majority- 7174
Luminescent Emission States of the Rare Earths, Factors Influencing the 7061
Lutetium, Electrical Resistivity of Polycrystalline 7016

M

Magnesium Oxide, Surface Energy of 6999
Magnesium Oxide Single Crystals, Secondary Electron Emission from 7023, 7024
Magnetic:
Anisotropies of Evaporated Nickel Films 7041
Core Logic, Impulse Selection for 7183
Cores and Transistors, Binary Counters Using 7184
Crystal Puller, Synthesis and Crystal Pulling of Gallium Arsenide in a 6956
Devices:
Faraday Rotators 7113
Ferromagnetic Thin Films 7190
Field Displacement Isolators 7112
Fine Wire Ferrite Limiters 7114
Isolators 7113
Yttrium Iron Garnet Resonance Isolators 7115

Film:
Memories, High Speed Thin 7191
Recording Channel, Transistor 7170
Films,
Spiral Walls in Thin 7038
Structure of Thin 6974, 6976
Films:
by Impact Evaporation, Preparation of 6975
Electrodeposited in a Magnetic Field, Influence of Substrates on Thin 7039
Materials, Generation of Microwave Electromagnetic Radiation in 7169
Moment Arrangements in Manganese Spinels, Triangular 7037
Properties of:
Cobalt and Cobalt-Nickel Alloys, Effect of Plating Parameters on the 6994
Electrodeposited Thin Nickel-Iron Films, Effects of Composition and Thickness on the 7040
Ferrite Thin Films 6976
Low Loss Nickel Zinc Ferrites 7056
Oblique-Incidence Permalloy Films 7042
Permalloy Films Evaporated at Grazing Incidence 6971, 6973
Permalloy Films, Use of Magnetoresistance Measurements to Study the 7044
the Heavy Rare Earth Metals 7016
Thin Ferrite Films 6974
Ultra Fine Ferrite Particles 6973
Yttrium-Iron Garnets Containing Neodymium 6977
Recording Heads, High-Resolution Ferrite 7171
Switching in Permalloy Films 7044
Transducer Heads, Fine-Grained Ferrite for 7171
Magnetization:
of $Mn_{2-x}Cr_xSb$ 7033
of Yttrium Iron Garnets Containing Neodymium, Saturation 6977
Process of a Helical Spin Configuration 7031
Magnetoresistance Measurements to Study the Magnetic Properties of Permalloy Films, Use of 7044
Manganese:
and its Alloys, Antiferromagnetic Domains in 7036
Spinels, Triangular Moment Arrangements in 7037
Manganese Chromium Antimonide, Exchange Inversion in 7033
Manganese Fluoride by High Magnetic Fields, Spin Flopping in 7050
Manganese Oxide, Infrared Antiferromagnetic Resonance in 7048
Masers, Slow-Wave Structures for Traveling Wave 7115
Mass Spectrometric Analysis of Molecules in Equilibrium with Silicon Carbide 6929
Measurement of:
DC Currents, Semiconductor Diode Modulator for 7202
Diode Impedance 7124
Drift Mobility Using the Field Effect Modulation of Photoconductors 7070
Humidity Using Peltier Cooling 7206
Radiation Emissivity Using the Peltier Effect 7072
Stress in Very Thin Electrodeposits 7078
the Match of a Crystal Mixer 7118
the Surface Energies of Crystals 6999
Medical Applications of Transistors:
Cardiotachometers 7161
Intercardiac Catheter Tip Piezoresistive Pressure Gauge 7117
Melting of $AgSeTe_2$, Incongruent 6954
Memories, High Speed Thin Magnetic Film 7191
Memory:
Cells, Ferroelectric 7193
Systems with Rapid Cycle Times, Ferrite-Core 7189
Mercury Selenide-Mercury Telluride Alloys,
Electrical Properties of 6931
Growth of Single Crystals of 6931
Metals on Silicon, Mechanisms of Electroless Deposition of 6991
Metals, Theory of Impurity Resistance in 7014
Microelectronics, Thin Circuit 7122
Microplasmas in Silicon 7088
Microsystem:
Bandpass Amplifier 7131
Electronics,
Categorization of the Solid-State Device Aspects of 7103
Titanium Thin Film Resistance for 7107
Use of Distributed Parameter Circuits in 7123
Microwave:
Applications, Garnets for 7216
Carrier Injection Modulator, Semiconductor 7109
Devices: Traveling Wave Masers 7115
Electromagnetic Radiation in Magnetic Materials, Generation of 7169
Modulator, Excess Carrier Injection 7109
Projectile Telemetry 7164
Properties and Applications of Garnets 7054
Spectrometers, Detectors for 7205
Mixers, Optimum Source Conductance of Crystal 7118
Mobilities in Zinc Arsenide and Cadmium Arsenide, Carrier 7027
Mobility:
Doping of Semiconducting Compounds 7012
in Lead Sulfide Photoconductive Films, Hole 7011
Using the Field Effect Modulation of Photoconductors, Measurement of Drift 7070
Modulator,
Excess Carrier Injection Microwave 7109
Magnetic Pulse Generator for Use as a Radar 7160
Modulators, Double-Sideband Doubly-Pumped Nonlinear Reactance 7155
Modulators for DC Current Measurement, Semiconductor Diode 7202
Molecular Solids, Domain Theory of Carrier Behavior in 7008
Molybdenum-Cobalt Alloys, Electrodeposition of 6996
Multiplier for Use at Radio Frequencies, Hall Effect 7105
Multivibrators, Transistor: Effect of Saturation on 7148

N

Néel Points of the Heavy Rare Earth Metals 7016
Negative Impedance Converter, Synthesis of Active Networks with One 7120
Neodymium in Yttrium-Iron Garnets, Incorporation of 6977
Network:
Synthesis with One Negative Impedance Converter 7120
Theory: The Node System of Equations 7119
Neutron:
Activation Analysis of Impurities 6942, 6943
Detectors, Silicon Surface Barrier 7209
Nickel, Electroless Deposition of Gold on 6992
Nickel:
Films, Magnetic Anisotropies of Evaporated 7041
Films by Impact Evaporation, Preparation of 6975
Nickel Oxide, Neutron and Optical Studies of Antiferromagnetic Domains in 7035
Nickel Zinc Ferrites, Preparation and Properties of Low Loss 7056
Nickel-Cobalt Alloys from a Pyrophosphate Bath, Electrodeposition of 6995
Nickel-Iron Films, Effects of Composition and Thickness on the Magnetic Properties of Electrodeposited Thin 7040
Noise:
in a Nonlinear R-C System 7021
in Semiconductors, Excess 7022
Properties of Varactor Diodes 7115
to Traps in Cadmium Sulfide and Zinc Oxide, Relation of 7022
Nuclear:
Instruments, Transistor 7207
Instruments:
Pulse Height Analyzer 7211
Time-To-Pulse-Height Converters 7210
Particle Detectors,
Semiconductor Junction 7212
Silicon Junction 7208
Silicon Surface Barrier 7209

O

Organic:
Molecular Solids, Variation of Energy Gap w
Size of the Conjugated Syste
in 7029
Polymer Films,
Dielectric Properties of 7013
Electric Charge Transport Through 7013
Photocurrents Excited by Visible Light in
7013
Solids, Surface Trapping in 7029
Orientation of Evaporated Tin Telluride Films, Cry
tallographic 6953
Oscillators,
Transistor:
Beta-Phase-Shift 7151
Calculation of Pulse Duration in Blocking
7149
LC 7147
Phase Stabilized VLF 7146
Tunnel Diode: Gallium Arsenide 7150
Oxidation of Indium Antimonide, Theory of 6979

P

Paramagnetic:
Behavior of Polycrystalline Samarium 7057
Resonance of Europium in Single Crystals of Cadmium Sulfide 7058
Parametric:
Amplifier Transistor Operating in an Up-Con-
version Mode 7137
Amplifiers,
Capabilities and Limitations of 7133
Coupled-Cavity Traveling Wave 7138, 7139
Limitation on the Noise Performance of 7136
Optimum Noise and Gain-Bandwidth Per
formance of 7134
Symmetrical Matrix Analysis of 7135
Tunable 7140
Harmonic Generators, Large Signal Analysis
7157
Modulators 7155
Particle:
Counters, Cadmium Sulfide and Zinc Sulfide 6967
Detectors, Semiconductor Junction 7208, 72
Growth During Zinc Sulfide Phosphor Prepara
tion 6969
Particles, Growth of Ultra Fine Ferrite 6972
Peltier:
Cooling, Automatic Dew-Point Hygrometer Using 7206
Effect for Cooling Diodes, Use of the 7075
Method of Measuring Radiation Emissivity 70
Perfection of Crystals, Determination of the 6945
Permalloy:
Films,
Annealing of Oblique-Incidence 7042
Magnetoresistance and Magnetic Switchi
in 7044
Films Evaporated at Grazing Incidence 6971
6973
Thin Films, Rotatable Anisotropy in 7043
Phase Diagram of Mercury Selenide-Mercury Tellu
6931
Phosphorescence Mechanisms, Theory of 7065, 7
7067, 7068
Phosphor Films by Evaporation, Formation of Zinc
Sulfide 6968

Phosphor Preparation, Particle Growth During Zinc Sulfide 6969
Phosphorometer 7066
Phosphors, Maintenance of Electroluminescent 7063
Photoconductive Films, Hole Mobility and Crystal Size in Lead Sulfide 7011
Photoconductivity in Microcrystalline Powders, Mechanism of 7069
Photoconductors, Measurement of Drift Mobility Using the Field Effect Modulation of 7070
Photocurrents Excited by Visible Light in Organic Polymer Films 7013
Photodevice Dose Ratemeter 7163
Photodevices, Two Color Input-Two Color Output Image Intensifier 7110
Photovoltaic Devices, Diffused Silicon 6949
Phthalocyanines, Rectification in Polycrystalline 7018
Piezoelectric:
  $Ga_{2-x}Fe_xO_3$, Ferromagnetic Resonance in 7046
  Properties, Effect of Random Inhomogeneities on 7019
Piezoelectricity, Effect of Random Inhomogeneities on 7019
Piezoresistance of Antimony Doped Germanium 7003
Piezoresistive Pressure Gauge, Intercardiac Catheter Tip 7117
Plastically Deformed Tellurium, Recombination at Dislocations in 6936
Plating:
  in Thin Electrodeposited Films of Fe-Ni Alloys, Initial Growth of 7078
  Parameters on the Structure of Cobalt and Cobalt-Nickel Alloys, Effect of 6994
Polarizability of Free Carriers in Germanium and Silicon 7010
Polarization Reversal in Deuterium-Doped Rochelle Salt 7007
Polystyrene Films, Electric Charge Transport Through 7013
Polytypism in Silicon Carbide Crystals 6937, 6952
Potassium Chloride,
  Electrical Properties of 6998
  Electron Microscope Studies of Colloids in 6981
Potassium Chloride:
  Crystals, Breakdown Strength of 6998
  Single Crystals, Diffusion of Color Centers into 6934
  Surfaces, Electron Microscope Studies of Cleaved 6981
Powder Metallurgy Techniques, Preparation of Lead Selenide by 6959
Powders, Mechanism of Photoconductivity in Microcrystalline 7069
Power:
  Converters, Transistor DC to DC 7201
  Regulators, Transistor DC 7196
  Supply, Transistor Regulated 7200
Precipitate in Silver Antimony Telluride, Widmanstatten 6954
Precipitated:
  Phase in Germanium 6935
  Phases in Crystal Lattices, Determination of 6945
Pressure Gauge, Intercardiac Catheter Tip Piezoresistive 7117
Projectile Telemetry with Microwaves 7164
Protection of:
  Semiconductor Rectifiers, Short-Circuiter for 7125
  Transistors in Circuits 7199
Pulse:
  Amplifiers, Regenerative 7168
  Amplitude Interpolation Computer for Doppler Radar 7195
  Code Modulation Repeaters, Transistor 7168
  Generator for a Radar Modulator, Magnetic 7160
  Generators, Transistor 7159
  Height Analyzer, Transistor 7211
Purification of Arsenic 6946
Pyrophosphate Bath:
  Electrodeposition of Cobalt-Molybdenum Alloys from a 6995
  Electrodeposition of Nickel-Cobalt Alloys from a 6995
Pyropolymers, Semiconduction in Aluminum-Doped 7028

Q

Quartz by Gallium, Dissolution of 6928

R

Radar, Pulse Amplitude Interpolation Computer for Doppler 7195
Radar:
  Modulator, Magnetic Pulse Generator for Use as a 7160
  Transponder, Solid State 7223
Radiation, Production of Color Centers in Alkaline Earth Fluorides by X-Rays and Electron 7059, 7060
Radiation:
  Damage in Crystals, Dynamics of 6997
  Emissivity, Peltier Method of Measuring 7072
  Monitor, Transistor 7213
  on the Thermal Conductivity of Synthetic Sapphire, Effects of 7073
Rare Earth Metals, Resistivity of the 7016
Rare Earths, Factors Influencing the Luminescent Emission States of the 7061
Ratemeters, Design of Transistor 7162
Raysistor 7221
Reactions between Gallium and Quartz 6928
Reactor Safety System, Transistor and Controlled Rectifier 7214
Recombination:
  at Dislocations in Plastically Deformed Tellurium 6936
  in Gallium Arsenide, Direct 7009
Recording:
  Channel, Transistor Magnetic Film 7170
  Heads Using Bonding Glass Spacers, High-Resolution Ferrite 7171
Rectifiers, Gallium Arsenide Power 7091
Rectification, Theory of Electrolytic 7017
Rectification in Polycrystalline Phthalocyanines 7018
Rectifying:
  Barrier at an AlC-SiC Interface 7026
  Contacts to Silicon Carbide 7026
Reflection Spectra of Sodium Iodide Single Crystals 7064
Reflectivity of Germanium and Silicon 7010
Regulators,
  Corbino Disk Voltage 7106
  Transistor:
    DC Power 7196
    Switched Voltage 7198
Relays, Electro-Optical 7221
Repeaters,
  Negative Impedance 7167
  Transistor Pulse Code 7168
Resistance:
  for Microsystems Electronics, Titanium Thin Film 7107
  in Metals, Theory of Impurity 7014
Resistivity:
  of Granular Silicon Carbide 6948
  of Silver Selenide 7077
  of the Heavy Rare Earth Metals 7016
  to Néel Point in the Heavy Rare Earth Metals, Relation of Electrical 7016
Resistors, Dynamic Current-Voltage Characteristics of Silicon Carbide 7108
Resonance, Nonlinear Effects of Crystalline Anisotropy on Ferrimagnetic 7049
Resonance:
  Due to Magnetic Field Generated by Displacement Currents in Ferrites, Ferromagnetic 7045
  Frequency of Antiferromagnets with Large Uniaxial Anisotropy 7047
  in a Single Crystal Disc of Yttrium Iron Garnet, in Manganese Oxide, Infrared Antiferromagnetic 7048
  in Piezoelectric $Ga_{2-x}Fe_xO_3$, Ferromagnetic 7046
  Line Width:
    in some Rare Earth Doped Yttrium Iron Garnet, Ferrimagnetic 7053
    Maximum in Yttrium Iron Garnet, Ferromagnetic 7051
  of Europium in Single Crystals of Cadmium Sulfide, Electron Paramagnetic 7058
Rochelle Salt,
  Electro-Optic Kerr Effect in Deuterium-Doped 7007
  Polarization Reversal in Deuterium-Doped 7007
Ruby, Decay Rate of the Phosphorescence of 7068
Rutile Single Crystals, Electrostrictive Effect in 6998

S

Samarium, Paramagnetic Behavior of Polycrystalline 7057
Sapphire, Effect of Irradiation on the Thermal Conductivity of Synthetic 7073
Saturable Reactors and Transistors, Systems Using 7144
Saucer Etch Pits Due to a Precipitated Phase 6935
Scaler, Gallium Arsenide Tunnel Diode Decade 7224
Scalers, Read-Out Systems for Transistor 7185
Scaling Reactions, Theory of Diffusion-Limited 6979
Secondary Electron Emission from Magnesium Oxide Single Crystals 7023, 7024
Segregation in Crystal Lattices, Determination of 6945
Selenium from Arsenic, Separation of 6946
Semiconducting Compounds, Mobility Doping of 7012
Semiconductor Surface, Catalysis at a 6980
Semiconductors,
  Electronic Structure of Group IV and III-V 7002
  Excess Noise in 7022
  Machine for Slicing 7217
Sensistor for Stabilizing Transistor Circuits, Use of 7126
Shift Registers, Tunnel Diode 7179
Short-Circuiter for Protecting Semiconductor Rectifiers 7125
Silicon,
  Electrical Properties of 6998
  Faraday Effect at Microwave Frequencies in 6998
  High Field Effects in 7088
  Impurity Variations in 6947
  Liquid-Solid Interface Reactions During Etching of 6988
  Mechanism of Chemical Etching of 6987
  Mechanisms of Electroless Deposition of Metals on 6991
  Method for Monitoring the Chemical Etching Rate of 6982
  Microplasmas in 7088
  Modified Closed Box System for the Diffusion of Boron in 6949
  Polarizability of Free Carriers in 7010
  Reflectivity of 7010
  Shape of Melt-Crystal Interfaces During Float Zoning of 6958
  Surface Energy of 6999
  Use of Low Temperature Hall Measurements for Determining Impurity Concentrations in 6941
Silicon:
  and Germanium, Comparison of the Etch Rate of 6985
  Contacts, Improved 7097
  Dendrites,
    Growth and Evaluation of 6964
    Growth Steps on the Surface of 6963
  in Gallium, Solubility of 6928
  Photovoltaic Devices, Diffused 6949
  Resistor for Stabilization of Transistor Circuits,

Single Crystals for Fabricating Diffused Junction Devices, Method of Evaluating 7092
Silicon Carbide,
Analysis of Impurities in 6940
Dislocation-Etch Pit Relation in 6937
Etching of 6989, 6990
Fused Contacts to 7026
Heat of Sublimation of 6929
Mass Spectrometric Analysis of Molecules in Equilibrium with 6929
Neutron Activation Analysis of 6943
Resistivity of Granular 6948
Silicon Carbide:
Crystal Growth, Role of Dislocations in 6937
Crystals, Polytypism in 6937, 6952
Device Fabrication, Thermocouple Furnace for 7093
Films,
Electrical Properties of 6960
Fabrication of Junctions by Epitaxial Deposition of 6960
Grains, Diffusion of Nitrogen in 6948
Resistors, Dynamic Current-Voltage Characteristics of 7108
Transistors, Analysis of Bipolar and Unipolar High Temperature 7101
Varactor Diodes 7087
Silicon Nitride Receptacle, Horizontal Growth of Germanium Single Crystals Using a 6955
Silver:
into Cuprous Oxide, Diffusion of 6951
Ions in Silver Chloride, Diffusion of 6950
Silver Antimony Telluride,
Anomalous Hall Effect in 7020
Structure of 6954
Thermal Conductivity of 7020
Silver Chloride,
Dember Effect in 7025
Single Crystals, Diffusion of Ions in 6950
Silver Selenide, Preparation and Properties of 7077
Silver Selenium Telluride, Incongruent Melting of 6954
Sintered Lead Selenide,
Electrical Properties of 6959
Thermoelectric Properties of 6059
Slicing Semiconductors, Machine for 7217
Sodium Iodide Single Crystals, Fluorescence and Reflection Spectra of 7064
Sodium Niobate:
Ferroelectric Memory Cells 7193
Films, Preparation of Ferroelectric 6978
Solid:
Solution in the Mercury Selenide-Mercury Telluride System 6931
Solutions of Metals and Tungsten Trioxide 6998
Solubility of Silicon in Gallium 6928
Space Physics Applications, Pulse Height Analyzer for 7211
Spectrometers, Detectors for Microwave 7205
Spin:
Configuration, Magnetization Process of a Helical 7031
Flopping in Manganese Fluoride by High Magnetic Fields 7050
Orbit Coupling in Inorganic Complexes 7006
Spinel Structure, Dislocations, Stacking Faults and Twins in the 6932
Spiral Walls in Thin Magnetic Films 7038
Spraying, Properties of Ferrite Thin Films Prepared by 6976
Stability of:
Inorganic Complexes, Geometrical 7006
Tuned Transistor Amplifiers 7132
Stabilization:
of Transistor:
Circuits, Use of the Silicon Resistor for the 7126
Trigger Circuits 7152
Networks for Functional Electronic Blocks, Optimum 7121
Stacking:
Fault Energy in Graphite 6938
Faults in the Spinel Structure 6932
Static:
Switching, Theory of 7175
Switching System, Elliott Sheffer Stroke 7176
Storage:
Capabilities of Thin Film Cryotrons 7192
Matrix Using Ferromagnetic Thin Films, Computer 7190
with Very Short Read Time, Digital Computer 7188
Stress in Very Thin Electrodeposits, Measurement of 7078
Structural Defects in Germanium 6935
Structure of:
Cobalt and Cobalt-Nickel Alloys, Effect of Plating Parameters on the 6994
Silver Antimony Telluride 6954
Thin Ferrite Films 6974, 6976
Sulfur from Arsenic, Separation of 6946
Superconducting Gallium, Nuclear Quadrupole Resonance in 7030
Superconductive Coaxial Line, Characteristics of a 7116
Surface, Catalysis at a Semiconductor 6980
Surface:
Characteristics of III-V Intermetallic Compounds 6983
Currents in Inversion Layers of Semiconductors 7080
Energies of Crystals, Measurement of 6999
States of Diamond and Graphite 7004
Structure of Silicon Carbide Crystals 6952
Trapping in Organic Solids 7029
Surfaces, Electron Microscope Studies of Cleaved Potassium Chloride 6981
Switches,
Electro-Optical 7221
High Current Transistor 7154
Switching, Theory of Static 7175
Switching:
Capabilities of Thin Film Cryotrons 7192
Circuits, Diode Current 7177
System, Elliott Sheffer Stroke Static 7176
Synthesis of Active Networks with One Negative Impedance Converter 7120

T

Telemetry, Microwave Projectile 7164
Telephone Circuits, Transistor: Negative Impedance Repeater 7167
Television:
Circuits, Applications of Transistors to 7165
High Voltage Generators, Transistor 7166
Horizontal Sweep Circuits, Transistor 7166
Tellurium, Recombination at Dislocations in Plastically Deformed 6936
Tellurium from Arsenic, Separation of 6946
Terbium, Electrical Resistivity of Polycrystalline 7016
Thermal:
Conductivity, Effect of Point Imperfections on Lattice 7074
Conductivity:
of Germanium 7071
of Silver Antimony Telluride 7020
of Synthetic Sapphire, Effects of Irradiation on 7073
Using the Peltier Effect, Measurement of 7072
Thermocouple Furnace for Silicon Carbide Device Fabrication 7093
Thermodynamics of a Nonlinear R-C System 7021
Thermoelectric:
Effect for Cooling Diodes, Use of the 7075
Properties, Effect of Random Inhomogeneities on 7019
Properties of:
Silver Selenide 7077
Sintered Lead Selenide 6059
Thin:
Circuit Microelectronics 7122
Electrodeposited Films of Fe-Ni Alloys, Initia
Growth of Plating in 7078
Ferrite:
Films Prepared by Spraying, Properties of 6976
Films, Structure of 6974, 6976
Film:
Computer Storage Matrix, Ferromagnetic 7190
Cryotrons, Fabrication of 7192
Resistance for Microsystems Electronics, Titanium 7107
Films,
Crystal Orientation Effects in Tin-Telluric 6953
Effects of Composition and Thickness on th
Magnetic Properties of Electr
deposited Nickel-Iron 7040
Rotatable Anisotropy in Permalloy 7043
Films by Impact Evaporation, Preparation of Magnetic 6975
Magnetic:
Film Memories, High Speed 7191
Films Electrodeposited in a Magnetic Fiel
Influence of Substrates on 70
Films, Spiral Walls in 7038
Thulium, Electrical Resistivity of Polycrystalline 7016
Tin Single Crystals, Transformation of Gray 6930
Tin Telluride Films, Crystallographic Orientation o
Evaporated 6953
Titanium Thin Film Resistance for Microsystems Elec
tronics 7107
Transformation of Gray Tin Single Crystals 6930
Transistor:
Adder 7187
Arithmetic Unit 7186
Building Blocks for Data Instrumentation 71
Cardiotachometer 7161
Circuits, Use of the Silicon Resistor to Stabi
7126
DC:
Galvanometer Driver Amplifier 7203
Regulators 7196
-Diode Logic Circuitry 7182
Frequency Dividers 7153, 7158
Functional Units, High Gain Cascaded 7104
Magnetic Film Recording Channel 7170
Multivibrators, Effect of Saturation on 7148
Network Theory: The Node System of Equation
7119
Nuclear Instruments 7207
Overload Safety Circuit 7199
Power Converters, DC to DC 7201
Pulse:
Code Repeaters 7168
Generators 7159
Radiation Monitor 7213
Ratemeters, Design of 7162
Reactor Safety Systems 7214
Regulated Power Supply 7200
Resistor Logic Gates, Design of 7181
Scalers, Read-Out Systems for 7185
Stabilized Voltage Supplied 7197
Switched Voltage Regulators 7198
Switches, High Current 7154
Television Circuits, 7165, 7166
Trigger:
Circuit Stabilization 7152
Circuits, Cascode 7153
Video:
Amplifiers, Design of 7130
Current Amplifiers 7165
Wave Analyzers 7204
Transistors,
Field-Effect: Effect of Electron-Hole Pair Gen
eration on the Characteristics
of Photoconductive 7070
Junction:

SUBJECT INDEX *(Continued)*

Analysis of Bipolar and Unipolar Silicon Carbide High Temperature 7101
Charge Control Parameters 7094
Dissipation of Heat in 7102
Double Diffused Silicon 6949
Epitaxial 7219
Generalized Padé Approximation for Current Gain 7096
Non-Linear Distortion in 7095
Operation at High Current and in Saturation 7099
Parametric Amplifier 7137
Physical Limitations on Current Gain 7097
Resorption Time of Excess Charge Carriers in the Base Region of 7148
RF Transconductance of Alloyed and Drift 7098
Small Signal Parameters of 7095
Switching Characteristics of 7099
Uniformity of Junctions in Diffused Silicon 7100
Transistors:
and Magnetic Cores, Binary Counters Using 7184
and Transductors, Systems Using 7144
Transponder, Solid State Radar 7223
Trapping in Organic Solids, Surface 7029
Traps to Noise in Cadmium Sulfide and Zinc Oxide, Relation of 7022
Triangular Moment Arrangements in Manganese Spinels 7037
Trigger Circuits,
Cascode Transistor 7153
Stabilization of Transistor 7152
Tunnel Diode 7179
Tungsten Trioxide, Solid Solutions of Metals and 6998
Tunnel Diode:
Amplifiers, Theory and Synthesis of 7143
Converters 7156
Decade Scaler, Gallium Arsenide 7224
Locked Pairs 7180
Logic Circuits 7178, 7179
Oscillators, Gallium Arsenide 7150
Trigger Circuits 7179
Tunnel Diodes,
Design of Germanium 7082
Fabrication of Gallium Arsenide 7150
Neutron Bombardment of 7083
Tunnel Diodes and Backward Diodes Designed for Use in Computer Logic Circuits 7218
Twins in the Spinel Structure 6932

U

Uranium Glass, Decay Rate of the Phosphorescence of 7068

V

Valley-Orbit Splitting of Antimony in Germanium 7003
Varactor Diodes,
Design of 7081
Figure of Merit for 7081
Impedance of Diffused Silicon Mesa 7124
Noise Properties of 7115
Silicon Carbide 7087
Varistors, Dynamic Current-Voltage Characteristics of Silicon Carbide 7108
Video:
Amplifiers, Design of Transistor 7130
Current Amplifiers, Design of 7165
Voltage:
Generators, Transistor Television 7166
Regulators,
Corbino Disk 7106
Transistor:
DC 7196
Switched 7198
Supplies, Transistor Stabilized 7197

W

Walls in Thin Magnetic Films, Spiral 7038
Wave Analyzers, Transistor 7204
Waveform Generator, Sawtooth 7153
Whiskers:
by the Hydrogen Reduction of Cuprous Iodide Vapor, Growth of Copper 6970
Under High Fields, Observation of Domains in Iron 7034

X

X-Ray Diffraction Microscopy, Determination of Crystal Perfection by 6945
X-Rays, Production of Color Centers in Alkaline Earth Fluorides by 7059, 7060

Y

Yttrium Garnets, Device Applications of 7054
Yttrium Iron Garnet,
Ferrimagnetic Resonance in a Single Crystal Disc of 7052
Generation of Microwave Electromagnetic Radiation in 7169
Nature of the Low Temperature Line Width Maximum in 7051
Non-Linear Response of 7055
Yttrium Iron Garnet:
Doped with Rare Earth, Temperature Dependence of Ferrimagnetic Resonance Line Width in 7053
Resonance Isolators 7115
Yttrium Iron Garnets, Incorporation of Neodymium in 6977

Z

Zinc Arsenide, Electrical Properties of 7027
Zinc Oxide, Relation of Traps to Noise in 7022
Zinc Sulfide,
Decay Rate of the Phosphorescence of Mn-Activated 7068
Theory of Electroluminescence in 7062
Zinc Sulfide:
Crystals for Use as Detectors in Crystal Counters, Properties of 6967
Electroluminescent Phosphors, Maintenance of 7063
Phosphor:
Films by Evaporation, Formation of 6968
Preparation, Particle Growth During 6969
Zinc, Surface Energy of 6999

CONFERENCE PROGRAMS ABSTRACTED

in SOLID STATE ABSTRACTS, Vol. I, No. 3 and No. 4

Conference on Silicon Carbide, Boston, Mass., Apr. 2-3, 1959 (Proc. Conf. Silicon Carbide)

Eastern Joint Computer Conference, New York, N.Y., Dec. 13-15, 1960 (Proc. 1960 Eastern Joint Computer Conf.)

Fifth National Symposium on Space Electronics and Telemetry, Washington, D.C., Sept. 19-21, 1960 (Trans. 1960 Natl. Symposium on Space Electronics and Telemetry)

ISA Fall Instrumentation-Automation Conference, New York, N.Y., Sept. 26-30, 1960 (ISA 1960 Fall Instr. Automation Conf.)

Joint Symposium of the Corrosion and Electronics Divisions of the Electrochemical Society on the Surface Chemistry of Metals and Semiconductors, Columbus, Ohio, Oct. 19-21, 1959 (Surface Chem. Metals and Semicon.)

Princeton University Conference on Semiconduction in Molecular Solids, Princeton, N.J., Feb. 16-17, 1960 (Proc. Princeton U. Conf. Semiconduction Molecular Solids)

Properties of Elemental and Compound Semiconductors Conference, Boston, Mass., Aug. 31 - Sept. 2, 1959 (Properties of Elemental and Compound Semicon. Conf.)

Sixth Conference on Magnetism and Magnetic Materials, New York, N.Y., Nov. 14-17, 1960 (Sixth Conf. Magnetism and Magnetic Materials)

1960 Electron Devices Meeting, Washington, D.C., Oct. 27-28, 1960 (1960 Electron Dev. Mtg.)

1960 Fall Meeting of the Electrochemical Society, Houston, Tex., Oct. 9-13, 1960 (1960 Fall Meeting Electrochem. Soc.)

1960 IRE International Convention, New York, N.Y., Mar. 21-24, 1960 (1960 IRE Int. Conv. Rec.)

1960 IRE WESCON Convention, Los Angeles, Calif., Aug. 23-26, 1960 (1960 IRE WESCON Conv. Rec.)

1960 National Electronics Conference, Chicago, Ill., Oct. 10-12, 1960 (Proc. 1960 Natl. Electronics Conf.)

AUTHOR INDEX

Abrahams, E. 7015
Adams, D. K. 7155
Aldrich, R. W. 7103
Allen, F. 7196
Amelinckx, S. 6937, 6938
Andrievskii, A. I. 6951
Ansel, G. 7208
Arajs, S. 7057
Armstrong, L. D. 7091
Armstrong, R. W. 6954
Arnoldt, P. 7153
Arrott, A. 7036
Aspinall, D. 7186
Avakian, P. 6966
Azaroff, L. V. 7005

Bady, I. 7045
Bagno, S. M. 7215
Ballentyne, D. W. G. 7062
Banks, E. 6974
Bartholomew, D. D. 7113
Baruch, P. 7208
Bate, R. T. 6941, 7072
Bell, J. S. 7197
Benanti, M. 7109
Benbow, T. G. 7185
Benjamin, R. 7109
Bergman, R. H. 7178
Bergman, R. S. 7055
Berman, I. 7090
Berman, R. 7073
Bernard, W. 7021
Billington, C. 7065, 7066, 7067, 7068
Bither, T. A. 7033
Blair, R. R. 7083
Blakemore, J. S. 6936
Blank, J. M. 7122
Blum, S. 6956
Bockemuehl, R. R. 7070
Bogusch, R. 7191
Bolling, G. F. 6957
Bonner, A. L. 7167
Booker, G. R. 6963
Bradley, E. M. 7190
Brand, F. A. 7109
Braun, J. H. 6958
Bregman, F. 7213
Brog, K. C. 7200
Brooks, H. 7010
Brophy, J. J. 7022
Brouillette, J. W. 7103
Brown, J. S. 7127
Brown, T. M. 6996
Brownson, J. W. 6947
Bube, R. H. 7069
Buelow, F. K. 7177
Burrus, C. A. 7150
Butler, S. A. 7179

Cali, J. P. 6942, 6943
Callaway, J. 7001, 7074
Callen, H. B. 7021
Cardona, M. 7010
Carlson, A. 6962
Carlson, A. W. 7084
Carroll, P. 6948
Caspari, M. E. 6998
Castro, P. S. 7123, 7131
Catlin, A. 7079
Chang, H.-C. 7101
Chien, R. T. 7120
Chirkin, L. K. 7108
Cloud, W. H. 7033
Coghill, H. D. 6968
Cohen, E. 7105
Cohen, M. S. 6973
Coles, B. R. 7036
Collins, D. A. 7007
Colvin, R. V. 7016
Comstock, R. L. 7112
Conn, J. B. 7077
Cooper, B. R. 7047
Coren, R. L. 7044
Cornish, A. J. 7012
Critchlow, D. L. 7179
Croft, W. J. 6976
Croll, I. M. 6994
Crosby, D. R. 7180
Crouch, W. M. 7203
Culligan, G. 7210
Cunningham, J. A. 7173
Currie, M. R. 7138
Czyzak, S. J. 6967

Davis, H. L. 7032
De Bolt, H. E. 7202
Deetscreek, V. D. 6972
Delavignette, P. 6938
De Maria, G. 6929
DeMars, R. D. 6993
Dermatis, S. N. 6964
Desai, U. D. 7211
Deutsch, S. 7135
Diemer, G. 7145
Dillon, Jr., J. F. 7053
Ditzenberger, J. A. 6946
Dorain, P. B. 7058
Downs, R. 7117
Drowart, J. 6929
Duinker, S. 7171
Dymanus, A. 7046

Easley, J. W. 7083
Ebhardt, R. 7080
Edwards, D. B. G. 7186, 7189
Eggers, F. G. 7169
Ellis, Jr., R. C. 6990
Enz, U. 7031
Eriksen, B. K. 7195
Ertel, A. 7092
Ewald, A. W. 6930

Faria, S. 6969
Farrell, L. B. 6931
Faust, Jr., J. W. 6954, 6964, 6989
Fine, M. E. 6930
Fisch, E. A. 7191
Fischler, A. S. 7027
Fochs, P. D. 6961
Foster, E. L. 7073
Foster, L. M. 6928
Fotland, R. A. 6978, 7193
Fowler, Jr., C. A. 7034
Frank, F. C. 6984
Fritzsche, H. 7003
Frolov, V. N. 7147
Fryer, E. M. 7034
Fuller, H. W. 7038
Fuller, W. D. 7131
Fullwood, R. 7207

Garrett, C. G. B. 6980
Garrison, J. L. 7167
Gatos, H. C. 6983
Gerthsen, P. 7206
Gibson, J. B. 6997
Gilman, J. J. 6999
Gilsing, J. A. A. 7206
Gittinger, N. C. 7140
Glassbrenner, C. 7071
Goering, H. L. 6965
Goetzberger, A. 7089
Goland, A. N. 6997
Goldring, G. 6977
Gooch, G. M. 7116
Goodman, A. M. 7025
Gottlieb, P. 7049
Gould, R. W. 7138
Grabowski, K. P. 7139
Graham, Jr., C. D. 7041
Gran, B. E. 7043
Greene, J. C. 7134
Greifer, A. P. 7056
Gremmelmaier, R. 7163
Grimes, Jr., E. S. 7113
Grimsdale, R. D. 7188
Groschwitz, E. 7080
Grossman, J. J. 6988

Haak, F. A. 7018
Hammond, R. H. 7030
Happ, W. W. 7123
Harman, T. C. 6931
Harten, G. A. 7161
Haszko, S. E. 7020
Helsdon, P. B. 7165
Henkels, H. W. 7104
Hergenrother, K. M. 6960
Herick, D. J. 7166
Herring, C. 7019
Hertz, C. H. 7163
Hilibrand, J. 7081
Hill, R. L. 7173
Hill, R. M. 7055
Himes, R. C. 6959, 6965
Hinckfuss, I. C. 7172
Hittle, C. E. 7170
Hodara, H. 7130
Hofmeister, E. 7080
Holmen, J. O. 7043
Holonyak, Jr., N. 7103
Holt, D. B. 7000
Hopper, A. L. 7128
Horn, F. H. 6971
Hornstra, J. 6932
Huber, F. 7017

Inoue, M. 6934
Irons, H. R. 7184

Jacobs, H. 7109
Jacobs, I. S. 7050
Johannessen P. R. 7160
Johnson, K. M. 7157
Johnson, R. E. 7076
Jones, A. R. 7212
Juretschke, H. J. 7044

Kaminow, I. P. 7046
Kaminsky, G. 7086
Karew, J. J. 7182
Kaupp, H. R. 7180
Kay, E. 6975
Keffer F. 7048
Keith, R. J. 7172
Kellett, P. 7176
Kendrick, W. M. 7164
Kesperis, J. S. 6949
Kharlamova, T. E. 7087
Kholuyanov, G. F. 7087, 7108
Kilburn, T. 7186, 7188, 7189
Kim, C. S. 7156
Kleinman, D. A. 7106
Klier, J. 7125
Klick, C. C. 6933
Knight, W. D. 7030
Kolk, A. J. 7078
Koller L. R. 6968
Konigsberg, R. L. 7194
Kontorovich, M. I. 7147
Kopp, W. J. 7167
Koroncai, A. K. 7161
Koutecky, J. 7004
Kramer, R. A. 6928
Kremheller, A. 6969
Krohn, A. 6996
Kuhlmann-Wilsdorf, D. 6939
Kuz'min, V. A. 7148, 7149
Kuznetzoff, P. 7091

Laherrere, J. P. 7028
Langer, J. S. 7014
Lanigan, M. J. 7189
Laponsky, A. B. 7023
La Rue, J. J. 7119
Lassiter, E. M. 7160
Lauriente, M. 7039
Lavine, M. C. 6983
LeCraw, R. C. 7051
Lee, C. A. 7086
Legvold, S. 7016
Lemaire, H. P. 6976
Le May, C. Z. 7101
Lesk, I. A. 7103, 7122
Lessoff, H. 7056
Liehr, A. D. 7006
Lindaman, R. 7174
Lipman, N. H. 7210
Loken, M. K. 7162
Lommel, J. M. 7041
Long, M. W. 7205
Lougher, E. H. 7072
Love, T. A. 7209
Lowe, L. F. 6943
Lumpkin, O. 7158
Lynch, J. T. 7182
Lyon, D. H. 6935

Macaulay, I. J. 7172
Maissel L. L. 7097
Mann, H. 7152
Martin, Jr., D. C. 6950
Marvin, J. F. 7162
Matlow, S. L. 6991, 7002
Mayburg, S. 7009
Mayer S. E. 6960
McCall, Jr., G. S. 7045
McMullen, C. W. 7141
McNally, F. X. 7039
Mead, C. A. 7099
Mehrtens, D. H. 7126
Meindl, J. D. 7109, 7121
Messner, D. 7060
Meyer, N. I. 7095
Milgram, M. 6997
Miller, A. 7015
Miller, D. P. 6953
Miller, J. F. 6959, 6965
Miller, L. E. 7100
Miller, W. D. 7162
Minamoto, M. T. 7093
Minner, W. 7098
Mizuno, H. 6934
Mlavsky, A. I. 6960
Mohanty, G. P. 7005
Mohr, R. J. 7118
Morelock, C. R. 6970
Morgan, J. V. 7011
Morgan, S. P. 7085
Morrison, G. H. 6940
Moruzzi, V. L. 7037
Mrozowski, S. 7029
Murray, R. B. 7209

Nahman, N. S. 7116
Nakada, Y. 7056
Neff, G. W. 7179
Nicoll, F. H. 7110
Nolta, J. P. 7018
Nomura, K. C. 6936
Nowalk, T. P. 7104

Ohlsen, G. T. 7175
Okwit, S. 7118

Partridge, G. R. 7168
Pasynkov, V. V. 7108
Paul, W. 7010
Payne, H. 6967
Pederson, D. O. 7142
Pellikan, S. G. 7147
Pellin, R. A. 6958
Pelzl, H. 7166
Pepper, R. S. 7142
Perkins, G. D. 6944
Peters, L. A. 7164
Peterson, W. C. 7119
Petrak, J. R. 7204
Pitzalis, O. 7121
Plotkin, S. 7158
Pohl, H. A. 7008, 7028
Pomerantz, M. A. 7024
Porreca, G. 7211
Porter, J. L. 6955
Price, Jr., C. H. 7154
Prosen, R. J. 7043

Quinn, H. F. 6994

Rama Char, T. L. 6995
Ramsay, D. A. 7144
Raskin, J. S. 7181
Ray, C. E. 7112
Reade, R. F. 6950
Redmond, K. 7199
Reed, H. J. 7196
Reese, W. E. 7027
Rettinger, M. 7170
Riederman, N. H. 6974
Robbins, H. 6985, 6986
Robinson, C. F. 6944
Rodrigue, G. P. 7054
Rosenberg, A. J. 6979
Rosenthal, L. A. 7159
Roth, W. L. 7035
Rowen, J. H. 7169
Rubinstein, H. 7038
Runyan, W. R. 7102
Rupp, R. L. 6940

Saha, A. R. 7151
Salter, F. 7187
Sandulova, A. V. 6951
Saphir, R. 6947
Sard, E. W. 7134
Scarr, R. W. A. 7111
Schawlow, A. L. 7106
Schieber, M. 6977
Schieve, W. C. 7024
Schlereth, F. H. 7195
Schleuning, H. W. 6974
Schmidt, J. D. 7195
Schmidt, P. F. 7017
Schneidmesser, B. 7073
Schuele, W. J. 6972
Schultz, J. W. 6936
Schwartz, B. 6985, 6986
Schwarz, R. F. 7017
Schwuttke, G. H. 6945
Scott, D. C. 7113
Scouler, W. J. 7059
Sears, G. W. 6970
Selig, T. R. 7082
Setterington, R. A. 7111
Shatas, R. A. 7024
Shiozawa, L. R. 6962
Shombert, D. J. 6941
Shortes, S. H. 6953
Sievers, III, A. J. 7048
Silber, L. M. 6974
Simon, R. 7072
Simon, R. E. 6981
Simonov, Iu, L. 7132
Singer, K. 7170
Slack, G. A. 7071
Sloan, S. C. 7113
Smakula, A. 6966, 7059, 7060
Smilen, L. I. 7143
Smith, A. W. 7052
Smith, D. O. 7042
Smits, F. M. 7085
Smulkowski, O. 7208
Smyth, R. R. 7201
Sorenson, A. A. 7198
Sparkes, J. J. 7094
Sparks, J. E. 7156
Spedding, F. H. 7016
Spencer, E. G. 7051
Spencer, H. E. 7011
Spencer, R. H. 7160
Spokas, J. J. 7013
Spratt, J. P. 7097
Sproull, R. L. 6981
Sree, V. 6995
Stafeev, V. I. 7075
Stern, E. 7114
Stewart, J. L. 7096
Stocker, C. F. 7081
Strauss, A. J. 6931
Strumane, G. 6937
Struthers, J. D. 6946
Strutt, M. J. O. 7129
Sullivan, D. L. 7038
Suran, J. J. 7122
Sussman, A. 7110
Swoboda, T. J. 7033

Tancrell, R. H. 7183
Taylor, R. C. 7077
Taylor, T. C. 7026
Thomas, R. C. 7082
Thompson, H. D. 6943
Thornton, W. A. 7063
Thurston, M. O. 7133
Tiller, W. A. 6954, 69
Tinkham, M. 7048
Timizi, S. M. A. 7073
Tomasek, M. 7004
Towns, G. 7076
Traite, M. 7117
Trambarulo, R. 7150
Trenholme, W. M. 721
Treves, D. 7034
Truesdell, R. M. 7146
Turner, D. R. 6982, 69
Turner, E. H. 7051
Turner, W. J. 7027

Vager, Z. 6977
Van Allen, R. L. 7211
van Berkum, P. A. 716
Van Santen, J. G. 714
Van Sciver, W. J. 706
van Tol, M. 7206, 7213
Van Uitert, L. G. 706
Verma, A. R. 6952
Vineyard, G. H. 699
Vinogradoso, B. N. 7 4
Vodicka, V. W. 7137
Vogel, J. S. 7129
von Baeyer, H. C. 707

Walker, W. P. 7079
Wallace, L. F. 7101
Waller, E. E. 7130
Walton, R. F. 6992
Warfield, G. 7025
Watanabe, A. 7052
Watkins, H. 7078
Weglein, R. D. 7136, 7
Weiner, J. R. 6942
Weingarten, L. R. 694
Weiser, K. 6956
Weiss, G. P. 7042
Welkowitz, W. 7117
Wernick, J. H. 7020
Whelan, J. M. 6946
Whetten, N. R. 7023
Wieder, H. H. 7007
Willardson, R. K. 6944
Wolf, I. 7040
Wolfe, R. 7020
Wolfson, R. G. 6930
Wright, P. G. 7197

Yatsko, R. S. 6949
Yefsky, S. A. 7130
Youla, D. C. 7143
Young, D. R. 7192
Yurkevich, M. I. 6951

Zakrzewski, J. T. 7126
Zuleeg, R. 7137

List of Periodicals scanned for SOLID STATE ABSTRACTS (Journal and Cards)

Acta Crystallographica (Acta Cryst.)
Acta Metallurgica (Acta Met.)
Acta Physica (Acta Phys.)
Acta Physica Hungaricae (Acta Phys. Hungar.)
Acta Physica Polonica (Acta Phys. Polon.)
Acta Polytechnica Scandanavica (Acta Polyt. Scand.)
Advances in Physics (Advances Phys.)
A.E.G. Progress (AEG Prog.)
Alta Frequenza (Alta Frequenza)
American Ceramic Society Bulletin (Am. Ceram. Soc. Bull.)
American Journal of Physics (Am. J. Phys.)
American Mineralogist (Am. Mineral.)
Analyst (Analyst)
Analytical Chemistry (Analyt. Chem.)
Annalen der Physik (Ann. Physik)
Annales de Chimie et Physique (Ann. Chim. et Phys.)
Annales de Physique (Ann. Phys., Paris)
Annales de Radioelectricite (Ann. Radioelect.)
Annales des Telecommunications (Ann. Telecommun.)
Annals of Physics (Ann. Phys.)
Applications and Industry (Applic. and Industr.)
Applied Scientific Research (Appl. Sci. Res.)
Archiv der Elektrischen Ubertragung (Arch. Elekt. Uber-tragung)
Archiv für Elektrotechnik (Arch. Elektrotech.)
Archiv für Technisches Messen (Arch. Tech. Messen)
Arkiv för Fysik (Arkiv Fysik)
Asea Journal (Asea J.)
A. T. E. Journal (ATE J.)
Audio (Audio)
Australian Journal of Physics (Aust. J. Phys.)
Australian Journal of Scientific Research (Aust. J. Sci. Res.)
Automatic Control (Auto. Control)
Automation and Remote Control (Russian Translation) (Automa. Remote Control)

Battelle Technical Review (Battelle Tech. Rev.)
Beama Journal (Beama J.)
Bell Laboratories Record (Bell Labs. Rec.)
Bell System Technical Journal (Bell Sys. Tech. J.)
British Communications and Electronics (Brit. Commun. Electronics)
British Journal of Applied Physics (Brit. J. Appl. Phys.)
Bulletin de L'Academie Pol. des Sciences (Bull. L'Acad. Pol. Sci.)
Bulletin of the Academy of Sciences of the USSR - Physical Series (Russian Translation) (Bull. Acad. Sci. USSR-Phys. Ser.)
Bulletin of the American Physical Society (Bull. Am. Phys. Soc.)
Bulletin of the Research Council of Israel (Bull. Res. Counc. of Israel)

Cables and Transmission (Cables and Transm.)
Canadian Journal of Chemistry (Can. J. Chem.)
Canadian Journal of Physics (Can. J. Phys.)
Ceramics Industry (Ceram. Ind.)
Ceskoslovensky casopis pro fysiku (Cs. cas. fys.)
Chemical Reviews (Chem. Revs.)
Chemical and Engineering News (Chem. Engrg. News)
Cobalt (Cobalt)
Communication and Electronics (Commun. and Electronics)
Communications of the Association for Computing Machinery (Commun. Assoc. Computing Mach.)
Comptes Rendus Hebdomadaires des Seances de l'Academie des Sciences (Comptes Rendus)
Control Engineering (Control Engrg.)
Croatia Chemica Acta (Croat. Chem. Acta)
Czechoslovak Journal of Physics (Czech. J. Phys.)

Direct Current (Direct Curr.)
Dissertation Abstracts (Diss. Abstr.)

Electrical Communication (Elect. Commun.)
Electrical Engineering (Elect. Engrg.)
Electrical Manufacturing (Elect. Mfg.)
Electrical World (Elect. World)
Electronic Applications (Electronic Applic.)
Electronic Design (Electronic Des.)
Electronic Engineering (Electronic Engrg.)
Electronic Equipment Engineering (Electronic Equipm. Engrg.)
Electronic Industries (Electronic Ind.)
Electronic Technology (Electronic Tech.) formerly Electronic and Radio Engineer
Electronics (Electronics)
Electronics and Communications (Electronics and Commun.)
Electrotechnical Journal of Japan (Electrotech. J. Japan)
Elektronische Rundschau (Elektron. Rundschau)
Elektrotechnicky Obzor (Elektrotech. Obzor)
Elektrotechnische Zeitschrift (Elektrotech. Z.)
Energia Nucleare (Energia Nucleare)
Engineering and Mining Journal (Engrg. Mining J.)
Ericsson Technics (Ericsson Technics)

Faraday Society Discussions (Faraday Soc. Disc.)
Fernmeldetechnische Zeitschrift (Fernmeldetech. Z.)
Fortschritte der Physik (Fortschritte Phys.)
Frequenz (Frequenz)

General Electric Review (GE Rev.)
General Telephone Technical Journal (Genl. Tel. Tech. J.)

Helvetica Physica Acta (Helv. Phys. Acta)
Hochfrequenztechnik und Elektroakustik (Hochfrequenztech. u. Elektroakust.)

I. B. M. Journal of Research and Development (IBM J. Res. and Dev.)
Indian Journal of Physics (Indian J. Phys.)
Industrial Laboratories (Indus. Labs.)
Instruments and Automation (Instr. and Automa.)
IRE National Convention Record (IRE Natl. Conv. Rec.)
IRE Transactions:
- on Aeronautical and Navigational Electronics (IRE Trans., Vol. ANE)
- on Audio (IRE Trans., Vol. AU)
- on Automatic Control (IRE Trans., Vol. AC)
- on Broadcast and Television Receivers (IRE Trans., Vol. BTR)
- on Broadcast Transmission Systems (IRE Trans., Vol. BTS)
- on Circuit Theory (IRE Trans., Vol. CT)
- on Communication Systems (IRE Trans., Vol. CS)
- on Component Parts (IRE Trans., Vol. CP)
- on Electron Devices (IRE Trans., Vol. ED)
- on Electronic Computers (IRE Trans., Vol. EC)
- on Industrial Electronics (IRE Trans., Vol. IE)
- on Information Theory (IRE Trans., Vol. IT)
- on Instrumentation (IRE Trans., Vol. I)
- on Medical Electronics (IRE Trans., Vol. ME)
- on Microwave Theory and Techniques (IRE Trans., Vol. MTT)
- on Military Electronics (IRE Trans., Vol. MIL)
- on Nuclear Science (IRE Trans., Vol. NS)
- on Production Techniques (IRE Trans., Vol. PT)
- on Reliability and Quality Control (IRE Trans., Vol. RQC)
- on Space Electronics and Telemetry (IRE Trans., Vol. SET)
- on Vehicular Communications (IRE Trans., Vol. VC)

Journal of the Acoustical Society of America (J. Acoust. Soc. Am.)
Journal of the American Ceramic Society (J. Am. Ceram. Soc.)
Journal of the American Chemical Society (J. Am. Chem. Soc.)
Journal of Applied Physics (J. Appl. Phys.)
Journal of the Audio Engineering Society (J. Audio Engrg. Soc.)
Journal of the British IRE (J. Brit. IRE)
Journal of Chemical Physics (J. Chem. Phys.)
Journal de Chimie Physique (J. Chim. Phys.)
Journal of the Electrochemical Society (J. Electrochem. Soc.)
Journal of Electronics and Control (J. Electronics Control)
Journal of the Franklin Institute (J. Franklin Inst.)
Journal of the Institution of Electrical Engineers (London) (J. IEE)
Journal of the Institute of Metals (J. Inst. Metals)
Journal of Metals (J. Metals)
Journal of Molecular Spectroscopy (J. Mol. Spectrosc.)
Journal of the Optical Society of America (J. Opt. Soc. Am.)
Journal of Physical Chemistry (J. Phys. Chem.)
Journal of the Physics and Chemistry of Solids (J. Phys. Chem. Solids)
Journal de Physique et le Radium (J. Phys. Radium)
Journal of the Physical Society of Japan (J. Phys. Soc. Japan)
Journal of Research of the National Bureau of Standards (J. Res. Natl. Bur. Stand.)
Journal of Scientific Instruments (J. Sci. Instr.)
Journal of the Society of Motion Picture and Television Engineers (J. Soc. Mot. Pict. TV Engrs.)
Journal of the Television Society (J. TV Soc.)

Marconi Review (Marconi Rev.)
Materials in Design Engineering (Matls. Des. Engrg.)
Metallurgical Reviews (Metal. Revs.)
Military Electronics (Mil. Electronics)
Missiles and Rockets (Missiles and Rockets)
Molecular Physics (Mol. Phys.)
Mullard Technical Communications (Mullard Tech. Commun.)

Nachrichtentechnik (Nachrichtentech.)
Nachrichtentechnische Zeitschrift (Nachrichtentech. Z.)
Nature (London) (Nature)
Naturwissenschaften (Naturwissenschaften)
NBS Technical News Bulletin (NBS Tech. News Bull.)
Nuclear Instruments and Methods (Nuc. Instr. Methods)
Nuclear Power (Nuc. Power)
Nuclear Science Abstracts (Nuc. Sci. Abstr.)
Nucleonics (Nucleonics)
Nuovo Cimento (Nuovo Cim.)

Onde Electrique (Onde Elect.)
Optics and Spectroscopy (Russian Translation) (Optics and Spectrosc.)
Optik (Optik)

Philips Research Reports (Philips Res. Rep.)
Philips Technical Review (Philips Tech. Rev.)
Philips Telecommunication Review (Philips Telecommun. Rev.)
Philosophical Magazine (Phil. Mag.)
Physica (Physica)
Physical Review (Phys. Rev.)
Physical Review Letters (Phys. Rev. Lett.)
Physics of Metals and Metallography (Russian Translation) (Phys. Metals Metallog.)
Physics Today (Phys. Today)
Physik (Physik)
Post Office Electrical Engineers Journal (P. O. Elect. Engrs. J.)
Power Apparatus and Systems (Power Appar. Sys.)
Proceedings of the Institution of Electrical Engineers (Proc. IEE)
Proceedings of the Institute of Radio Engineers (Proc. IRE)
Proceedings of the IRE, Australia (Proc. IRE, Aust.)
Proceedings of the National Academy of Sciences (U.S.A.) - (Proc. Natl. Acad. Sciences)
Proceedings of the Physical Society (Proc. Phys. Soc.)
Proceedings of the Royal Society (Proc. Roy. Soc.)
Proceedings of the Royal Netherlands Academy of Science (Proc. Roy. Neth. Acad. Sci.)
Process Control and Automation (Proc. Control Automation)
Product Engineering (Prod. Engrg.)
Progress in Metal Physics (Prog. Metal Phys.)
Progress of Theoretical Physics (Prog. Theoret. Phys.)

Radiation Research (Rad. Res.)
RCA Review (RCA Rev.)
Radio Engineering (Russian Translation) (Radio Engrg.)
Radio Engineering and Electronics (Russian Translation) (Radio Engrg. Electronics)
Refrigeration Engineering (Refrig. Engrg.)
Research (Research)
Research Reviews (Res. Revs.)
Reviews of Modern Physics (Revs. Mod. Phys.)
Review of Scientific Instruments (Rev. Sci. Instr.)
Revista Electrotechnica (Rev. Electrotech.)
Ricerca Scientifica (Ricerca Sci.)
Rozprawy Elektrotechniczne (Rozpr. Elektrot.)
RRE Journal (RRE J.)
Russian Journal of Inorganic Chemistry (Russian Translation) (Russ. J. Inorg. Chem.)

Science (Science)
Scientia Sinica (Sci. Sinica)
Scientific American (Sci. Amer.)
Semiconductor Products (Semicon. Prod.)
Siemens Edison Swan Journal (Siemens Ed. Swan J.)
Siemens Review (Siemens Rev.)
Siemens Zeitschrift (Siemens Z.)
Signal (Signal)
Solar Energy (Solar Energy)
Solid State Journal (Solid State J.)
Solid State Electronics (Solid State Electronics)
Note: The six items below are Russian Translations
Soviet Physics - Crystallography (Soviet Phys.-Cryst.)
Soviet Physics - Doklady (Soviet Phys.-Doklady)
Soviet Physics - JETP (Soviet Phys.-JETP)
Soviet Physics - Solid State (Soviet Phys.-Solid State)
Soviet Physics - Technical Physics (Soviet Phys.-Tech. Phys.)
Soviet Physics - Uspekhi (Soviet Phys.-Uspekhi)
Sperry Engineering Review (Sperry Engrg. Rev.)
Sylvania Technologist (Sylvania Technologist)
Telecommunications (Russian Translation) (Telecommun.)
Telefunken Rohre (Telefunken Rohre)
Telefunken Zeitung (Telefunken Z.)
Transactions of the Faraday Society (Trans. Faraday Soc.)
Transactions of the Metallurgical Society of AIME (AIME Trans.)
Transactions of the New York Academy of Sciences (Trans. N. Y. Acad. Sci.)

U. S. Government Research Reports (U. S. Gov. Res. Rep.)

Vacuum (Vacuum)
Vestnik Akademii Nauk SSR (Vestnik Akad. Nauk SSR)

Welding Engineer (Welding Engr.)
WESCON Convention Record (WESCON Conv. Rec.)
Western Electric Engineer (Western Elec. Engr.)
Westinghouse Engineer (Westinghouse Engr.)
Wireless World (Wireless World)

Zeitschrift für Angewandte Chemie (Z. Angew. Chem.)
Zeitschrift für Angewandte Physik. (Z. Angew. Phys.)
Zeitschrift für Elektrochemie (Z. Elektrochem.)
Zeitschrift für Instrumentenkunde (Z. Instrumentenk.)
Zeitschrift für Kristallographie (Z. Krist.)
Zeitschrift für Metallkunde (Z. Metallkde.)
Zeitschrift für Naturforschung (Z. Naturforsch.)
Zeitschrift für Physik (Z. Physik)
Zeitschrift für Physikalische Chemie (Z. Physik. Chem.)
Zhurnal Eksperimental'noi i Teoreticheskoi Fiziki (Zhur. Eksp. i Teoret. Fiz.)
Zhurnal Fizicheskoi Khimii (Zhur. Fiz. Khim.)
Zhurnal Neorganicheskoy Khimii (Zhur. Neog. Khim.)

Abridged Table of Contents for SOLID STATE ABSTRACTS ON CARDS

Category M: Solid State Metallurgy

Alloys (Phase Diagrams, Solubility, Segregation)

Crystal Structure (Lattices, Imperfections, Impurities)

Crystal Growth (Methods, Crystal Forms)

Crystal Surfaces (Surface Chemistry, Crystal Processing, Connections)

Environmental Effects (Heat Treatment, Radiation)

Category P: Solid State Physics

Crystal Physics (Binding and Lattice Properties, Energy Bands and Levels)

Electrical Properties (Dielectric, Carrier, Conductive, Breakdown, Magnetoelectric, Noise, Surface)

Magnetic Properties (Ferro-, Ferri-, Para-, and Diamagnetic)

Optical Properties (Absorptive, Radiative, Luminescent, Photoconductive, Photovoltaic)

Thermal Properties (Thermoelectric)

Mechanical Properties (Deformation)

Category D: Solid State Devices

(Theory, Fabrication, Properties, Measurements)

Conductive Devices (Diodes and Rectifiers, Varistors, Transistors, Functional Units)

Magnetoelectric Devices (Hall Effect, Magnetoresistive)

Photodevices (Photoconductive, Photodiode and Phototransistor, Photovoltaic, Luminescent)

Thermal Devices (Thermistor, Thermoelectric)

Ferrite Devices (Isolators, Circulators, Memory Elements, etc.)

Paramagnetic Devices (Masers)

Dielectric Devices (Transducers, Memory Cells, Amplifiers)

Superconductive Devices (Cryotrons)

Category B: Solid State Device Circuits

Amplifiers

Oscillators

Switching Circuits

Signal Converters (Modulators, Detectors, Mixers, Frequency Multipliers and Dividers)

Wave Generators

Pulse Circuits

Category A: Solid State Device Applications

Communications (Radio, Television, Telephony)

Radar

Telemetry

Computers

Power

Control

Instrumentation

ORDER FORM

CAMBRIDGE COMMUNICATIONS CORPORATION
238 Main St., Cambridge 42, Mass.

Gentlemen:

Please enter my order for the publications which I have checked below:

☐ **SOLID STATE ABSTRACTS** (Journal) — Vol. 1 (1960 abstracts) $25.00

SOLID STATE ABSTRACTS ON CARDS — Vol. 1 (1960 abstracts) [A subscription to **Solid State Abstracts** (Journal) — Vol. 1 is included with any order for one or more card categories without additional charge.]

☐ All Categories (Complete) $250.00

☐ Semiconductor Abstracts 175.00
(selected from all categories)

☐ Magnetic, Dielectric, etc. Abstracts 100.00
(selected from all categories)

☐ Category M (Metallurgy) 50.00

☐ Category P (Physics) . . . . . $ 75.00

☐ Category D (Devices) 50.00

☐ Category B (Circuits) 50.00

☐ Category A (Applications) 50.00

Name .....

Address .....

.....

.....

☐ Payment Enclosed ☐ Bill me

FOR SURFACE STUDIES

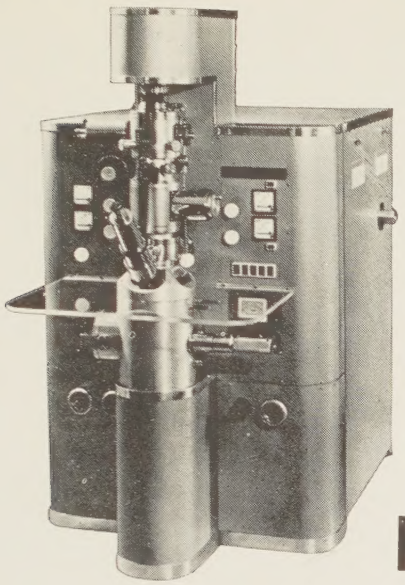

KE1

Trüb, Täuber Secondary Electron Emission Microscope

for direct viewing of metallic and semiconducting specimens by means of secondary electrons released from ion bombardment of the surface — featuring . . .

- Images free of distortion and deformation
- Enlargement up to 1500 X electronoptically
- Resolution 500–600Å
- Object temperature 150°–800° C
- Observable surface of the object 25 mm square
- Differentiation of the material

The Instrument Includes . . .

Electrostatic immersion objective
Ion beam system
Revolving contrast diaphragms
2 electromagnetic projectors
Observation chamber with fluorescent image screen
Recording chamber with plate cassette
High-intensity optical microscope
All-metal housing with vacuum equipment including diffusion pump
High-voltage equipment for 45 kV
Measuring instruments and control equipment

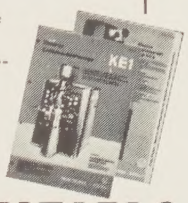

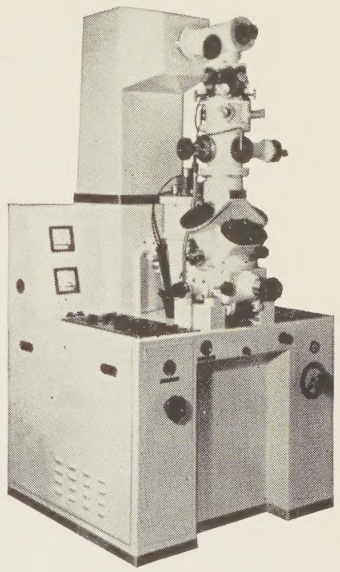

KD3

Trüb, Täuber Electron Diffractograph

for determining the crystalline structure of surfaces, thin layers, and extremely small quantities of material, including dynamic processes — featuring . . .

- Cold-cathode electron gun with practically unlimited life
- Simple design — dependable operation, extreme flexibility
- Balanced optical system
- High resolving power
- Large variety of specimen holders for various methods of investigation
- Devices for heating and cooling the test specimens (from liquid nitrogen to 1000°C)
- Devices for discharging, etching, surface evaporating
- Various cameras for photographic recording on plates and films
- Unique kinematic recorder

Specifications

Acceleration Voltage —	
continuously adjustable:	10 to 50 kV
ripple (fractional):	$\approx 10^{-4}$
stability:	$\pm 0.1\%$
Final vacuum:	approx. 2 x 10^{-5} mm Hg
Magnification with electronic lens:	75X
Minimum line width:	0.001 mm
Minimum diameter of beam for focussing on specimen, without additional diaphragms:	4μ

Distributed by:

NEW ENGLAND SCIENTIFIC INSTRUMENTS CO.

238 MAIN STREET • CAMBRIDGE 42, MASSACHUSETTS • Klrkland 7-1997

Electron Microscopes • Nuclear Induction Spectrographs • High Voltage Oscillographs • Precision Laboratory Instruments • Nuclear Track Microscopes

may cost your company many times the price of

SOLID STATE ABSTRACTS ON CARDS

These cards enable anyone — scientist, engineer, librarian, file clerk — to maintain a cumulative reference file of up-to-date information in the solid state field. Classification numbers on each card make it easy to file this information in a logical sequence and hundreds of guide cards make it possible to locate required references immediately.

This service, which amounts to a continuous literature search on more than 4000 topics, covers conference papers, U.S. patents, and commercial new product releases in addition to some 250 technical journals published throughout the world.

Take full advantage of the billions of dollars of research results that are reported each year. This annotated and classified bibliography of current research in the solid state field is inexpensive insurance that your scientific efforts are not duplicating the work of others.

CAMBRIDGE COMMUNICATIONS CORPORATION
238 Main Street • Cambridge 42, Massachusetts